Review

Recent Advances in Preparation and Testing Methods of Engine-Based Nanolubricants: A State-of-the-Art Review

Sayed Akl [1,*], **Sherif Elsoudy** [1], **Ahmed A. Abdel-Rehim** [1], **Serag Salem** [1] and **Mark Ellis** [2]

1. Department of Mechanical, Faculty of Engineering, The British University in Egypt, Cairo 11837, Egypt; sherif.elsoudy@bue.edu.eg (S.E.); ahmed.azim@bue.edu.eg (A.A.A.-R.); Serag.salem@bue.edu.eg (S.S.)
2. Mechanical Engineering and Design, School of Engineering, London South Bank University, London SE1 0AA, UK; ellism3@lsbu.ac.uk
* Correspondence: Sayed.akl@bue.edu.eg

Abstract: Reducing power losses in engines is considered a key parameter of their efficiency improvement. Nanotechnology, as an interface technology, is considered one of the most promising strategies for this purpose. As a consumable liquid, researchers have studied nanolubricants through the last decade as potential engine oil. Nanolubricants were shown to cause a considerable reduction in the engine frictional and thermal losses, and fuel consumption as well. Despite that, numerous drawbacks regarding the quality of the processed nanolubricants were discerned. This includes the dispersion stability of these fluids and the lack of actual engine experiments. It has been shown that the selection criteria of nanoparticles to be used as lubricant additives for internal combustion engines is considered a complex process. Many factors have to be considered to investigate and follow up with their characteristics. The selection methodology includes tribological and rheological behaviours, thermal stability, dispersion stability, as well as engine performance. Through the last decade, studies on nanolubricants related to internal combustion engines focused only on one to three of these factors, with little concern towards the other factors that would have a considerable effect on their final behaviour. In this review study, recent works concerning nanolubricants are discussed and summarized. A complete image of the designing parameters for this approach is presented, to afford an effective product as engine lubricant.

Keywords: nanotechnology; engine-based nanofluids; energy saving; engine performance

1. Introduction

Transportation activities employing internal combustion engines will require more efficient and advanced approaches through the upcoming years. This appears as a crucial challenge regarding the enhancement of vehicular tribology and fuel consumption [1]. This corresponds to energy conservation demands and the lessening of greenhouse gas emissions in the light of the Paris protocols on climate change [2–4]. A direct strategy to address this situation is to promote fuel economy, which is the primary driving force behind the improvement in modern combustion engines' performances [5]. Numerous approaches have been successfully employed to enhance engine efficiency. This includes the insertion of heating waste recovery systems, combustion efficiency refinement, and scaling down frictional losses in the engine [6–10]. Friction reduction has been receiving considerable interest from scientists, as a cost-effective method to empower engine efficiency. The development in engine lubricants is considered one of the leading approaches for this purpose. Additives are usually added to the lubricants to improve their efficiency. In light of engine oil additives and other applications with high-loaded conditions, dialkyl dithiophosphate (ZDDP) has been used for several decades for its impressive tribological performance [11–14]. For instance, a recent study by Vyavhare [15] showed that a reduction in the coefficient of friction, by 47%, had been observed when ZDDP was dispersed with ZnO nanoparticles into the base lubricant. Despite that, ZDDP is known for its poisonous

emissions of phosphorus and sulphur species [16,17]. To a certain degree, commercial lubricants cannot afford a better performance under severe conditions, such as higher mechanical stresses, higher speeds, and higher working temperatures.

Consequently, novel approaches regarding engine lubricants have been raised to meet these conditions. For instance, the current requirements of ILSAC GF6 (International Lubricants Standardization and Approval Committee for gasoline-fueled vehicles grade) assess the lubrication industry, to embark on a new generation of lubricants with advanced anti-wear and friction properties [18]. Figure 1a represents the proposed standardized development in gasoline lubricants, in terms of fuel consumption and greenhouse gas emissions, during the upcoming years. Accordingly, this would reduce the percentage of frictional and thermal power losses reported in recent studies with the current engine oil technology, as shown in Figure 1b [19].
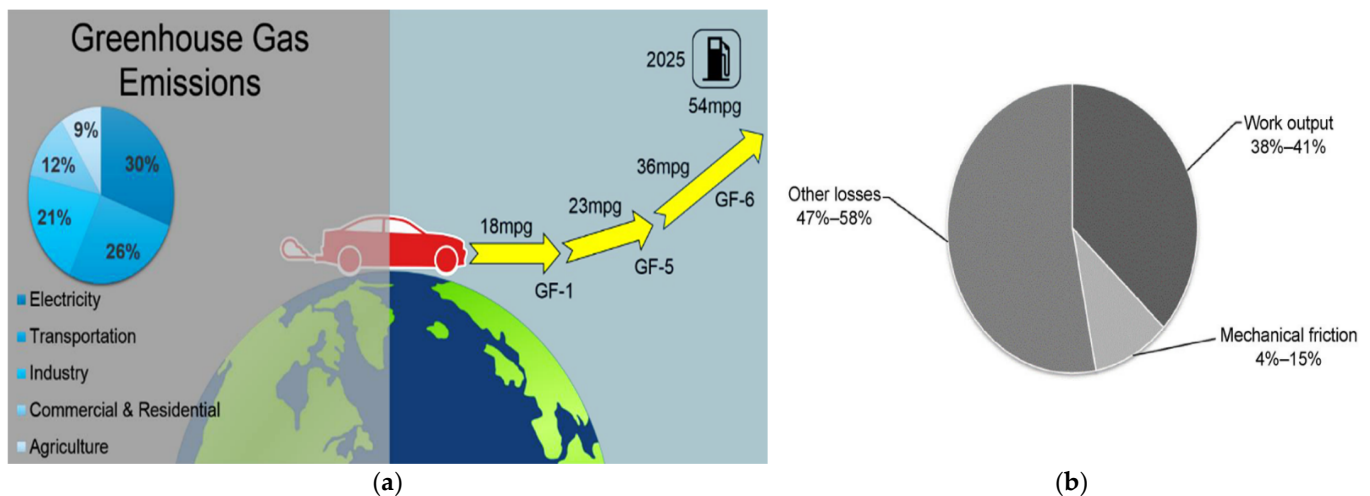

Figure 1. (**a**) Recent fuel economy standards of ILSAC [18] Adapted with permission. (**b**) energy losses distribution in a fired engine [19] Adapted with open access permission.

Nanomaterials have been studied intensively as additives for promoting lubricant capabilities. The application of nanoparticles in the engine's lubrication system showed a great deal of boosting the overall engine performance in many studies [20–24]. Nanolubricants have a major effect on promoting the wear process, which is the durability of the engine parts, with a considerable role in engine thermal efficiency [25]. Plenty of nanomaterials have been used for this objective. This includes carbon and its derivatives (Gr [26], MWCNT [27], ND [28,29]), oxides of inorganic compounds (ZnO [30,31], CuO [32] MgO [33], TiO_2 [34]), and transition metal dichalcogenide (MoS_2 [35]).

The current review study is considered a step towards developing a novel class of lubricant additives, which are considered less harmful to humans and the environment, besides their substantial performance [36,37]. Moreover, it offers a systematic outline of the research outcomes introduced in previously declared data through the last decade, regarding engine-based nanolubricants. The study is intended to be a helpful directory for researchers, concerning the development in the field of engine lubricants. The overview starts with the standard preparation methods. A detailed review of the tribological, rheological, and engine performance follows. Finally, a discussion on the challenges regarding selecting possible nano candidates and future directions for this purpose is included.

2. Preparation Methods and Dispersion Stability of Nanolubricants

2.1. Basic Concepts

Any host liquid is known as a nanofluid, where nanoparticles are presented in a stable suspended state. A significant challenge in employing nanoparticles in lubricants is linked to their dispersion stability in these fluids. This is because nanoparticles easily agglomerate

due to their high surface tension, forming non-dispersible aggregate clusters [38]. The aggregation of nanoparticles can effectively limit the nanolubricant's lubricity at the contact area, and could even increase friction in some cases [39,40]. The dispersion stability of nanolubricants can be clarified by colloidal theories [41]. In these theories, nanoparticle aggregation is attributed to the interaction between the nanoparticles and their thermal agitation energy received from the base liquid. The thermal agitation energy has a value of K_bT, where K_b and T are the Boltzman constant and the liquid temperature, respectively. The thermal agitation energy induces the nanoparticles to move in the solvent, causing the random Brownian motion [42]. This random motion urges the interaction between colloidal nanoparticles in the form of van der Waals attractive forces and repulsive forces. A stable dispersion of nanolubricant formed when the repulsive forces between the particles overcame the attractive forces caused by thermal agitation [42]. The repulsive force's nature has been explained through the two widely accepted electrostatic stabilization theories by DLVO and the steric stabilization [28,43], as shown in Figure 2a. In the DLVO theory, the repulsive force between nanoparticles is referred to as the electrostatic charge originated at the surface of the particles. This electrostatic interaction is typical in polar solvents, and is characterized by their high dielectric constant (ϵ). On the contrary, in solvents with a low dielectric constant, as in lubricants, the electrostatic interaction is weak, even when nanoparticles have a high surface charge [39]. The electrostatic stabilization is enhanced by dispersing agents, which can enrich the total surface charge of nanoparticles [43].
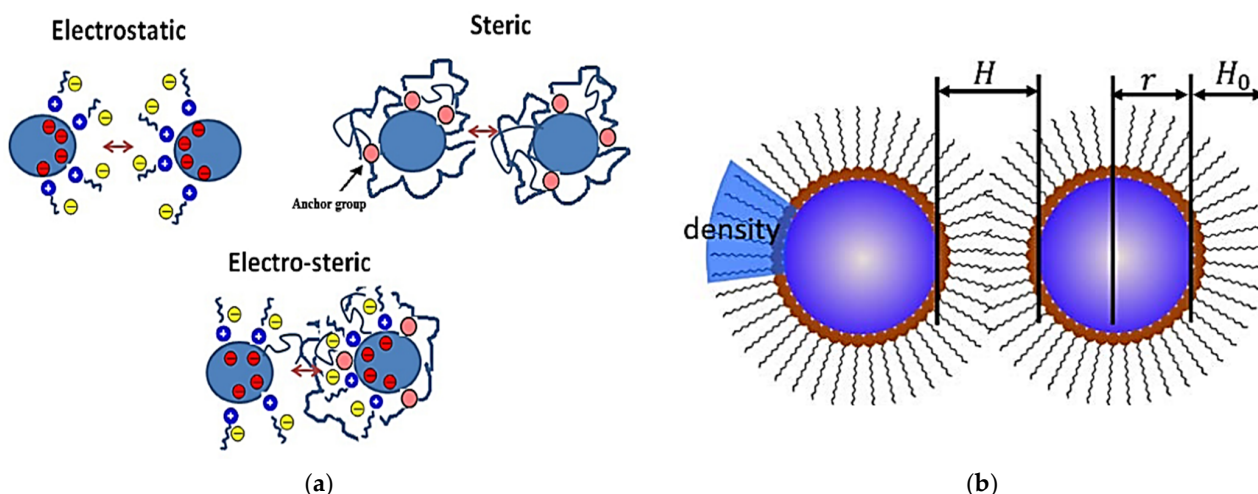

(**a**)   (**b**)

Figure 2. Summary of colloidal stability theories of nanofluids. (**a**) Electrostatic, steric, and electro-steric stabilization [28] Adapted with permission. (**b**) Steric stabilization [39] Adapted with open access permission.

In steric stabilization, dispersing agents cover the suspended nanoparticles to form a grafted layer on the particle's surface, as shown in Figure 2b. Ho is the thickness of the grafted layer, H is the distance between the particles, and r is the particle's radius. The steric repulsive force originates from the elastic deformation of the grafted surface layers. When two grafted particles approach each other, the grafted surface layer deforms, leading to the steric stabilization [39]. In some studies, both stabilization methods had been used to produce stabilized nanolubricants [28].

2.2. Preparation Methods of Nanolubricants

The preparation of nanolubricants is considered a substantial step in building a stabilized and durable nanofluid system. Based on nanofluid preparation, two methods have been utilized to produce nanofluids, named single-step and two-step methods [37,39,44–49].

In the single-step method, nanoparticles are prepared with the base fluid and an appropriate dispersing agent simultaneously to produce the nanolubricant. This could be

done using many techniques, such as physical vapor deposition, liquid chemical methods, laser ablation, and submerged arc synthesis systems [47,48]. However, this method is limited by its high cost and small-scale production rates [38]. In the two-step method, the nanoparticles are first prepared separately. The nanoparticles are then added with the dispersing agent into the base fluid as a second processing step, using many techniques such as magnetic stirring, probe sonication, bath sonication, homogenizing, high shear mixing, and planetary ball mill. Most researchers use the second-step type, as it is considered the most economical method to prepare nanolubricants with large-scale productions [43,50]. Figure 3 provides the approaches reported in the literature for the preparation and stability testing techniques of nanofluids.
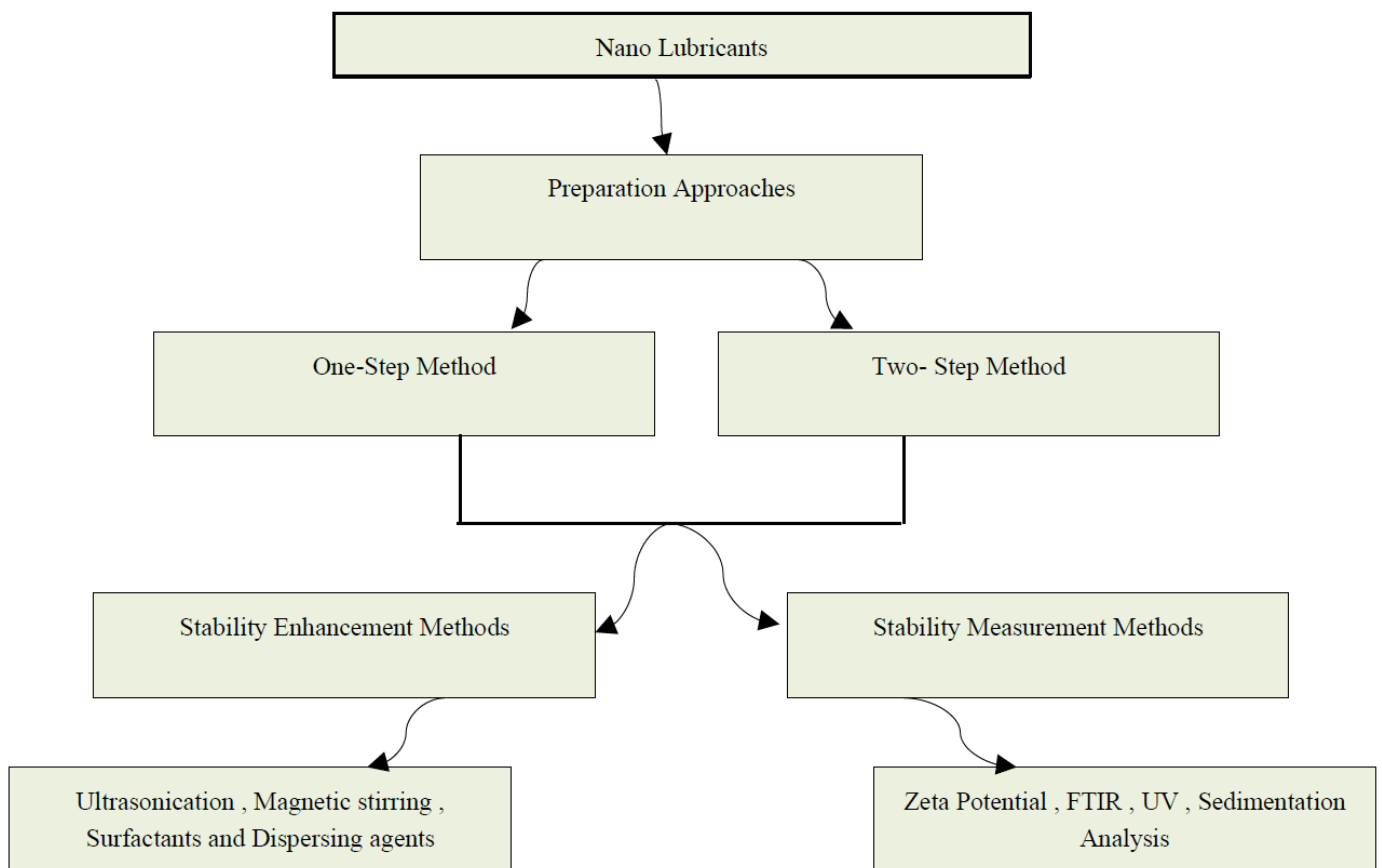

Figure 3. Preparation approaches and stability measurement techniques of nanolubricants mentioned in the literature.

A surface modification for the nanoparticles through dispersing agents is conducted to stabilize the particles in the base medium for the two preparation methods. This is to prevent particle aggregation and sedimentation. Functionalization by steric or electrostatic stabilization is the most commonly used method for surface modification. In both of the methods, ionic surfactants or polymers are used to coat the nanoparticle surface [39].

For studies regarding engine nanolubricants, researchers investigated many techniques to enhance the dispersion stability in terms of one- or two-step methods. In a recent study by Mello [38], the dispersion stability of CuO nanoparticles in the base lubricant of PAO was studied using the following four different dispersing agents: oleic acid, toluene, hexane, and ethylene glycol. The study used two different techniques, electrostatic and steric surface functionalization methods, during the preparation of nanolubricants. Oleic acid had been used, firstly, as an ionic surfactant, and then three different organic dispersants had been added to keep the nanoparticles in a stable suspension. The stability results of ultraviolet¬–visible spectrometry (UV) and sedimentation showed that the best stability

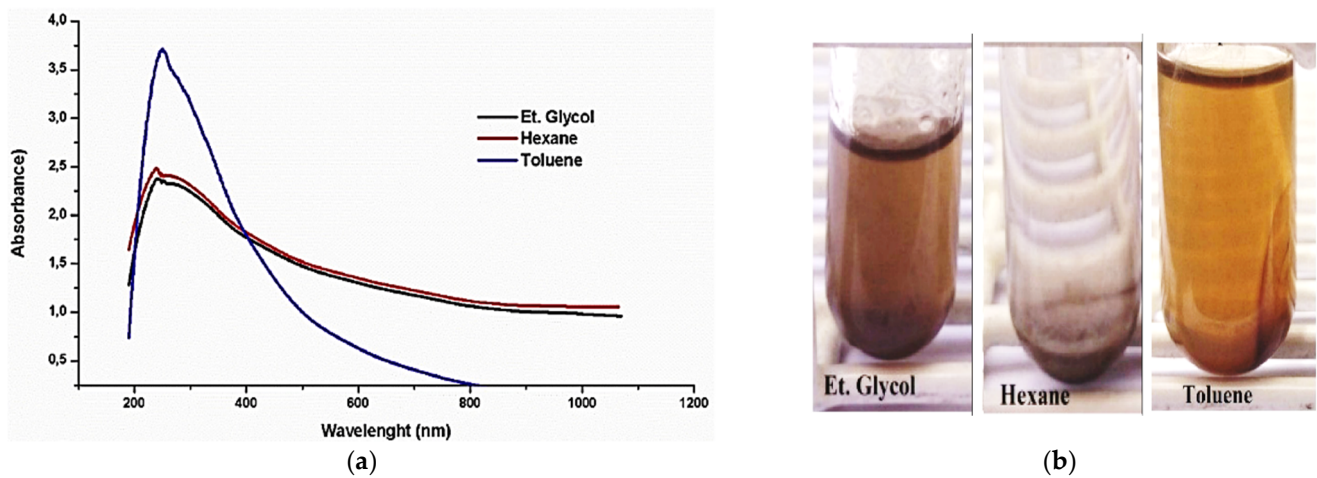dispersion of nanolubricants was toluene and hexane, for a stable time of 30 days, as shown in Figure 4.

Figure 4. Dispersion stability of CuO nanolubricant with different dispersing agents. (**a**) UV–visible spectra, (**b**) sedimentation analysis [38]. Adapted with permission.

In another study by Hemmat [51], the nanolubricant of ZnO/10W-40 was prepared using the second-step method, without dispersing agents. The stability of the suspended nanoparticles lasted for only 72 h. This shows how important the addition of dispersing agents is, and how it can effectively promote stability performance. Hybrid nanoparticles of ZnO/MWCNT were added to the engine lubricant of 10W-40 [30]. The sedimentation results showed a stability duration of 15 days when the nanoparticles had been functionalized by oleic acid, with an optimum concentration of 0.25 wt.%. There is no experimental relationship in all the stability studies that can link nanoparticles, their size, and base lubricant to the duration of stability. In light of that, many concerns about nanolubricant dispersion stability still need to be explored in future studies. In another recent study by Kamal [50], the dispersion stability had been conducted on Al_2O_3/TiO_2 hybrid nanoparticles added to PAO6 as a base engine lubricant. The nanoparticles had been functionalized using bis(2-Ethylhexyl) phosphate (HDEHP) as a surfactant. Many dispersion analyses were conducted, such as FTIR, UV, and zeta potential. The results revealed a superb dispersion performance of the prepared nanolubricants, reaching a stable period of 70 days, as shown in Figure 5b.
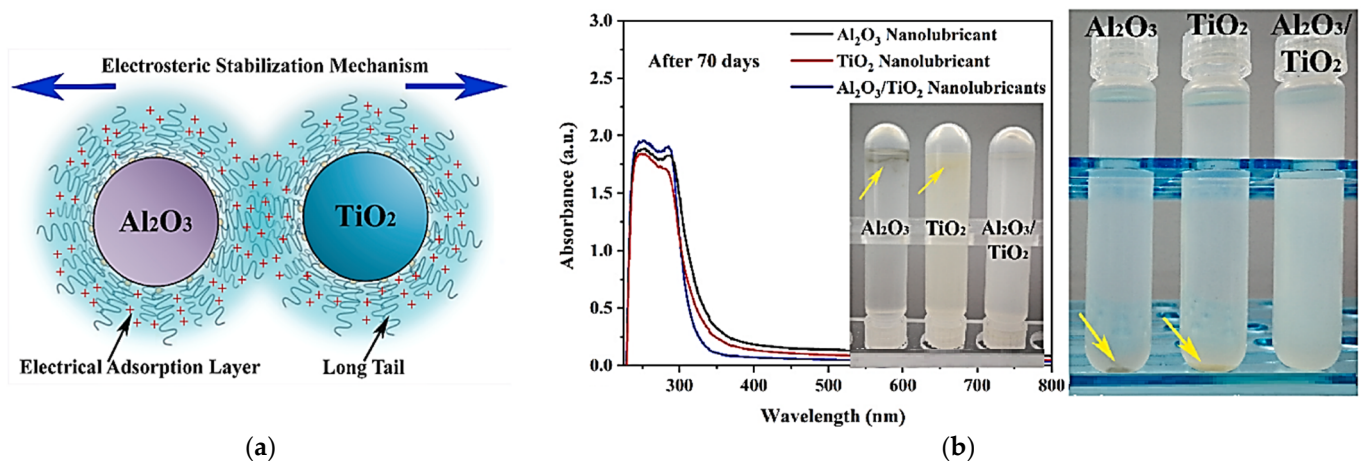

Figure 5. Dispersion stability of hybrid Al_2O_3/TiO_2 nanolubricant. (**a**) Electro-steric stabilization mechanism, (**b**) sedimentation and UV analyses after 70 days [50]. Adapted with permission.

The outstanding dispersion capabilities of the prepared nanolubricants were attributed to the electrostatic, electro-steric, and steric stabilization mechanisms (Figure 5a), which were promoted through the addition of HDEHP. All of the stability studies of engine lubricant-based nanofluids during the last ten years are concluded in Table 1.

In some studies, it had been reported, in many cases, that a low quality of dispersion stability can affect the tribological, rheological, and thermophysical properties of the nanolubricant.

For instance, it had been reported by Abdel-Rehim that CuO would aggregate at a high concentration of 1 wt.% [52]. These aggregates led to instability of tribo-film formation, which had been demonstrated through the surface analysis of EDX. The authors claimed that at a high concentration of nanoparticles, the aggregations of the nanoparticles would form high-weight particles compared to their nominal size. These aggregations would then aggravate the wear behaviour of the lubricant, as they can experience some difficulty getting involved with the contact asperities.

In another study by Ali [53], the absence of dispersion of the hybrid Al_2O_3/TiO_2 engine-based nano-lubricant had been observed by UV after 55 days. These low qualities of dispersion stability would then cancel the beneficial effect of the nanolubricant on the tribological and thermophysical properties. The study declared that nanoparticles would provide a thermal path between the fluid layers when nanolubricants are afforded at an acceptable dispersion stability, thus presenting the most significant enhancement in the thermal conductivity.

Numerous considerations can be revealed from Table 1. For instance, there is no specific trend to be followed that can guarantee an acceptable stability behaviour, and thus the longer shelf life of these nanolubricants. This includes the preparation techniques, surface modification methods, and testing parameters as well. This might be returned to the particular nature of each element that had been used in every single study.

Further, all testing conditions regarding dispersion stability were conducted based on the static condition of the prepared nanolubricant. For instance, all of the studies monitored suspension quality through UV, zeta, FTIR, and sedimentation, after a specific period of storing the nanolubricant. This means that there is no evidence of what can happen to the colloidal stability of nanolubricants if they undergo a real engine test at elevated temperatures and working loads.

In consequence, a study by Mello had considered a part of this issue by testing the stability of a CuO nanolubricant dispersed by toluene and oleic acid, before and after the tribological testing [38]. One more vague issue that needs to be treated is the effect of degradation on the engine lubricant life span, which is observed under specific testing conditions [54,55].

Table 1. A summary of the literature on the dispersion stability of engine oil-based nanofluids.

Ase Lubricant	Nano-Additive	Preparation Method	Optimal Concentration in Terms of Stability	Dispersing Agents	Testing of Depression	Stable Condition/Duration	Processing Method/Processing Time	Reference	Year
Base as lubricant/PAO6	Al_2O_3/TiO_2	Two-step method	0.1 wt.%	HDEHP	Sedimentation, Zeta potential, FTIR, UV	Stable/70 days	Ultrasonic dispersion/6 h Magnetic stirrer	[50]	2021
SAE 5 W-30	ZnO/TiO_2	Two-step method	All concentrations	Oleic acid	Sedimentation	Stable/1 week	Ultrasonic dispersion/2 h Magnetic stirrer	[56]	2021
SAE 20 W-40	$MWCNT/TiO_2$	Two-step method	0.1	-	Zeta potential	Stable/72 h	Ultrasonic dispersion/3 h	[57]	2021
SAE 40	SiO_2	Two-step method	All concentrations	-	Sedimentation	Stable/1 month	Ultrasonic dispersion/40 min Magnetic stirrer/30 min	[58]	2021
SAE 30	Graphite	0.3 wt.%	0.3 wt.%	Tween-80, Ethylene glycol	Sedimentation, zeta potential,	Stable/ 15 days	Ultrasonic dispersion/1.5 h	[59]	2021
Base as lubricant/paroline oil	MoS_2	One-step method	All concentrations	Not reported	Sedimentation	Stable/10 days	Ultrasonic dispersion	[35]	2020
Base as lubricant/HD 50	Gr	Two-step method	0.01 wt.%	Sodium dodecyl persulfate (SDS), Oleic acid (OA)	Sedimentation, FTIR, XRD	Stable/30 days	Magnetic stirrer/3 h, Ultrasonic dispersion/12 h	[6]	2020
SAE 10W-40	Gr-MS-Zn	One-step method	0.5 wt.%	PEHA	Sedimentation	Stable/30 days	Not reported	[60]	2020
SAE 10W-40	ZnO/MWCNT	Two-step method	0.25 wt.%	Oleic acid (OA)	Sedimentation	Stable/15 days	Ultrasonic dispersion/2 h	[30]	2020
SAE 40	ZnO, MoS_2	Two-step method	0.1 wt.%	Not reported	Sedimentation	Stable-ZnO/6 days	Ultrasonic bath/45 min	[61]	2020
SAE 5W-30	MWCNT	Two-step method	0.03 wt.%	Liqui Moly	Not reported	Stable	Not reported	[27]	2020
Base as lubricant/PAO	CuO	One-step method	0.1 wt.%	Toluene/OA, Hexane/OA, Et.Glycol/OA	Sedimentation, UV	Sable-Toluene/30 days	Magnetic stirrer/7 h	[38]	2020
SAE 20W-50	$La(OH)3/rGO$	One-step method	Not reported	Not reported	Sedimentation, XRD	Stable/28 days	Ultrasonic dispersion/1 h	[62]	2020
SAE 5W-30	Cu/Gr	Two-step method	0.4 wt.%	Oleic acid (OA)	UV	Stable/11 days	Magnetic stirrer/4 h	[63]	2019
Base as lubricant/hexadecane	GO	Two-step method	10 mg L^{-1}	Oleylamine	Sedimentation	Stable	Ultrasonic dispersion	[64]	2019
SAE 5W-30	GO	Two-step method	0.1 wt.%	Dodecylamine, Ethanol, Xylene	UV, Sedimentation, XRD	Stable/32 Days	Ultrasonic dispersion/6 h	[65]	2019
SAE 10W-40	TiO_2	Two-step method	Not reported	Oleic acid (OA)	Sedimentation, Zeta sizer	Not stable	Magnetic stirrer/15 min Ultrasonic dispersion/20 min	[66]	2018
SAE 5W-30	Gr	Two-step method	0.4 wt.%	Oleic acid (OA)	Sedimentation, UV	Stable/11 days	Magnetic stirrer/4 h	[67]	2018
SAE 5W-30	Al_2O_3/TiO_2	Two-step method	0.1 wt.%	Oleic acid (OA)	Not reported	Not reported	Magnetic stirrer/4 h	[68]	2018
SAE 10W-40	ZnO	Two-step method	0.25–2 vol.%	Not reported	Sedimentation	Stable/72 h	Magnetic stirrer/2 h, Ultrasonic dispersion	[51]	2017
Base as lubricant/PAO	Al_2O_3	Two-step method	1 wt.%	Oleic acid (OA)	Not reported	Not stable	Magnetic stirrer	[69]	2017
SAE 5W-30	MoS_2	Two-step method	-	Not reported	Not reported	Not reported	Magnetic stirrer, Ultrasonic dispersion	[70]	2017
SAE 50	ZnO	Two-step method	0.125–1.5 vol.%	Not reported	Sedimentation	Stable/2 days	Ultrasonic dispersion/5 h	[71]	2017
Base as lubricant/60SN	ZnO	Two-step method	0.5 wt.%	Oleic acid (OA)	Sedimentation	Stable/12 h	Magnetic stirrer/20 min, Ultrasonic dispersion/30 min	[72]	2017
SAE 40	MWCNT/CuO	Two-step method	0.0625–1 vol.%	Not reported	Sedimentation	Stable/1 week	Magnetic stirrerUltrasonic dispersion	[73]	2017
Base as lubricant/paraffin	MoS_2	Two-step method	1 wt.%	ZDDP, Polyisobutylene amine succinimide (PIBS)	SEM	Stable	Ultrasonic dispersion/ 40 min	[74]	2017

Table 1. *Cont.*

Ase Lubricant	Nano-Additive	Preparation Method	Optimal Concentration in Terms of Stability	Dispersing Agents	Testing of Depression	Stable Condition/Duration	Processing Method/Processing Time	Reference	Year
SAE 50	MWCNT/SiO$_2$	Two-step method	0.0625–2 vol.%	Not reported	Sedimentation	Stable	Magnetic stirrer/2 h, Ultrasonic dispersion	[75]	2016
SAE 5W-30	Al$_2$O$_3$, TiO$_2$	Two-step method	0.25 wt.%	Oleic acid (OA)	UV, Zeta sizer	Stable/336 h	Magnetic stirrer/4 h	[76]	2016
SAE 10W-40	MWCNT/ZnO	Two-step method	0.125–1 vol.%	Not reported	Sedimentation	Stable/1 week	Magnetic stirrer/2 h Ultrasonic dispersion/1 h	[77]	2016
Base as lubricant/PAO	ZnO	One-step method	0.2–1.5 wt.%	Oleic acid (OA)	FTIR	Stable	Magnetic stirrer	[78]	2016
Base as lubricant/PAO	Gr	Two-step method	0.01 wt.%	Span-80	Sedimentation	Stable/4 weeks	Magnetic stirrer/10 min, ultrasonic dispersion/15 min	[79]	2016
SAE 10W-40	GO, Ag, GNP	Two-step method	0.06–0.1 wt.%	Stearic amine, ethanol, SDS, glucose	Sedimentation, FTIR	Stable/2 weeks	Ultrasonic dispersion/5 h	[80]	2016
SAE 10W-40	GO	One- step method	0.04 mg mL^{-1}	Octadecylamine (ODA)	XRD, FTIR	Stable/30 days	Ultrasonic dispersion	[81]	2015
Base as lubricant /500 N	MoS$_2$	One-step method	0.58 wt.%	Sodium dodecyl persulfate (SDS), heptane	Sedimentation, UV	Stable/1 year	ultrasonic shaker/1 h	[82]	2015
Base as lubricant/PAO	Cu/rGO	One-step method	0.5–2 wt.%	Oleic acid (OA)	FTIR	Stable/ 7 days	Ultrasonic dispersion	[83]	2015
SAE 40	C	Two-step method	0.01 vol.%	Not reported	Zeta sizer	Stable/14 days	Ultrasonic dispersion/ 1 h	[84]	2014
Rapeseed oil/SAE20W40	CuO	Two-step method	0.5 wt.%	Not reported	UV	Stable/29 days	Rotary Shaker /5 h, ultrasonic dispersion/2 h	[85]	2014
SAE 15W-40	MoS$_2$	Two-step method	All concentrations	Span-80	Sedimentation	Stable/14 days	High shear homogenizer/ 30 min	[86]	2014
Base as lubricant/PAO	Gr	Two-step method	0.5–1.5 wt.%	Oleic acid (OA)	FTIR	Stable/ 7 days	Magnetic stirrer/30 min	[87]	2014
SAE 10W-40	rGO	One-step method	0.04 mg mL^{-1}	Octadecylamine (ODA)	Sedimentation, XRD, zeta potential, FTIR	Stable/30 days	Ultrasonic dispersion	[88]	2014
SAE 20W-50	MWCNT	One-Step method	0.1 wt.%	SOCL2, DMF, THF, dda	Sedimentation, XRD	Stable/720 h	Ultrasonic dispersion, Magnetic stirrer	[89]	2013
SAE 20W-50	MWCNT	Two-step method	0.1 wt.%	Dodecylamine	Sedimentation	Stable/720 h	planetary ball mill/3 h	[90]	2013
Base as lubricant/PAO	MoS$_2$	Two-step method	3 wt.%	Benzethonium chloride	Sedimentation	Stable	Ultrasonic dispersion	[91]	2012
500 W	GO	Two-step method	0.025 mg mL^{-1}	DMF	FTIR	Stable	Ultrasonic dispersion/1 h	[92]	2011

3. Tribological Performance of Nanolubricants

Nanoparticles perform a vital function between friction pairs, specifically at the boundary lubrication regime where the wear and friction margins are at their top worth [93]. Their tiny dimensions allow them to penetrate the surface asperities at the contact area, as shown in Figure 6 [94]. According to the tribological hypotheses, these particles as nano additives exfoliate under high normal loads of surface asperities and form a layer of tribo-film [95]. Yang [74] also believed in this mechanism of film formation, as shown in Figure 6c. The formation of a tribo-layer was a result of the action of the dragging and extrusion of MoS_2 nanoparticles along the contact area. Hou [96] suggested the same point (generation of tribo-layer) as a significant opportunity to diminish the wear rate by 29% and 21% when TiO_2 and Al_2O_3 were used, respectively. In this study, the action of the tribo-film was explained as an ultra-thin layer of lubricating film or a solid lubricant.

In another study [97], the coefficient of friction and wear rate had been reduced by 20% and 50%, respectively, when the MoS_2 nanolubricant was used. This had also been clarified by the mechanism of tribo-sintering (tribo-film). Nanoparticles were trapped and stuffed at the valleys of the pairing surfaces. This enhances the surface roughness, and thus reduces the shear forces between the asperities. The study also discussed the effect of working speed and loads on the mentioned nanolubricants' tribological properties. It was found that raising the contact load and speed led to increasing the shear rate of the asperities, due to the flash temperature growth at contact. Hirani [65] studied the reason behind the formation of this tribo-film. Analyses using EDX and XPS suggest a chemical reaction between the base material of the friction pair and the nanoparticles, which is responsible for this tribo-film formation.
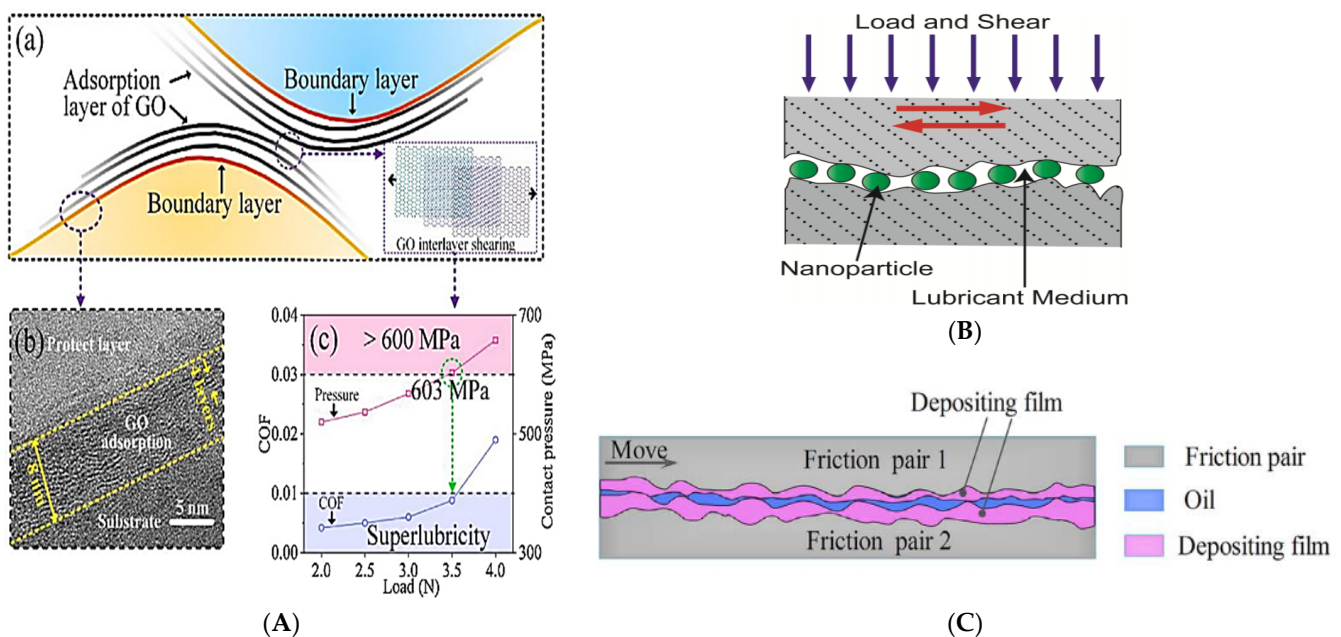

Figure 6. Different lubrication mechanisms of nanolubricants. (**A**) Tribo-film formation of GO nanosheets [94]. (**B**) Ball-bearing mechanism of ZnS nanowires [98]. (**C**) Tribo-film mechanism of MOS_2 nanolubricant [74]. Adapted with permission.

The friction coefficient was reduced by 40% when functionalized graphene nanoparticles were used in contrast with the base engine oil. Hou [76] reported a study of using the hybrid nanoparticles of Al_2O_3/TiO_2 for engine lubricants through 50 km of sliding distance. The mentioned hybrid nanolubricant showed an amended performance, with a reduction in frictional power losses by 40–51%, compared to the base engine oil. Also, the wear rate was reduced by 17% after the end of the test. Rivera [99] studied the multilayer graphene doped with polyaniline and copper, respectively (MLG¬–PANI, MLG–Cu). The study revealed a significant reduction in the coefficient of friction and wear rate by

20–40% and 43–60%, respectively, as shown in Figure 7. According to the surface analysis results using AFM, a combined effect of both polishing and tribo-sintering mechanisms was proposed, due to the enhancement in the average surface roughness. Prabaharan [100] investigated the tribological effect of adding different concentrations of CuO nanoparticles. Based on a statistical study on the experimental work, the study concluded that sliding speed and load are directly related to paired surfaces wear rate. The study reported that the concentration of 0.5 wt.% CuO would be the effective concentration to achieve the least specific wear rate and friction coefficient.
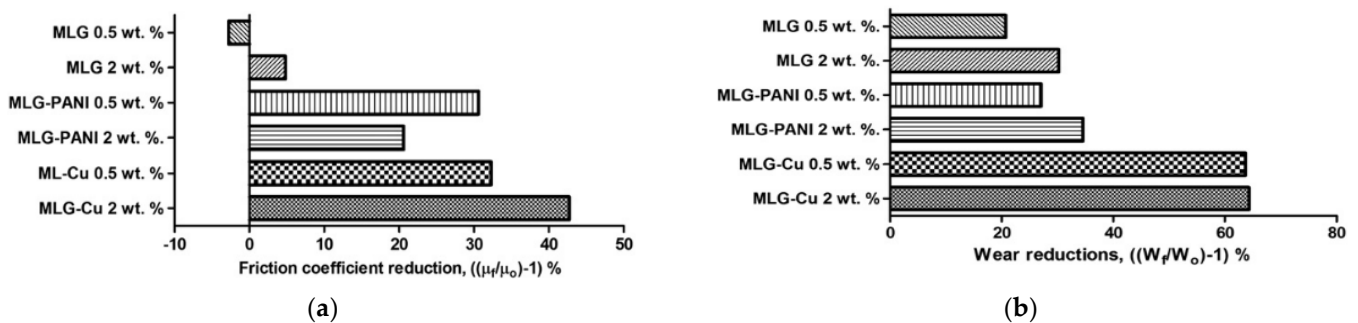

Figure 7. Tribological characteristics of multi-layer graphene engine-based nanolubricant. (**a**) Friction coefficient reduction, (**b**) wear reduction [99]. Adapted with permission.

Chuan. [62] made an intensive study on using reduced graphene oxides (rGO) as nano additives for diesel engine lubricants. The study introduced the reduced graphene oxide doped with lanthanum hydroxide nanoparticles (La (OH)$_3$)/rGO) as a new composite of nano additives. The composite of lanthanum hydroxide/reduced graphene oxide showed a substantial tribological performance under different conditions of load and working temperatures, as shown in Figure 8a.

The study proposed that this type of nanocomposite can be decomposed under high contact pressures, to form a tiny lamellar that can enter the contact interface and generate tribo-films, as shown in Figure 8b. Guangneng [35] showed that the coefficient of friction and wear had been reduced by 26.2% and 41.9%, respectively, for MoS$_2$ nanolubricants. Many studies regarding nanolubrication in engines, for both fully formulated and base lubricants, are mentioned in Table 2. Besides the tribo-sintering mechanism, other lubrication mechanisms were contributed to nanolubricants in many studies. These are mending, polishing, and rolling mechanisms. In the rolling mechanism, the spherical nanoparticles' surface morphology allows them to act as nano ball bearings [34]. The tiny-sized nanoparticles will roll over the surface asperities of the contacted surfaces. In this way, rolling friction is provided and will be a replacement for the sliding friction of the asperities. Despite that, for nanoparticles to act as a ball bearing, their size must be greater than the average surface roughness of the paired surfaces, so they can roll among the surface asperities [101].

Table 2. A summary of the tribological properties for engine-based nanolubricants.

Base Lubricant	Nano Additive	Reduction in COF %	Tribological Configuration	Testing Load/Speed	Testing Temperature °C	Concentration wt.%	Effective Concentration wt.%	Reference	Year
SAE-40	ZnO MoS$_2$	5 16	Pin-on-Disc	20–75 N 150 rpm	Ambient Temperature	0.1, 0.4, 0.7	0.4 0.7	[102]	2021
SAE-30	Graphite	91.6	Pin-on-Disc	20–50 N 300 rpm	Ambient Temperature	0.3	0.3	[59]	2021
SAE-40	SiO$_2$	18.46	Pin-on-Disc	120–180 N 120 rpm	Ambient Temperature	0.1–1 vol.%	0.1 vol.%	[58]	2021
Base as lubricant—Group III	ZrO$_2$	11	Ball-on-Disc	50–100 N 50 Hz	100	0.1–0.6	0.4	[103]	2021
SAE 20 W-50	hBN	20.5	Four-ball Tribometer	392.5 N 1200 rpm	75	0.025 vol.%	0.025 vol.%	[104]	2021
Base as lubricant—Group III	ZnO	7.8	Cylinder-on-flat	500–530 Mpa 300 rpm	100	0.33	0.33	[15]	2021
SAE 20W-50	Boron nitride (BN) Tungsten disulphide (WS2) Graphene (Gr)	56 37 2.5	Ball-on-Disc	40–100 N 150 rpm	Ambient Temperature	0.5	0.5	[26]	2020
SAE 10W-40	Gr-MS-Zn	37	Four-ball Tribometer	392.5 N 1200 rpm	75	0.025–0.1	0.05	[60]	2020
SAE 20W-50	Nano-lanthanum hydroxide/reduced graphene oxide (LaOH3/rGO)	16.7	Ball-on-Disc	1.96–5.88 N 0.1 m/s	40–80	0.05, 0.1	0.1	[62]	2020
SAE 10W-30	Hairy silica particles (HSP)	15	Ball-on-Three-plate testing module	2 N 0.05 m/s	25–100	0.1, 0.3, 0.5, 1	0.3	[105]	2020
SAE 10W-40	ZnO/MWCNT	32	Ball-on-Disc	35–55 N 5–15 Hz	Ambient Temperature	0.25, 0.50, 0.75, and 1	0.25	[30]	2020
SAE 40	ZnO MoS$_2$	5.9 12	Pin-on-disc	75 N 150 rpm	Ambient Temperature	0.1, 0.4, and 0.7	0.4 0.7	[61]	2020
Base as lubricant—Paroline oil	MoS$_2$	64	Ball-on-disc	6 N 1.5 Hz	Ambient Temperature	0.1, 0.2, 0.3 and 0.5	0.3	[35]	2020
Base as lubricant—Ionic liquid	Gr	40	Pin-on-disc	0.5 N 0.01 m/s	Ambient Temperature	0.5	0.5	[106]	2020
Diesel oil	ZnO	5.86	Pin-on-disc	75 N	Ambient Temperature	0.1, 0.4, 0.7	0.4	[31]	2020
Base as lubricant—PAO 40	CuO	24	Ball-on-disc	10 N 0.01 m/s	50	0.5	0.5	[32]	2020
SAE 5W-30	Gr	40	Ball-on-Plate	10–50 N 3 mm/s	Ambient Temperature	0.01, 0.05, 0.1	0.1	[65]	2019
SAE 5W-30	Cu/Gr	26–32	Piston Ring/Cylinder Liner	90–368 N 0.154–0.6 m/s	100	0.03, 0.2, 0.4, and 0.6	0.4	[63]	2019
SN/GF-5 lubricant	C	32	piston ring/cylinder liner interface	50–400 N 10 Hz	100	1, 3 and 5	3	[107]	2019
SAE 5W-30	Al$_2$O$_3$, TiO$_2$	53	piston ring/cylinder liner interface	250 N 0.5 m/s	Ambient Temperature	0.1	0.1	[68]	2018
SAE 5W-30	Graphene (Gr)	29–35	Piston Ring/Cylinder Liner	90–368 N 0.154–0.6 m/s	70–90	0.03, 0.2, 0.4, 0.6	0.4	[67]	2018

Table 2. *Cont.*

| Base Lubricant	Nano Additive	Reduction in COF %	Tribological Configuration	Testing Load/Speed	Testing Temperature °C	Concentration wt.%	Effective Concentration wt.%	Reference	Year
SAE 10W-30	Copper oxide (CuO)	76	Piston skirt-Liner Contact Tester	2–9 N 200–300 rpm	Ambient Temperature	0.005–0.01	0.008	[108]	2018
SAE 10W-30	TiO_2	86	Pin-on-Disc	40–60 N 1 m/s	Ambient Temperature	0.3, 0.4, 0.5	0.5	[34]	2018
Base as lubricant—SN 500	$Ni-MoS_2$	21	Four-ball Tribometer	392 N 1200 rpm	75	0.1–0.5	0.5	[97]	2018
Base as lubricant—Mineral	Cu	40–60	Four-ball Tribometer, Pin-on-Disc	392 N 1200 rpm	40–100	0.3, 3	0.3	[109]	2018
Base as lubricant—SN 500	Graphene oxide (GrO)	33	Four-ball Tribometer	147 N 1200 rpm	Ambient Temperature	0.04	0.04	[110]	2017
Base as lubricant—Liquid paraffin	MoS_2	12.2–35.3	Ball-on-Disk	30 N 0.036 m/s	Ambient Temperature	1	1	[74]	2017
SAE 5W-30	ND	36	Block-on0ring	30 kg 200 rpm	Ambient Temperature	0.016	0.016	[28]	2017
Base as lubricant—60SN base oil	ZnO	41	Four-ball Tribometer	500 N 1000 rpm	Ambient Temperature	0.2, 0.5, 0.5, 0.8,and 1	0.5	[72]	2017
SAE 5W-30	Al_2O_3, TiO_2	48–50	Piston Ring/Cylinder Liner	30–250 N 50–800 rpm	100	0.05, 0.1, 0.25, 0.5	0.25	[96]	2016
SAE 20W-50	Gr	21	Four-ball Tribometer	400 N 1200 rpm	75	0.01	0.01	[111]	2016
SAE 5W-30	Al_2O_3, TiO_2	51	piston ring/cylinder liner interface	40–230 N 0.5–1.45 m/s	100	0.05, 0.1, 0.25 and 0.5	0.1	[76]	2016
SAE 5 W- 30	Al_2O_3 TiO_2	35 51	piston ring/cylinder liner interface	185–340 0.25–0.66 m/s	60	0.25	0.25	[112]	2016
Chevron Taro 30 DP 40	Cu	18.2	Pin-on-disc	0.1–180 mN 0.02 mm/s	25	0.3 vol.% 3 vol.%	3 vol.%	[113]	2016
Base as lubricant—Mineral	Fe–Carbon capsules	8	Block-on-ring	650 N 1.65 m/s	Ambient Temperature	0.01–0.1	0.07	[114]	2015
SAE 75 W- 85	CuO Al_2O_3	14 -	Four-ball Tribometer	7000 N 500 rpm	Ambient Temperature	0.5, 1 and 2	2 -	[115]	2015
SAE 40	SWCNH	12	Ball-on-disc	600 MPa 0.001–1.8 m/s	25,40,60 and 80	0.005, 0.01 and 0.02	0.01	[84]	2014
SAE 10	CuO Cu Fe Co Fe/Cu Fe/Co Co/Cu	18 49 39 20 53 36 53	Four-ball Tribometer, Pin-on-Disc	150 N 1420 rpm	Ambient Temperature	0.5, 0.25 0.5 0.5 0.5 0.25/0.25 0.25/0.25 0.25/0.25	All concentrations	[116]	2013
Base as lubricant—PAO 10	MoS_2 BN	57 No improvement	Piston Skirt/Cylinder Liner	250 N 2 Hz	20–100	3	3	[91]	2012
SAE 15 W-40	Cu	37	Ball-on-disc	50 N 10–30 Hz	Ambient Temperature	0.0125, 0.025, 0.0375 and 0.05	0.0375	[117]	2011
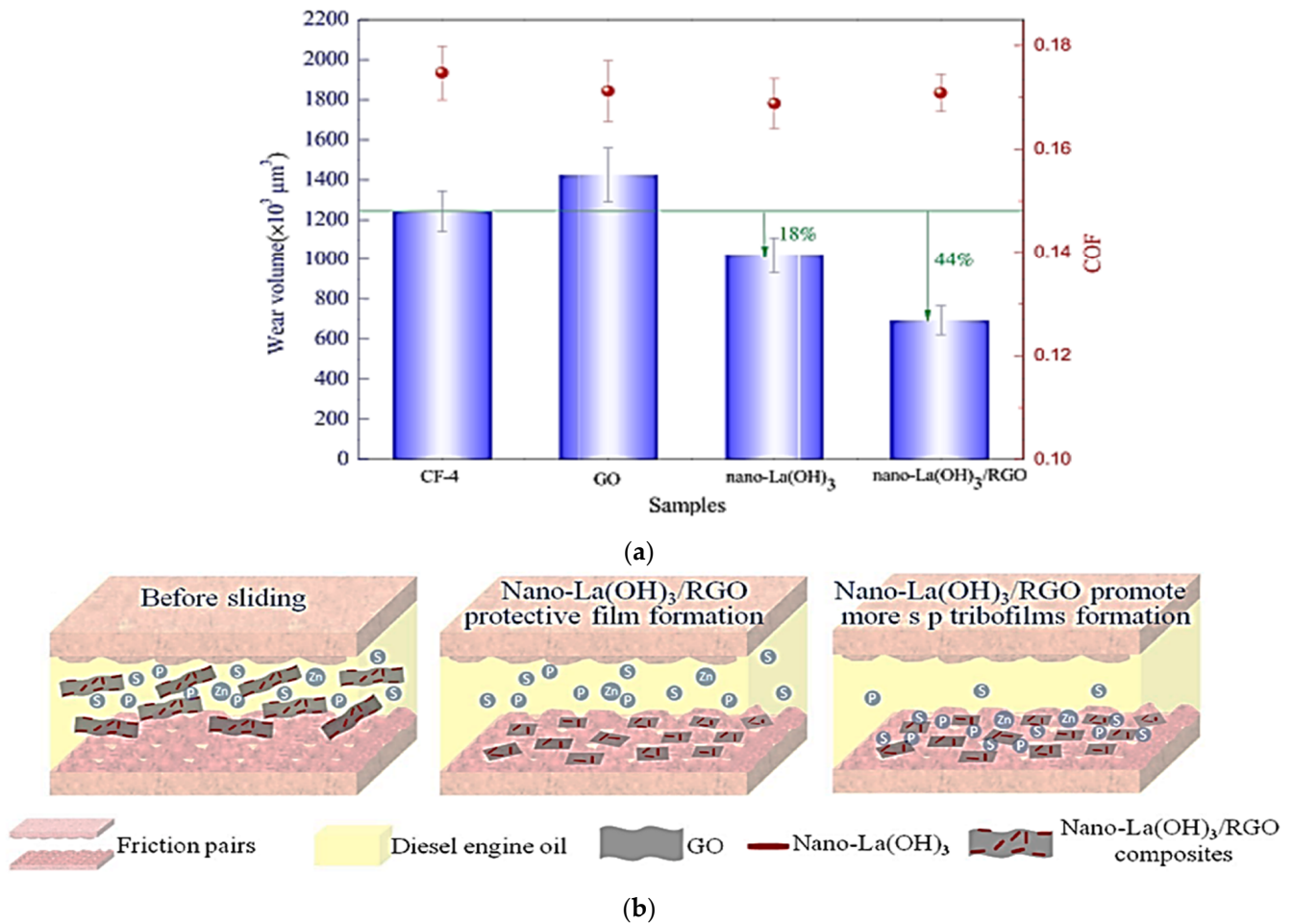
Figure 8. Tribological performance of diesel engine oil with nano-lanthanum hydroxide/reduced graphene oxide composites. (**a**) Reduction in coefficient of friction and wear volume, (**b**) hypothesized wear mechanism of nanolubricant [62]. Adapted with permission.

In the polishing mechanism, nanoparticles reduce the surface roughness of the asperities [118]. This reduces the shear stresses of the asperities, and thus improves the tribological performance [84]. In the mending mechanism, a self-repairing action of the nanoparticles takes place. In this mechanism, the nanoparticles would have the ability to fill out the scars, and tiny grooves resulted from contacting friction on the mating surfaces. Recent studies revealed that the previous hypotheses of both tribo-sintering and mending mechanisms are considered the same [30]. Kamal [63] introduced the tribological properties of hybrid copper/graphene (Cu/Gr) nanoparticles as engine lubricant additives. Under various conditions of normal load and sliding speed, the hybrid nano-lubricant of Cu/Gr showed improvement in tribological properties, with a moderation in the wear rate and coefficient of friction in the ranges of 25–30% and 26–30%, respectively. The consolidation in the tribological properties was referred to as the formation of a tribo-film or the self-lubricating layer of nanoparticles, as shown in Figure 9.
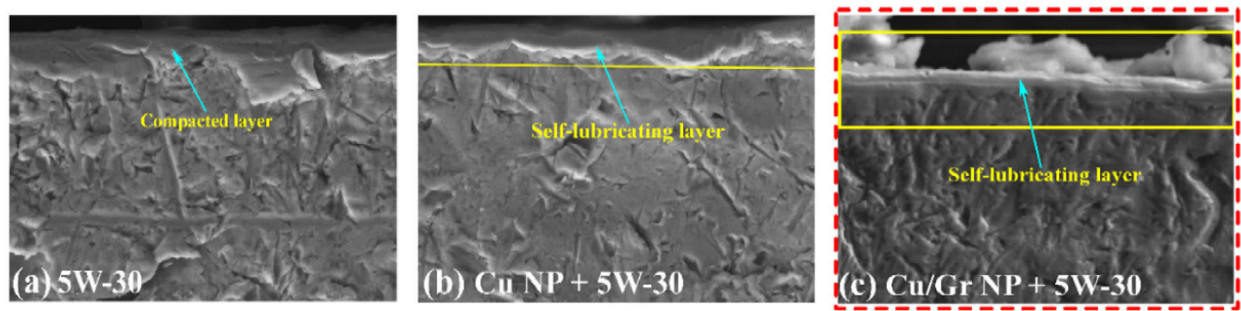
(A)

(B)
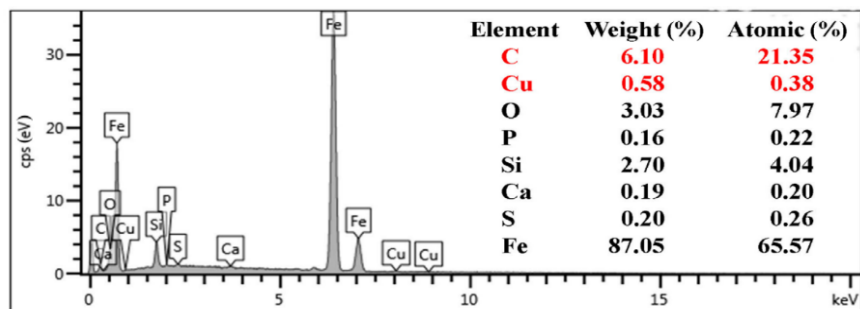
(C)

Figure 9. Tribo-sintering mechanism of Cu/Gr of automobile engine nano-lubricant. (**A**) SEM analysis of the tribo-lubricating layer (**B**,**C**), EDS mapping and spectrum of the tribo-film elements [63]. Adapted with open access permission.

In another study by Ajay [30], friction reduction, by 32%, was introduced through the ZnO/MWCNT hybrid nanolubricant. The synergetic effect of hybrid nanoparticles affords a protective tribo-film during the rubbing process of the surface asperities. In another study regarding hybrid engine-based nanolubricants [24], the ZnO-decorated reduced graphene oxide/Mos2 nanolubricants showed a reduction in COF by 37%. The authors claimed that the enhancement in the friction properties returns to the formation of a protective thin tribo-layer with a low shear strength.

A statistical and analytical multi-scale contact model, based on the Greenwood and Williamson model (GW), was conducted by Ghaednia [119]. This was to investigate the working methodology of CuO and Ag nanolubricants, and their lubrication mechanism of the resulting tribo-films (Figure 10). The study suggested that there is no integrated film of nanoparticles on the contacted surfaces, and it seems that tribo-films are randomly distributed on the surfaces. Moreover, the tribo-film can effectively reduce the real area of contact, thus diminishing the coefficient of friction.
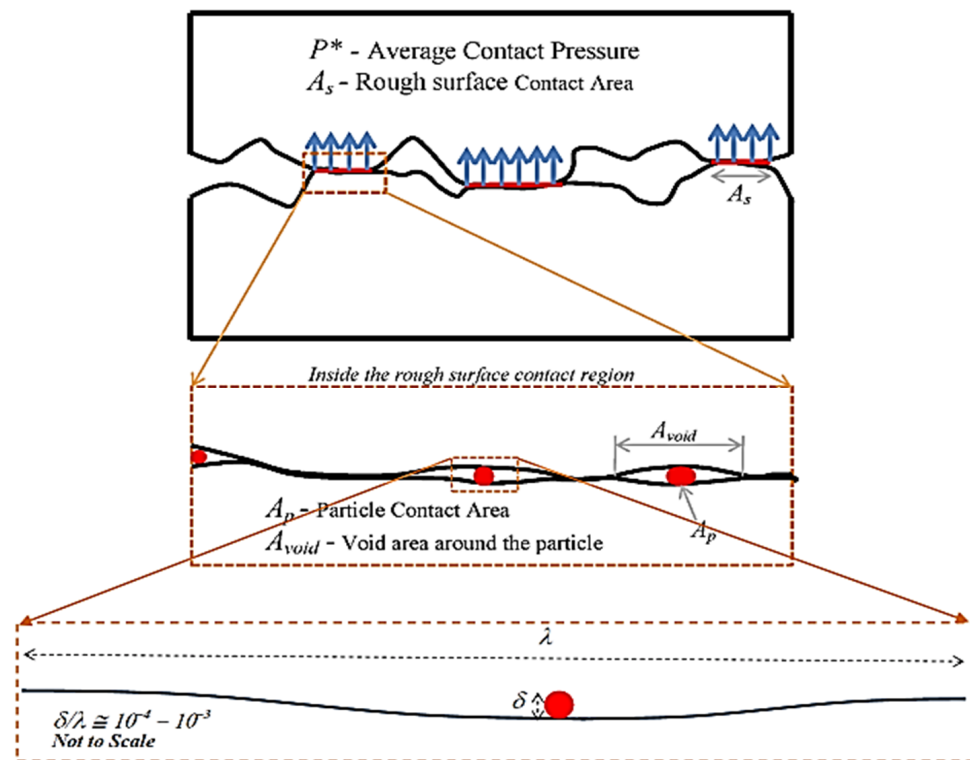
Figure 10. Illustration of the contact model regarding SAE 5W-20 CuO nano-lubricant [119]. Adapted with permission.

A comprehensive study by Pena-Paras [120] was conducted theoretically and experimentally to investigate the effect of the nanoparticle size of TiO_2 on the tribological properties of the polyalphaolefin (PAO) base as a lubricant.

The study was conducted with one level of nanoparticle concentration of 0.05%, under the different surface roughness conditions of 0.3, 0.7, and 1.4 um, respectively.

An atomistic simulation using molecular dynamics was performed as thermotical evidence of the mending and tribo-sintering mechanisms [120]. The concept of the Lennard–Jones method and solid–liquid interactions were utilized through LAMMPS software. The reduction in wear loss (86%) through the experimental test block-on-ring tribometer was justified by simulation studies, as shown in Figure 11. The study suggested that smaller nanoparticles than the average surface roughness of the surface asperities can fill the valleys of those asperities. While nanoparticles that are larger than the average roughness cannot effectively perform this function. Varrla [92] reported an enormous improvement in the graphene (Gr) nanolubricant, with a concentration of 0.025 mg/mL. The friction and wear were reduced by 80% and 33%, respectively. A significant role for this developed performance of the Gr nanolubricant returns to the nanoparticles' nano ball-bearing mechanisms, as had been hypothesized by the study.

In another study, Yuan [80] investigated the tribological properties of fully formulated 10 W-40 engine oil with silver nanoparticle-decorated graphene. Thanks to protective film formation, the COF and wear rate were diminished by 30% and 27%, respectively. Vaitkunaite [121] discussed the correlation between the viscosity of different fully formulated lubricants and the linkage of the tribo-film formation of MoS_2 nanolubricants. The study concluded that lubricant viscosity has a considerable action on the tribochemistry in the contact region. There is a linear relationship between the coverage area of tribo-films and the achieved value of friction coefficient for the lubricants of lower viscosities. However, at higher viscosities, the formation of tribo-films is affected by the low asperity contact.
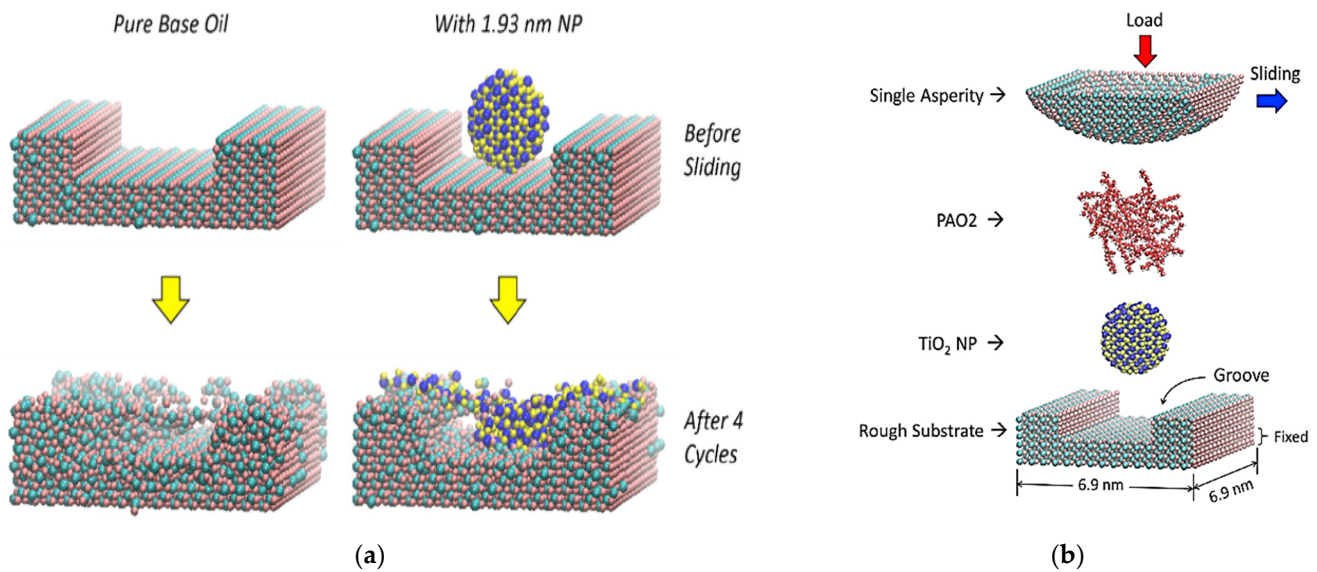
Figure 11. Snapshots of molecular dynamic simulations regarding TiO$_2$ nanolubricant with PAO2 as base oil. (**a**) Illustration of tribo-film mechanism with the addition of nano additives. (**b**) Components of the simulation model [120]. Adapted with permission.

Demas [69] concluded that at very high concentrations of TiO$_2$ and Al$_2$O$_3$ nanoparticles of 1 wt.%, nanolubricants showed a fading effect on the tribological performance compared to the bare fully formulated lubricants. The fully formulated lubricant of 5W-30 gives a coefficient of friction that is 25% lower than the nanolubricant base of PAO. ZnO nanolubricants were evaluated using a four-ball tribometer [78]. A reduction in the coefficient of friction and wear rate were observed, by 9.9% and 31.2%, respectively, compared to the lubricant base of PAO. The nanolubricant of ZnO succeeded in forming a tribo-film with adequate coverage alongside the contacted areas of the sliding pairs.

In a recent study by Tóth [103], the formation of a tribo-film had been verified by SEM/EDX analyses. A considerable number of ZrO$_2$ nanoparticles formed a cluster on the surface grooves, as shown in Figure 12. It had been claimed by authors that these clusters were formed due to strong van der Waals attractive forces between the nanoparticles and the contacted metal surface. In this way, nanoparticles can continuously fill wear grooves, resulting in a smoother and refined contact surface. This refined surface can decrease the load pressure, and hence, help to provide a longer lifetime of engine components.
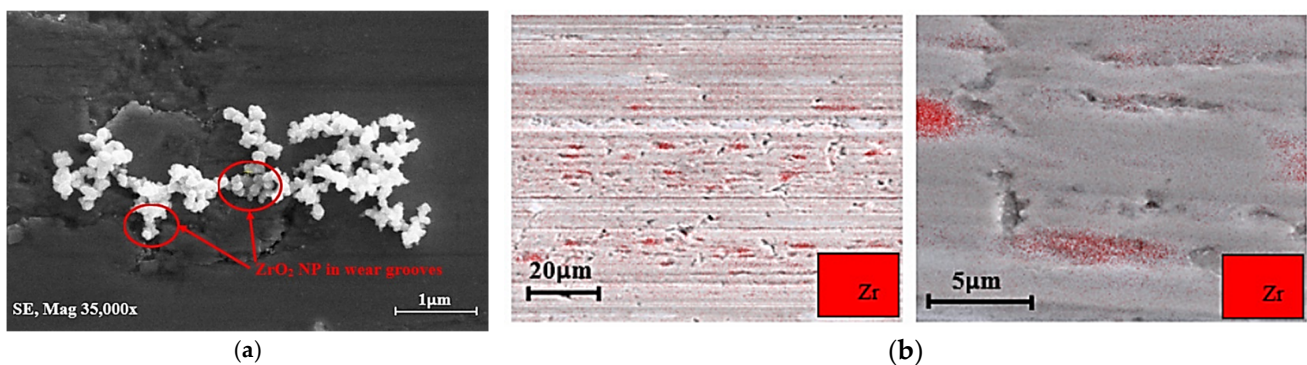

Figure 12. Tribo-sintering mechanism of ZrO$_2$ engine-based nanolubricants. (**a**) SEM analysis, (**b**) EDX anal-ysis [103]. Adapted with open access permission.

4. Rheological and Thermophysical Properties of Engine Lubricant-Based Nanofluids

A significant factor that is necessary during the design process of engine nanolubricants is to estimate these systems' rheological and thermophysical properties. This is to ensure that other specifications, such as tribological properties and overall engine performance, would not be affected. This includes viscosity, density as rheological properties, thermal conductivity, flash point, and pour point as thermophysical properties. This section discusses all these thermophysical and rheological parameters, based on recent studies regarding engine nanolubricants.

4.1. Viscosity

The viscosity of engine lubricant is considered one of the most critical parameters that defines the final behaviour of the lubricant system of an engine. Adding nano additives to these systems would directly affect the viscosity, meaning the pumping power and pressure loss [45,122]. A substantial factor to be considered when studying engine lubricant viscosity is to classify the type of fluid behaviour when nanoparticles are added; this would be whether it is a Newtonian or non-Newtonian behaviour. A fluid is called Newtonian when the shear rate or flow velocity does not affect the fluid's viscosity [123]. In other respects, the viscosity of a non-Newtonian fluid is affected by the shear rate.

Moreover, the viscosity of both the Newtonian and non-Newtonian fluids has a temperature-dependent behaviour [123,124]. Non-Newtonian fluid is classified into two main categories, which are pseudoplastic and dilatant fluids. The viscosity will be diminished under high shear rates for pseudoplastic fluids, so they have a shear-thinning behaviour. Furthermore, for dilatant fluids, the value of viscosity rises with the increasing the shear rate, so they have shear-thickening behaviour [125].

Most commercially available engine lubricants are typically considered a non-Newtonian fluid with shear-thinning behaviour [124]. Engine lubricants are commonly categorized as multigrade oils, such as SAE 10W-40, SAE 10W-60, and SAE 5W-40, as they work under different temperature ranges. The non-Newtonian behaviour of multigrade engine oils had been proposed by the constitutive equation [124], as follows:

$$\eta = \mu_1 \frac{k + \mu_2 \, \dot{\gamma}}{k + \mu_2 \, \dot{\gamma}} \tag{1}$$

where η is the non-Newtonian viscosity, $\dot{\gamma}$ is the shear rate, μ_1 is the first Newtonian viscosity, μ_2 is the second Newtonian viscosity, and k is the curve-fitting parameter. The value of k determines the range of shear rate required for the shear-thinning behaviour of the multigrade engine oil, which takes place between μ_1 and μ_2, as shown in Figure 13. At any specific working temperature and at low values of shear rates, the viscosity of engine lubricant reaches the first Newtonian viscosity μ_1, while at higher values of shear rates, the viscosity reaches the second Newtonian viscosity μ_1. Therefore, a nanolubricant design process for fully formulated engine oils requires a thorough investigation for these three regions of different viscosity behaviours. In many rheological studies regarding engine nanolubricants, Newtonian behaviour was noticed at specific conditions. The rheological properties of the fully formulated nano engine oil 20W-50 were investigated [126]. CuO nanoparticles were added at different concentrations, in the range of 0.2–6 wt.%. The study reported a linear correlation between the shear rate and the shear stress under various conditions of working temperatures (5–70 °C), demonstrating that CuO nanolubricant has a Newtonian behaviour, as shown in Figure 14a.

In another study [127], hybrid nanoparticles of Al_2O_3,/MWCNT were added to the engine oil of SAE 40. Under different working temperature conditions and shear rate ranges of 25 to 50 °C and 1333 to 131,333 s^{-1}, respectively, the nanolubricant showed no relationship between the shear rate and viscosity under all the testing temperatures. Thus, this hybrid nanolubricant is considered a Newtonian fluid. Other hybrid nanoparticles of MWCNT/MgO were used for SAE 50 engine oil [128]. The rheological properties of engine

nanolubricants were investigated under different particle concentration ranges, from 0.25 to 2 vol.%.
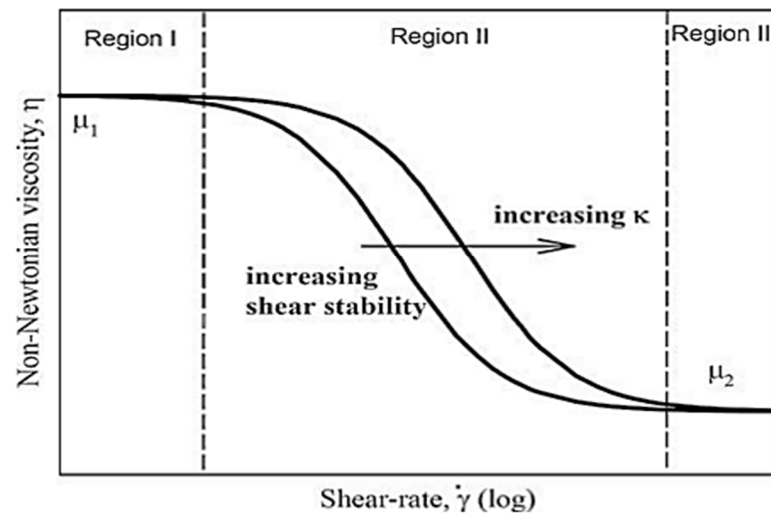

Figure 13. Effect of the shear rate on the non-Newtonian multigrade engine lubricants [124]. Adapted with permission.
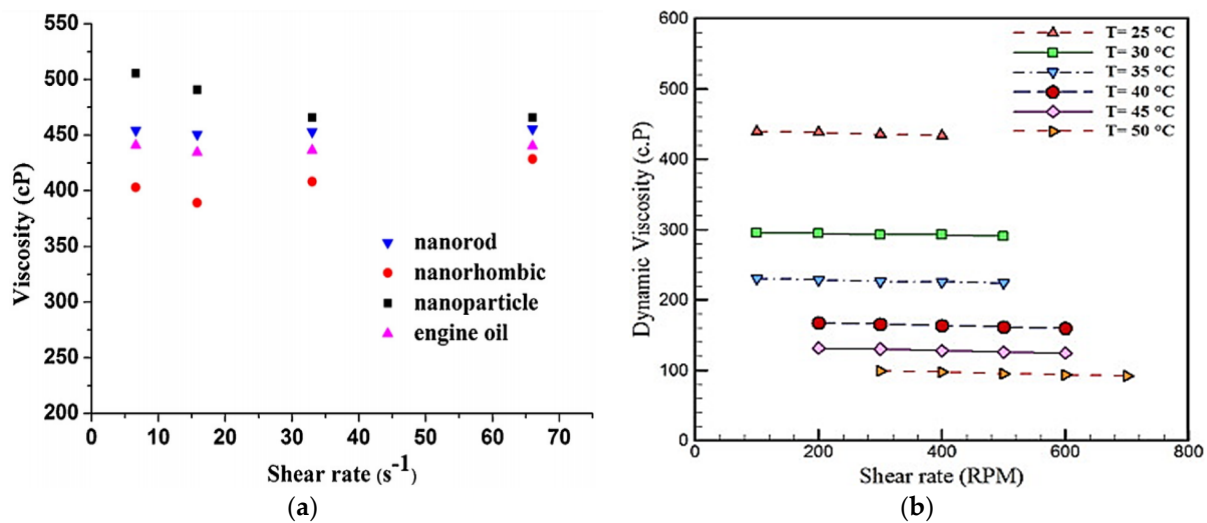

Figure 14. Effect of the shear rate on different types of engine-based nanolubricants. (**a**) CuO nano additives with different mor-phologies added to 20W-50 engine oil [126]. (**b**) MWCNT/MgO engine-based nanolubricant [128]. Adapted with permission.

The study concluded that the prepared nanolubricant has a Newtonian behaviour at the mentioned working conditions, as shown in Figure 14b. Furthermore, the non-Newtonian behaviour of nanolubricants, regarding engine oil, was noticed in many studies. Hybrid nanoparticles of MWCNT/SiO$_2$ were added to the SAE40 engine lubricant [75]. Nanoparticles were added in different concentrations, in the range from 0.625 to 2 vol.%. The experiments were conducted under a shear rate range from 100 to 500 rpm, with a working temperature range of 25 to 50 °C. The study disclosed that the nanolubricant has two different viscosity behaviours; up to 1 vol.%, Newtonian behaviour was observed. However, non-Newtonian behaviour was remarked at concentrations higher than 1 vol.%, as shown in Figure 15. Many studies regarding nanolubrication in engines for different viscosity behaviours are illustrated in Table 3.
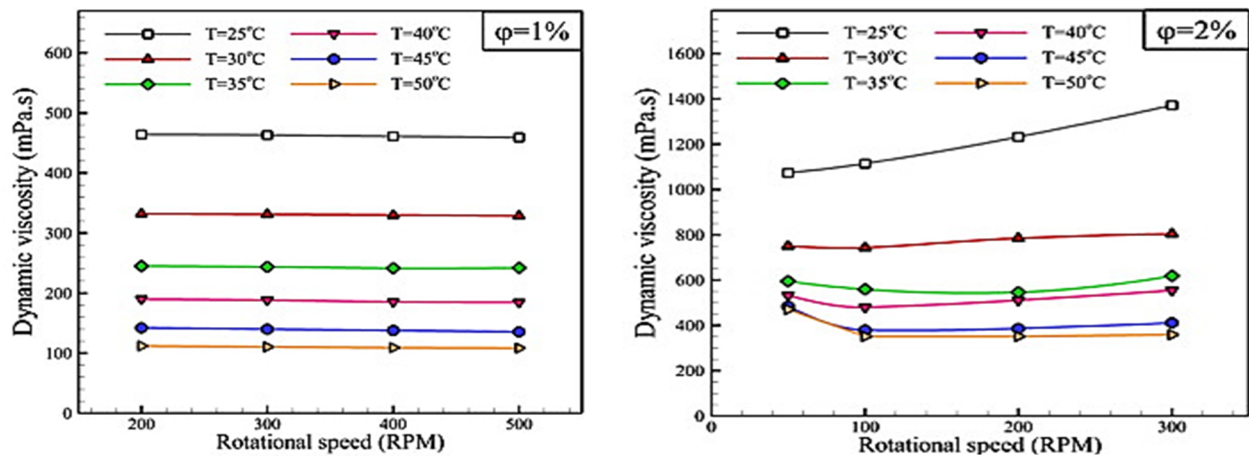
Figure 15. Effect of the volumetric percentage of MWCNT/SiO$_2$ nano additive on the final viscosity behaviour of an engine oil [75]. Adapted with permission.

Other factors that would affect the engine nanolubricant's viscosity are the working temperatures and added nanoparticles concentration. Hojjat [89] studied the kinematic viscosity of the MWCNT nanolubricant at different conditions. The nanoparticles were added to the base engine lubricant of 20W-50, under different concentrations of 0.1, 0.2, and 0.5 wt.%, and testing temperatures of 40 and 100 °C. At a temperature of 100 °C and a concentration of 0.1 wt.%, the viscosity of the nanolubricant met its maximum decrease, by 0.25%, while the maximum rise of 1.7% occurred at the concentration of 0.5 wt.% and the temperature of 40 °C. The study proposed that the low concentration of nanoparticles would ease the sliding of the lubricant layers by going through the fluid layers; thus, diminishing the values of viscosity. Whereas at high concentrations, the nanoparticles would aggregate, thus increasing the viscosity. In another study [129], the hybrid nanolubricant of MWCNT/ZnO showed an impressive performance regarding the viscosity index of 5W-50 engine lubricant. At a concentration of 0.75 vol.% and a high operating temperature of 55 °C, the degree of viscosity dependence on temperature decreased. Therefore, a high viscosity index is obtained. Hemmat [75] discussed the effect of adding hybrid MWCNT/ SiO$_2$ to SAE 40 engine lubricant. The study revealed that the dynamic viscosity of nanolubricant decreases with increasing the working temperature.

Table 3. A summary of the published literature of the viscosity behaviour for engine-based nano lubricants.

Base Lubricant	Nano Additive	Testing Temperature °C	Testing Shear Rate	Concentration	Viscosity Behaviour	Reference	Year
SAE 5W-30	MgO	5–55	666.5–13, 330 s^{-1}	0.1–1.5 vol.%	non-Newtonian	[33]	2020
SAE 50	ZnO	25–65	5–55 s^{-1}	0.125–1.5 vol.%	Newtonian	[130]	2020
SAE 10W-40	ZnO, MgO	5–75	5–1000 rpm	0.125–1.5 vol.%	Newtonian for both nanolubricants	[131]	2019
Engine lubricant 20W-50	MWCNT/Mg(OH)$_2$	25–60	100–600 rpm	0.125–1.5 vol.%	Newtonian	[132]	2018
	MWCNT/SiO$_2$	40–100	10–70 s^{-1}	0.05–1 vol.%	Newtonian	[133]	2018
SAE 40	MWCNT/MgO	25–45	100–1000 rpm	0.25–2 vol.%	non-Newtonian	[134]	2018
SAE 10W-40	ZrO$_2$/MWCNT	5–55	666.66–11, 999.97 s^{-1}	0.05–1 vol.%	non-Newtonian	[135]	2018
SAE 10W-40	MWCNT/SiO$_2$	5–55	666.5–11, 997 s^{-1}	0.05–1 vol.%	non-Newtonian	[136]	2017
SAE 10W-40	ZnO	5–55	666.5 and 11, 997 s^{-1}	0.25–2 vol.%	Newtonian	[51]	2017
SAE 50	TiO$_2$	25–50	666.5–9331 s^{-1}	0.125–1.5 vol.%	Newtonian/non-Newtonian	[137]	2017
Engine lubricant	Cu	40–100	5–40 s^{-1}	0.2–1 wt.%	Newtonian/non-Newtonian	[138]	2017
SAE 50	MWCNT/MgO	20–50	670–8700 s^{-1}	0.0625–1 vol.%	non-Newtonian	[139]	2017
SAE 40	MWCNT/ZnO	25–60	1333–13,333 rpm	0.05–1 vol.%	Newtonian	[140]	2017
SAE 40	MWCNT/SiO$_2$	25–50	100–500 rpm	0.625–2 vol.%	Newtonian/non-Newtonian	[75]	2016
SAE 40	Al$_2$O$_3$/MWCNT	25–50	1333–13, 333 s^{-1}	0.0625–1 vol.%	Newtonian	[127]	2016
SAE 40	MWCNT/SiO$_2$	25–60	667–6667 s^{-1}	0.0625–1 vol.%	Newtonian	[141]	2016
SAE 10W-40	MWCNT/ZnO	5–55	5–1000 rpm	0.125–1 vol.%	Newtonian	[77]	2016
SAE 50	MWCNT/MgO	25–50	100–700 rpm	0.25–2	Newtonian	[128]	2016
SAE 20W-50	CuO	5–70	10–70 s^{-1}	0.2–6 wt.%	Newtonian	[126]	2015

The maximum decrease in viscosity is 30.2% at the temperature and nano concentration of 40 °C and 1 vol.%, respectively. Moghaddam [73] investigated the viscosity improvement of hybrid MWCNT/CuO engine nanolubricant. The viscosity of the nanolubricant increased by 29.47% at a concentration of 1 vol.% compared to the SAE 40 base lubricant. Ali [53] studied different nano additives of Al_2O_3, TiO_2, and hybrid Al_2O_3/TiO_2 added to 5W-30 engine lubricant. The nanolubricants were tested under one concentration of 0.25 wt.%, and two different working temperatures of 40 and 100 °C. At 40 °C, a reduction in viscosity was noticed, by 3%, 3.7%, and 4.3% for Al_2O_3, TiO_2, and Al_2O_3/TiO_2, respectively. While, at 100 °C, a reduction in viscosity was noticed by 2% for all nanolubricants. MWCNT was added to the engine lubricant in a concentration that ranges from 0.01 to 0.2 wt.% [142]. The results showed that the maximum increase in viscosity was 14.11% at 0.2 wt.%

Four different types of nanoparticles, including MWCNT, graphene nanosheets (G), carbon nanoballs (CNBs), and fullerene nanoparticles, were added to 20W-50 engine lubricant [90]. The study revealed that the viscosity of nanolubricant is a function only in the nano concentration. All of the lubricants showed no appreciable changes in the values of viscosities in contrast to the base lubricant. Many studies regarding the viscosity enhancement of engine nanolubricants are illustrated in Table 4.

Table 4. A summary of the published literature of the viscosity improvement for engine-based nanolubricants.

Base Lubricant	Nano Additive	Testing Temperature °C	Concentration	Effective Concentration	Most Viscosity Refinement	Reference	Year
SAE 40	ZnO and MoS$_2$	40–100	0.1–0.7 wt.%	0.7 wt.%	Increase by 9.57%/MOS$_2$, 10.12%/ZnO, at 100 °C	[102]	2021
SAE 20W-40	SiO$_2$	50–90	0.3–1.5 wt.%	0.3 wt.%	Increase by 99%, at 90 °C	[143]	2021
SAE 50	ZnO	25–65	0.125–1.5 vol.%	1.5 vol.%	Increase by 25.3%	[130]	2020
SAE 40	ZnO and MoS$_2$	40–100	0.1–0.7 wt.%	0.7 wt.%	Increase by 9.58%/MOS$_2$, 10.14%/ZnO, at 100 °C	[61]	2020
SAE 5W-30	MgO	5–55	0.1–1.5 vol.%	1.5 vol.%	Increase by 25% at 15 °C	[33]	2020
Engine lubricant	MgO and ZnO	5–55	0.125–1 vol.%	1.5 vol.% for both nanolubricants	Increase by 124.3%/ZnO, 75%/MgO, at 55 °C	[131]	2019
SAE 10W-40	MWCNT/ZrO$_2$	5–55	0.05–1 vol.%	1 vol.%	Increase by 31% at 55 °C	[135]	2018
Engine lubricant	MWCNT/Mg	25–60	0.25–2 vol%	2 vol%	Increase by 60% at 60 °C	[132]	2018
SAE 20W-50	°C MWCNT/SiO$_2$	40–100	0.05–1 vol.%	1 vol.%	Increase by 171% at 100 °C	[133]	2018
Engine lubricant	Cu	4–100	0.2–1 wt.%	1 wt.%	Increase by 37% at 40 °C	[138]	2017
SAE 50	MWCNT/MgO	25–50	0.0625–1 vol.%	1 vol.%	Decrease by 75% at 50 °C	[139]	2017
SAE 40	MWCNT/CuO	25–50	0.0625–1 vol.%	1 vol.%	Increase by 29.47% at 30 °C	[73]	2017
SAE 40	MWCNT/ZnO	25–60	0.05–1 vol.%	1 vol%	Increase by 33.3% at 40 °C	[140]	2017
SAE 40	Al$_2$O$_3$/MWCNT	25–50	0.0625–1 vol.%	1 vol.%	Increase by 46% at 35 °C	[127]	2016
SAE 50	MWCNT/MgO	25–50	0.25–2 vol.%	2 vol.%	Increase by 65% at 40 °C	[128]	2016
SAE 40	MWCNT/SiO$_2$	25–60	0.0625–1 vol.%	1 vol.%	Increase by 37.4% at 60 °C	[141]	2016
SAE 40	MWCNT/SiO2	25–50	0.0625–2 vol.%	0.5 vol.%	Increase by 1.7% at 40 °C	[75]	2016
SAE 10W-40	MWCNT/ZnO	5–55	0.125–1 vol.%	1 vol.%	Increase by 55% at 55 °C	[77]	2016

Prediction Models for the Viscosity

According to many studies regarding nanolubricants in engines [47], the classical models of colloidal systems could not predict the rheological and thermophysical properties under different conditions of temperatures and concentrations. The issue with these models is their concentration and temperature limit, at which the prediction can be proposed with relevant and accurate results. For viscosity prediction, the classical model of Einstein and Brinkman [144] is applicable only for extremely diluted colloidal systems of spherical particles, as follows:

$$\mu_{eff} = \mu_{bf}(1 + 2.5\ \varphi) \tag{2}$$

where μ_{eff} is the effective nanofluid viscosity, μ_{bf} is the viscosity of the base fluid, and φ is the solid volume fraction of the nanoparticles. Recent studies have developed many correlations concerning many factors of engine nanolubricants, including the type of nanoparticles, concentration, and working temperature range [122,130,145]. Hemmat [146]

proposed a new correlation model for the hybrid Al_2O_3/MWCNT engine nanolubricant of 5W-50, as presented in Equation (3), where μ_{nf} is the viscosity of the nanofluid.

$$\mu_{nf} = -744.8 + \frac{1806 \; \varphi \; 0.01386}{T^{0.2}} \tag{3}$$

The model is applicable only for predicting the dynamic viscosity of Al_2O_3/MWCNT, with a concentration range of 0.05 to 1 vol.%, and temperatures between 5 and 55 °C, with high accuracy results regarding the R-squared value (R2) 99.23% compared to the experimental testing. In another study by Asadi [77], a correlation model is proposed for the engine nanolubricant of MWCNT/ZnO with 0.9803 of R2, as follows:

$$\mu_{nf} = 796.8 + 76.26 \; \varphi + 12.88 \; T + 0.7695 \; \varphi \; T + \frac{-196.9 \; T - 16.53 \; \varphi \; T}{T^{0.5}} \tag{4}$$

The model is valid under the nanoparticle concentration of 0.125–1 vol.% and a temperature range from 5 °C to 55 °C. Many studies regarding the viscosity prediction models proposed for engine nanolubricants are illustrated in Table 5. All of the proposed correlations are valid only for the tested ranges of nano concentrations, temperatures, and other tested factors.

Table 5. A summary of the proposed models to estimate the viscosity of engine-based nanolubricants.

Reference	Year	Base Lubricant	Nano Additive	Proposed Model	Accuracy of the Model
[129]	2018	SAE 5W-50	MWCNT/ZnO	$\frac{\mu_{nf}}{\mu_{bf}} = 0.866 \quad + 0.802\varphi + 8.38(10^{-3} * T)$ $- (7.86 * 10^{-6} * \dot{\gamma})$ $- (5.83 * 10^{-4} * \varphi * T)$ $- (6.26 * 10^{-7} * T * \dot{\gamma}) - (1.081 * \varphi^2)$ $- (2.44 * 10^{-4} * T^2)$ $+ (2.83 * 10^{-9} * \dot{\gamma}^2)$ $+ (1.26 * 10^{-8} * T^2 * \dot{\gamma}) + (0.572 * \varphi^3)$ $+ (1.63 * 10^{-6} * T^3)$	R2 = 0.9715
[133]	2018	SAE 20W-50	MWCNT/SiO$_2$	$\frac{\mu_{nf}}{\mu_{bf}} = 0.09422 - [(\frac{T}{\varphi})^2 +$ $0.100556 \; T^{0.8827} \varphi^{0.3148}] \exp(72,474.75\varphi^{3.7951})$	Margin of deviation < 1%
[140]	2017	SAE 40	MWCNT/ZnO	$\frac{\mu_{nf}}{\mu_{bf}} = A + B \; \varphi + C\varphi^2 + D\varphi^3$	Maximum error = 2%
[147]	2017	SAE 10W-40	TiO$_2$/MWCNT	$\frac{\mu_{nf}}{\mu_{bf}} = a_0 + a_1 \; \varphi + a_2\varphi^2 + a_3\varphi^3$	Margin of deviation = 1.1%
[51]	2017	SAE 10W-40	ZnO	$\frac{\mu_{nf}}{\mu_{bf}} = a_0 + a_1 \; \varphi + a_2\varphi^2 + a_3 \; \varphi \; \ln(\varphi)$	Margin of deviation < 1%
[73]	2017	SAE 40	MWCNT/CuO	$\frac{\mu_{nf}}{\mu_{bf}} = a_0 + a_1 \; \varphi \; \exp(\varphi) + a_2\varphi^2 + a_3\varphi^3$	-
[128]	2016	SAE 50	MWCNT/MgO	$\mu_{nf} = 328,201 \times T^{-2.053} \times \varphi^{0.09359}$	Maximum error = 8%
[148]	2016	SAE 40	MWCNT/SiO$_2$	$\frac{\mu_{nf}}{\mu_{bf}} = 0.00337 + \exp(0.07731 \; \varphi^{1.452})$	Margin of deviation = 4%
[75]	2016	SAE 40	MWCNT/SiO$_2$	$\frac{\mu_{nf}}{\mu_{bf}} = a_0 + a_1 \; \varphi + a_2\varphi^2 + a_3\varphi^3$	Margin of deviation = 1.2%
[127]	2016	SAE 40	Al_2O_3/MWCNT	$\frac{\mu_{nf}}{\mu_{bf}} = 1.123 \quad + 0.3251 \; \varphi - 0.08994 \; T + 0.002552 \; T^2$ $- 0.00002386 * T^3 + 0.9695(\frac{T}{\varphi})^{0.01719}$	Margin of deviation = 2%

4.2. Heat Transfer Performance

Internal combustion engines can only operate at specific temperature ranges that can exceed 250 °C at the contact of the piston ring/cylinder liner [25]. Engine lubricant enhances the lubricity of the internal parts and has a significant role in the engine heat sink system, including the cooling system of the water pump, radiator, and hoses [149]. The thermophysical properties of engine lubricant are vital to be studied when nano additives are added. These properties include thermal conductivity, flash point, and pour point. The thermal conductivity of engine lubricant measures the rate of heat transfer from the engine. The larger the thermal conductivity, the more efficiently the engine lubricant will transfer heat [150,151]. The engine lubricant's pour point is the minimum temperature at which the lubricant can sufficiently flow without any agglomeration.

In contrast, the flash point is the minimum temperature at which the lubricant is converted, under pressufre, to steam, creating a flammable mixture that can be ignited during the engine's working. The pour and flash points of engine lubricants are considered the minimum and maximum allowable lubricant operating temperatures [61,124]. Therefore, the improvement in the thermal behaviour of engines using nano lubricants is considered pivotal regarding thermal losses and fuel economy.

4.2.1. Flash Point and Pour Point

Mousavi [61] studied the flash point and pour point for the nanolubricants of ZnO and MoS$_2$, as shown in Figure 16. Both of the nanoparticles were added to the SAE-40 engine lubricant, with three different concentrations of 0.1, 0.4, and 0.7 wt.%. According to the study, the effective concentration for the flash point improvement is at 0.7 wt.% for both of the nanolubricants, with a maximum increase in the flash point by 5.01% and 5.88% for ZnO and MoS$_2$, respectively. This was clarified by the high values of these nanolubricants' thermal conductivity. Whereas the optimum concentration regarding pour point enhancement was achieved at 0.4 wt.% with both of the nanolubricants. The maximum decrease in the pour point was 5.05% and 15.2% for MoS$_2$ and ZnO, respectively.
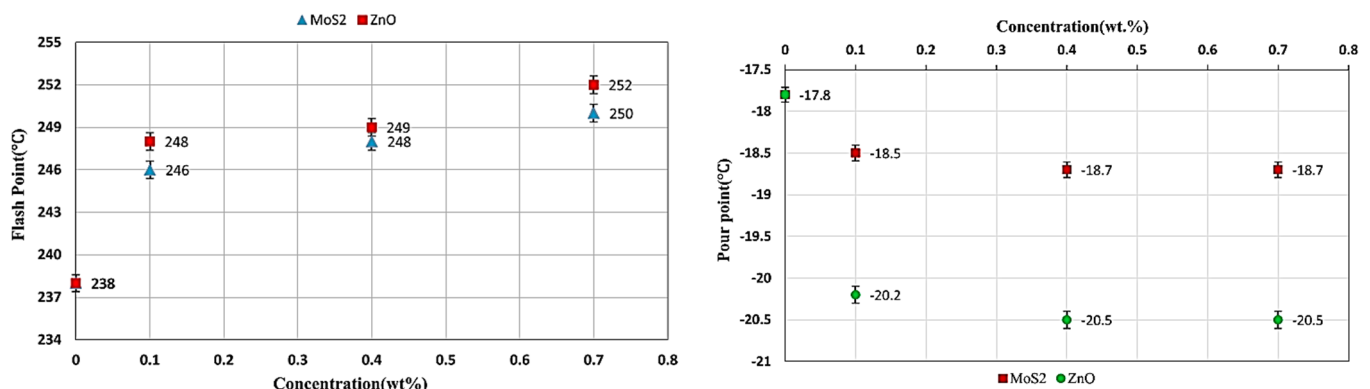
Figure 16. Flash and pour point of MoS$_2$ and ZnO engine–based nanolubricants [61]. Adapted with open access permission.

The flash and pour points of the MWCNT nano engine lubricant of 20W-50 were investigated by Ettefaghi [89]. Nanoparticles were added at three different concentrations of 0.1, 0.2, and 0.5 wt.%. The flash point and pour point had been improved by 13% and 3.3%, respectively, at an optimum concentration of 0.2 wt.%. In another study by Ehsan [90], four different nanoparticles were investigated for the thermophysical properties regarding flash and pour points. MWCNT, graphene, carbon nano balls, and fullerene nanoparticles were added to SAE 20 W-50 engine lubricant at the following two different concentrations: 0.1 and 0.2 wt.%. The study revealed that the greatest improvement in flash point was 13.8%, through the nanolubricant of carbon nano balls at a concentration of 0.2 wt.%. On the other hand, the maximum enhancement in pour point was 11%, through the nanolubricant of graphene at 0.2 wt.%.

In another study by Neha [152], the flash and fire points of SAE 20W-40 had been improved by 12.73% and 12.20%, respectively, for 0.2 wt.% of TiO$_2$ nano additives.

4.2.2. Thermal Conductivity

Many studies regarding engine nanolubricant thermal conductivity pointed to a considerable development in these systems' thermal conductivity, especially at high working temperatures and nano concentrations [53,151,153]. Researchers attributed this thermophysical improvement to the migration of nanoparticles under the base fluid's high vibrational energy. As the nanolubricant temperature increases, the energy level, vibration, and movement of the base fluid layers increase. This, in turn, weakens the bonds of molecules between the lubricant layers. Thus, it will assist the base fluid molecules to receive high

velocity, high striking, and collision rate of solid nanoparticles. Moreover, this causes the Brownian motion of the solid nanoparticles. This phenomenon is called the thermophoresis of nanofluids. The thermal conductivity of nanofluids is enhanced by the movement and migration of nanoparticles at high rates, from the warm to cold areas of the suspension system of the nanofluid suspension system [53,154–156].

Aberoumand [138] studied the effect of adding copper nanoparticles on the engine lubricant thermal conductivity. Nanoparticles were added at three different volume fractions, 0.2, 0.5 and 1%, with testing temperatures of 40 and 100 °C. The maximum improvement in the thermal conductivity was 49%, obtained at 1 vol.% and 100 °C. Yang [151] performed an experimental study on the engine lubricant of SAE 50 when ZnO nano additives were added at different volume fractions, from 0.125% to 1.5% in the temperature range from 25 to 55 °C. The maximum enhancement in the thermal conductivity was 8.74% at 1.5% and 55 °C, as shown in Figure 17a. The thermal conductivity of SAE 20W-50 also improved by 22.7% when MWCNT was added at 0.5 wt.% [89]. Amin [132] investigated the thermal conductivity of the hybrid $Mg(OH)_2$/MWCNT engine lubricant of SN 5W-50. Six different concentrations of nanoparticles, of 0.2, 0.75, 1, 1.5, and 2 vol.%, were studied, with a temperature range from 25 to 60 °C. The maximum enhancement in thermal conductivity improvement was 30.5% at 2 vol.% and 60 °C, as shown in Figure 17b. In another experimental work [53], thermal conductivity was improved by 10.3% for the hybrid Al_2O_3/TiO_2 engine nanolubricant of SAE 5W-30. A summary of recent studies on the thermal conductivity of engine lubricant-based nanofluids is presented in Table 6.
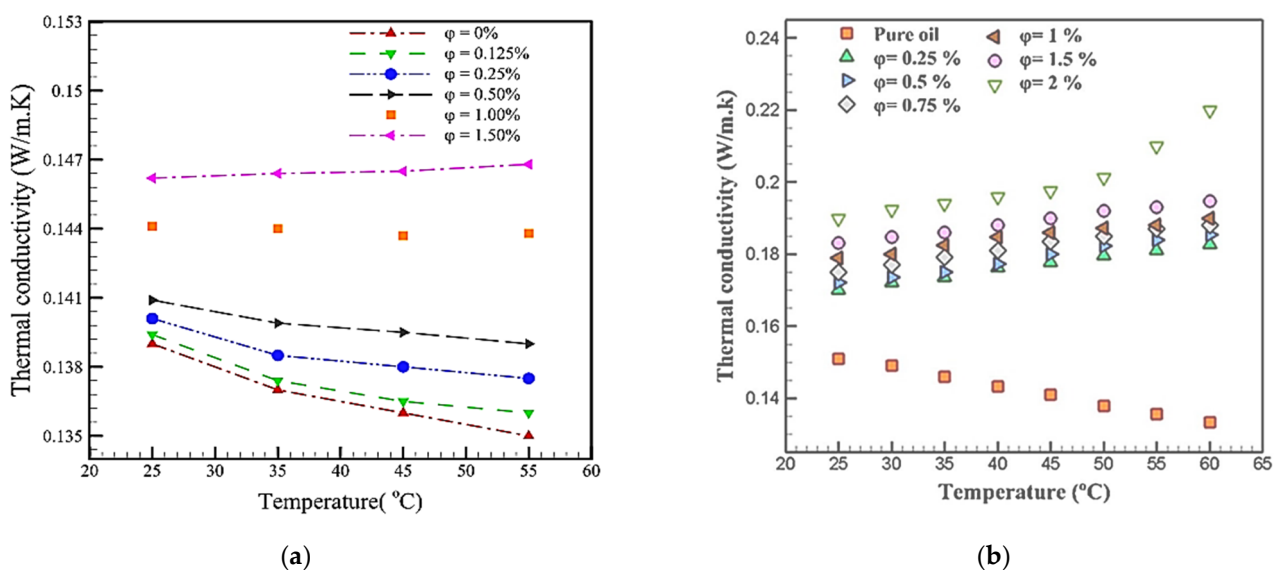

Figure 17. Thermal conductivity improvement of engine-based nanolubricants and different concentrations and temperatures. (**a**) ZnO nanolubricant paper [151], (**b**) hybrid nanolubricant of $Mg(OH)_2$/MWCNT [132]. Adapted with permission.

Table 6. A summary of the literature on the thermal conductivity of engine-based nanolubricants.

Base Lubricant	Nano Additive	Testing Temperature °C	Concentration	Effective Concentration	Improvement in Thermal Conductivity	Reference	Year
SAE 20 W-40	MWCNT/TiO$_2$	20–70	0.1–0.8 vol.%	0.8 vol.%	Increase by 24.42% at 70 °C	[57]	2021
SAE 50	ZnO	25–55	0.125–1.5 vol.%	1.5 vol.%	Increase by 8.74% at 55 °C	[151]	2019
Engine oil	ZnO, MgO	15–55	0.125–1.5 vol.%	1.5 vol.% for both nanoparticles	Increase by 28%/ZnO, 32%/MgO, at 55 °C	[131]	2019
Engine oil	Al$_2$O$_3$/MWCNT	25–50	0.125–1.5 vol.%	1.5 vol.%	Increase by 45% at 50 °C	[157]	2018
SAE 10W-40	MWCNT/ZnO	15–55	0.125 0 1 vol.%	1 vol.%	Increase by 40% at 55 °C	[158]	2018
SAE 5 W-50	Mg(OH)$_2$	25–60	0.25–2 vol.%	2 vol.%	Increase by 50% at 60 °C	[132]	2018
SAE 50	MWCNT/MgO	25–50	0.25–2 vol.%	2 vol.%	Increase by 62% at 50 °C	[128]	2016
Engine oil	Cu	40–100	0.2–1 wt.%	1 wt.%	Increase by 37% at 100 °C	[138]	2016
SAE 20W-50	Gr	10–180	0.01 wt.%	0.01 wt.%	Increase by 23% at 80 °C	[111]	2016
SAE 20W-50	CuO	20	0.1–0.5 wt.%	0.1 wt.%	Increase by 3%	[159]	2013

4.2.3. Prediction Models for the Thermal Conductivity

Numerous studies have been conducted to predict the behaviour of nanolubricants, regarding their thermal conductivity enhancement [47,151,160,161]. The empirical model of Maxwell and Hamilton [162] is considered one of the classical models that have been widely used to predict the thermal conductivity of spherical nanosuspensions, as follows:

$$\frac{K_{nf}}{K_{bf}} = \left[\frac{\left(K_p + (n-1)K_{bf} + (n-1)\varphi\left(K_{bf} - K_p\right) \right)}{K_p + (n-1)K_{bf} + \varphi\left(K_p - K_{bf}\right)} \right] \tag{5}$$

where K_{nf}, K_{bf}, K_p are the thermal conductivity of the nanofluid, base fluids, and nanoparticles, respectively. Whereas n is the nanoparticle's shape factor, with n = 3 for spherical nanoparticles. New empirical-based correlations have been proposed to investigate nanofluids' thermal conductivity, as the classic ones have many limitations regarding the nano concentration, size, type of base fluid, and the range of accuracy.

For nano engine lubricants, few numbers of studies proposed empirical-based correlations for certain types of nanolubricants, as shown in Table 7. These correlations are valid only at the tested working conditions and concentrations of nanolubricants.

Table 7. A summary of the proposed models for estimating the thermal conductivity of the engine-based nanolubricants.

Reference	Year	Base Lubricant	Nano Additive	Proposed Model	Accuracy of the Model
[151]	2019	SAE 50	ZnO	$\frac{K_{nf}}{K_{bf}} = (0.0055\,T^{0.632}\varphi^{0.831}) + 0.964$	Margin of deviation < 1%
[157]	2018	Engine oil	MWCNT/ Al$_2$O$_3$	$K_{nf} = 0.1534 + 1.1193\ \varphi + 0.00026\,T$	Maximum error = 2%
[132]	2018	SAE 5W-50	MWCNT/Mg(OH)$_2$	$K_{nf} = 0.159 + 1.1112\ \varphi + 0.003\,T$	Maximum error = 2%
[128]	2016	SAE 50	MWCNT/MgO	$K_{nf} = 0.162 + 0.691\ \varphi + 0.00051\,T$	Maximum error = 3%

5. Fuel Economy and Emissions

As a rule of thumb, upgrading the engine's lubricants can advance the fuel economy and the overall engine's system [163]. A valuable advantage of nanolubricants is their ability to bring down both the fuel consumption and the harmful exhaust emissions of engines.

This returns to the superior tribological and thermal properties of those lubricants, which are typically linked to the improvement of the engine efficiency, in terms of brake thermal efficiency (BTE) and brake-specific fuel consumption (BSFC) [4,68]. Interestingly, nanolubricants can afford a delicate balance between tribology and sustainability, to minimize the environmental effects of carbon footprints and greenhouse gas emissions [2,70,164,165]. In a recent study by Kamal [25], a hybrid nanolubricant of Al$_2$O$_3$/TiO$_2$, with a concentration of 0.1 wt.%, showed an improvement in brake thermal efficiency, in the range of 3.9–8.6%, concerning the base engine lubricant of SAE 20 W-40. The maximum enhancement in the thermal efficiency was observed at higher engine speeds with complete throttle valve

opening, as shown in Figure 18.The effect of Al_2O_3/TiO_2 hybrid nanolubricants on the fuel economy had been considered in another study [68]. The BSFC has been reduced dramatically, by 16–20%, with an economical fuel consumption of 4 L/100 km. The study claimed an upgrade in mechanical efficiency by 1.7–2.5%.
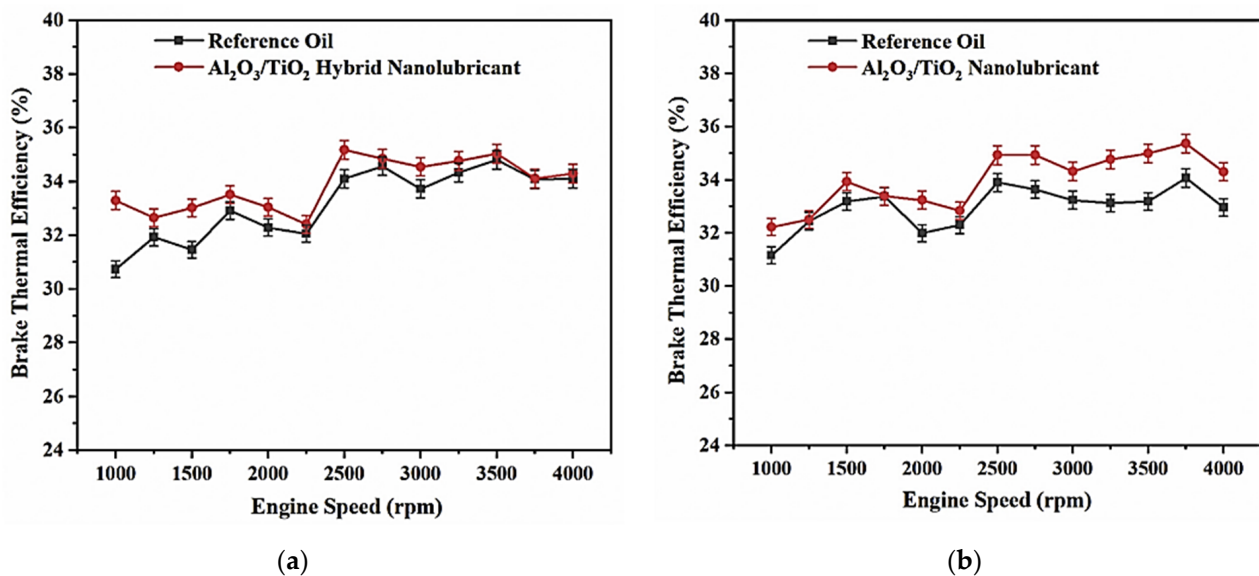

(a)　　　　　　　　　　　　　　　　　　(b)

Figure 18. Improvement in the thermal efficiency 5W-30 engine-based nanolubricant through hybrid Al_2O_3/TiO_2. (**a**) A 75% throttle valve opening, (**b**) 100% throttle valve opening [25]. Adapted with permission.

In another study by Pullela [166], the brake thermal efficiency had been improved by 4–7% when the nanolubricant of Cu nanoparticles was used with a concentration of 0.05, 0.1, and 0.2 wt.%, with respect to the base engine oil.

According to the New European Driving Cycle (NEDC) [67], a graphene nanolubricant with an adequate concentration of 0.4 wt.% was investigated. The results showed an impressive improvement regarding fuel consumption and exhaust emissions as well. The cumulative fuel consumption had been reduced by 17%, due to the improvement in the anti-wear and anti-friction properties (Figure 19I), whereas the results of the exhaust emissions for CO_2, HC, and NO_x showed a reduction of 2.79–5.42%, due to the enhancement in the heat transfer properties and the tribological properties, in terms of the tribo-films formed on the liner surfaces (Figure 19II). The nanolubricants of SiO_2 and Al_2O_3 were investigated under different concentrations of 0.3–0.9 wt.%, with a four-stroke diesel engine attached to a DC dynamometer [167]. The study concluded that SiO_2 nano additives decayed the engine's performance in terms of all concentrations compared to the plain engine oil of SAE 15W-40. In comparison, Al_2O_3 at 0.3 wt.% showed an auspicious development regarding BSFC and BTE (Figure 20).
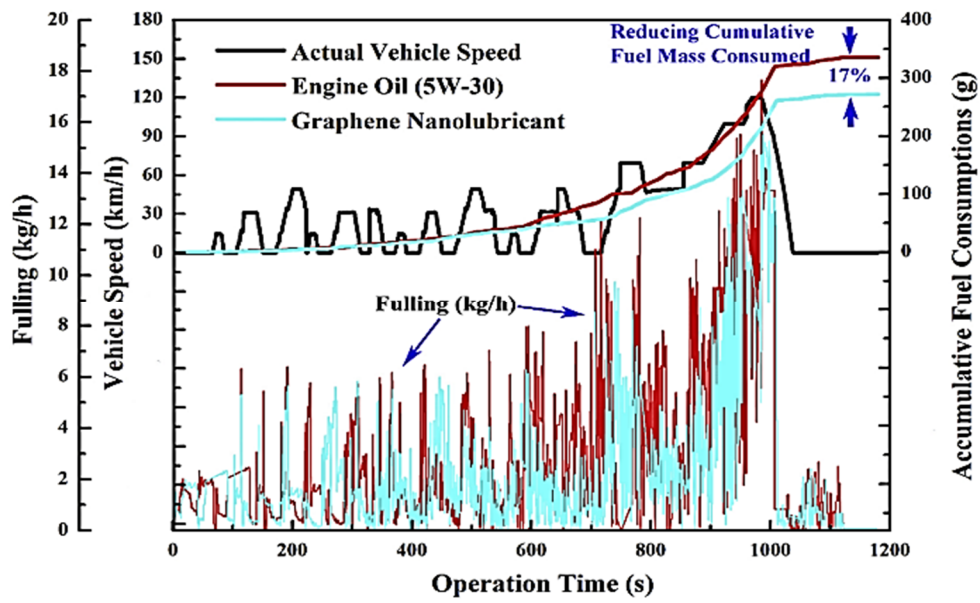
(I)
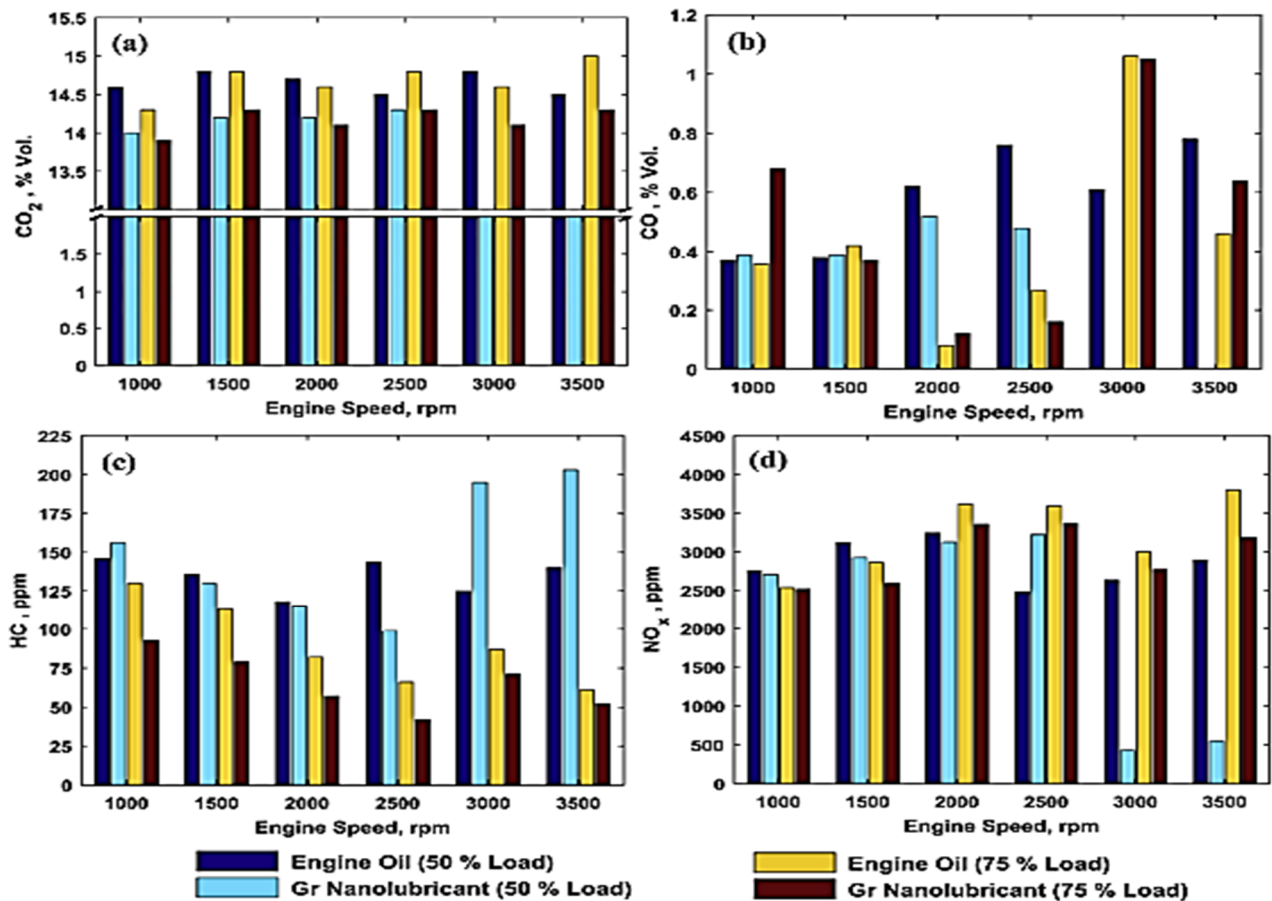
(II)

Figure 19. Energy-saving revenue from employing graphene engine -based nanolubricant. (**I**) Fuel consumption during New European Driving Cycle (NEDC). (**II**) Exhaust emissions under various operating conditions [67]. Adapted with permission.
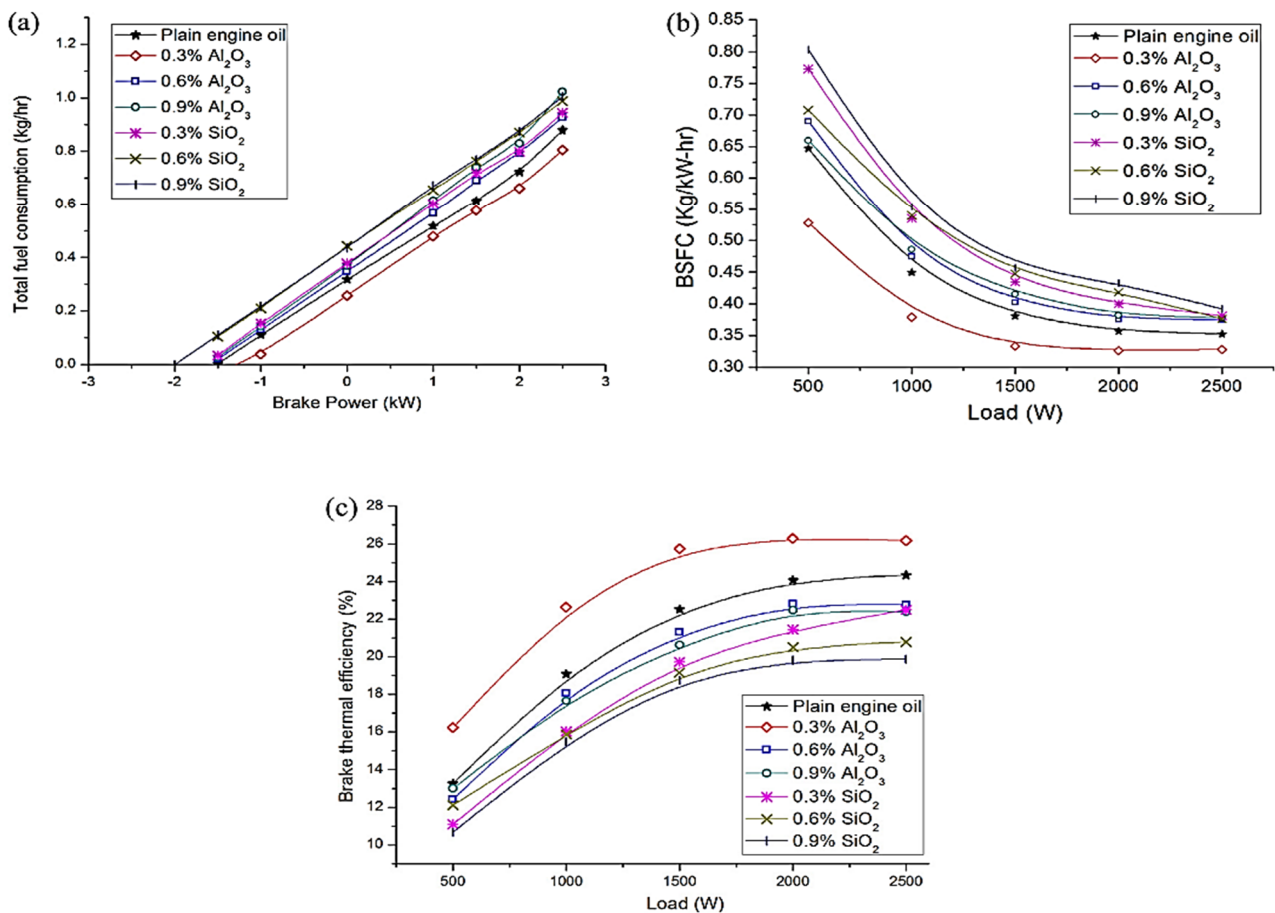
Figure 20. Effect of Al$_2$O$_3$ and SiO$_2$ nanolubricants on engine performance [167]. (**a**) Total fuel consumption. (**b**) brake-specific fuel consumption. (**c**) Brake thermal efficiency. Adapted with permission.

In another work, MoS$_2$ nanolubricants had been investigated, regarding the emissions of solid and gas pollutants through real diesel engine testing [168]. The study suggested that the presence of MoS$_2$ nanoparticles in the engine lubricant did not show a significant impact on minimizing both the emissions of ultrafine soot particles and greenhouse gases.

Interestingly, in another study by Sgroi [70], an average reduction in fuel consumption by 0.9% was obtained. The MoS$_2$ nanolubricant had been tested on the basis of the NEDC driving cycle of the real engine bench test. The study also reported a unique vehicle road test analysis with 5000 km of operating distance. A complete analysis of the nanolubricant degradation had been conducted after the road test. The degradation analysis confirmed a substantial upgrade regarding the wear particle analysis and chemical analysis as well.

Singh [59] reported a development in engine performance and exhaust emissions when graphite nanoparticles had been used. The reduction in the total fuel consumption and brake thermal efficiency was by 15.2% and 22%, respectively (Figure 21).

In another recent study by Bharath [56], vehicle noise pollution and vibrational characteristics were measured. The study was conducted for the hybrid nanolubricant of ZnO/ TiO$_2$, with a real automotive engine test. The hybrid nanolubricant showed a maximum reduction in the engine noise levels by 4.5% (Figure 22). At the same time, the reduction in the engine vibration was around 27–59% for the longitudinal vibration and 20–49% for the lateral vibration (Figure 23). It had been claimed, by the researchers of this study, that the noise and vibration reduction return to improvement in the tribological, rheological, and heat transfer properties provided by the hybrid nanolubricant. The better cooling and friction effect of the hybrid nanolubricant helped to dissipate the excessive heat of the engine. This will help in avoiding the knocking and vibration generated due to friction. Hence, reducing the mechanical losses and fuel consumption as well.
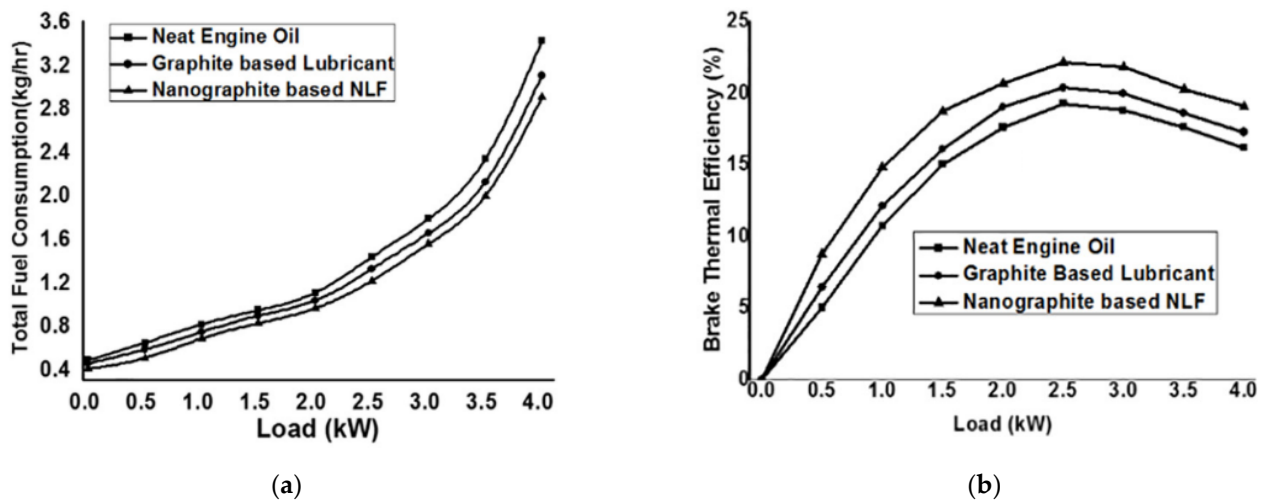
Figure 21. Enhancement of engine performance with nanolubrication. (**a**) Total fuel consumption, (**b**) brake thermal efficiency [59]. Adapted with permission.
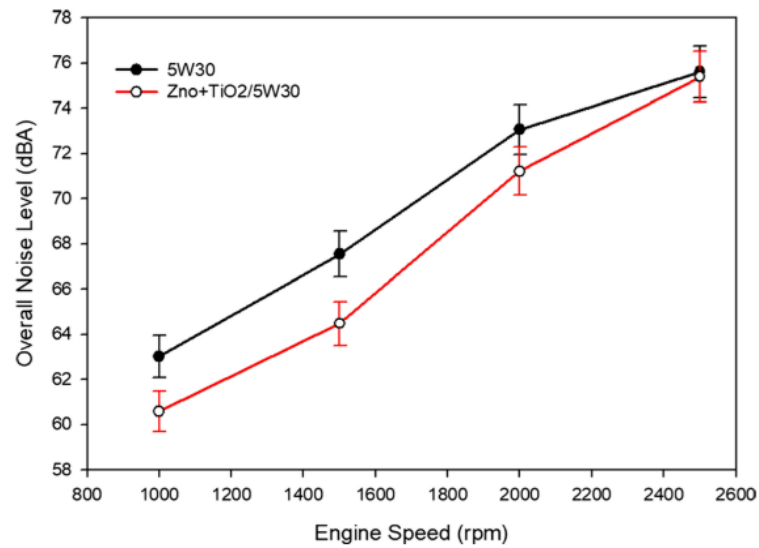

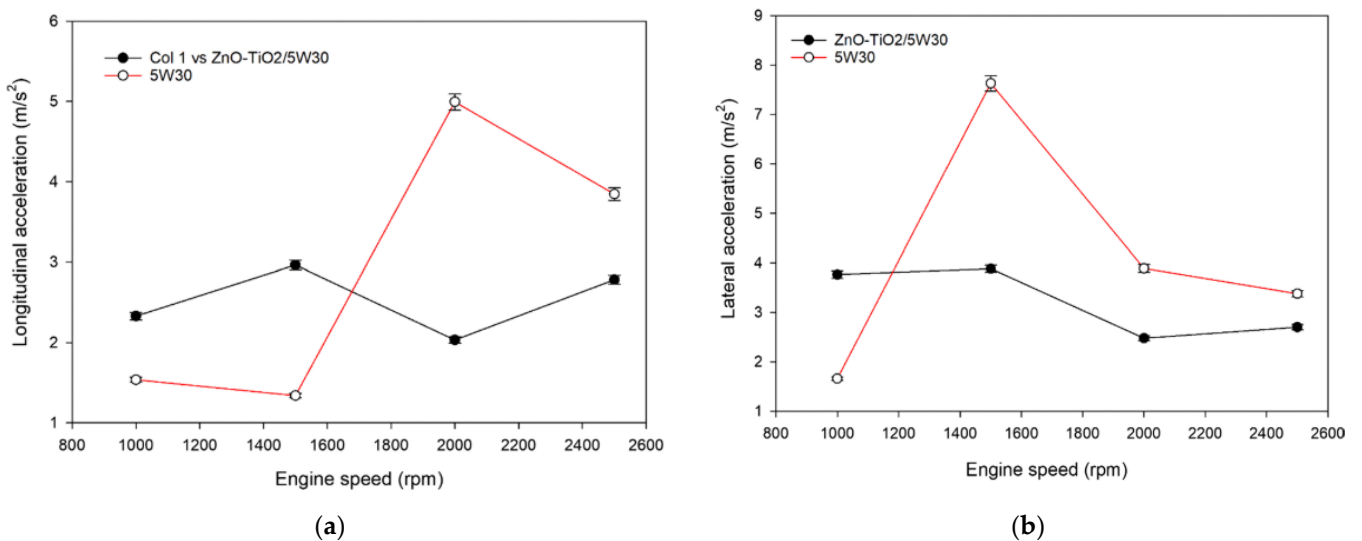**Figure 22.** Noise level reduction for engine-based nanolubricant [56].

Figure 23. Reduction in vibration acceleration, (**a**) Longitudinal vibration, (**b**) lateral vibration [56]. Adapted with permission.

6. Discussion

This section tries to afford a recommendation for potential candidates regarding engine lubricant-based nanofluids, and critically discuss the current findings of the literature. For instance, it is known that those fluids' tribological properties are considered the key parameter in designing such kinds of systems. This is because the lubricant tribological properties can predict the fuel economy, wear behaviour, and frictional power losses. Further, those fluids' dispersion stabilities and rheological characteristics should be then followed up to present the entire judgment on the selection, and screen out other candidates.

As stated by this review study, it appears that the nano additive of TiO_2 has the best tribological performance in contrast with other nanoparticles, as shown in Figure 24. This is due to its contribution to the high polishing of the surface asperities. Moreover, it showed excellent tribological performance in many studies, either as a single additive [68] or as a part of hybrid nanoparticles [67]. On the contrary, TiO_2 showed a fragile colloidal stability even when a surface-active agent was used to enhance their dispersion [112]. Figure 22 was constructed based on 55 studies published during the last decade, regarding the tribological properties of engine-based nanolubricants.
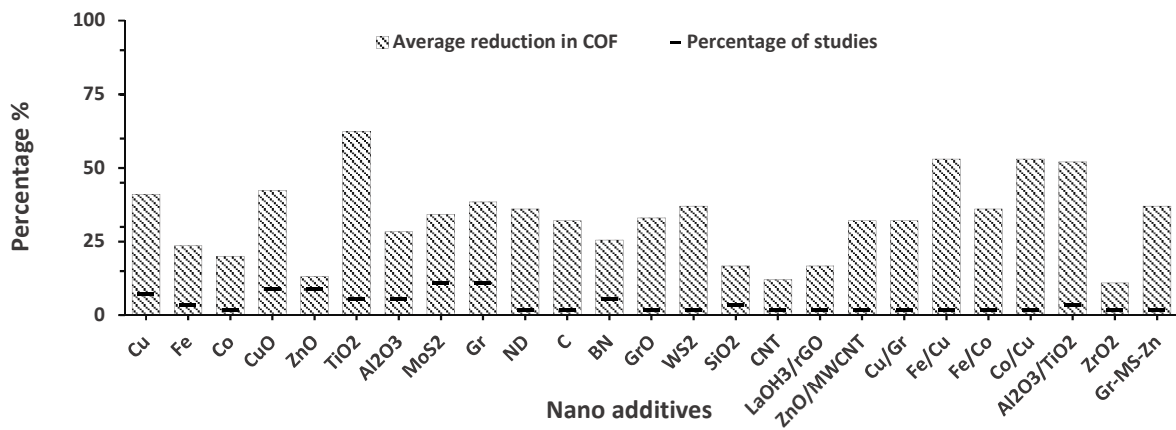

Figure 24. Nano additives that have been used for engine lubricants as friction modifiers published during the last decade.

Nanolubricants of base elements, such as Fe, C, Gr, Cu, Co, and other base candidates, showed promising improvement in tribological and thermal properties [20,169]. Despite that, in contrast with the types of nanoparticles, oxides such as CuO, ZnO, and GrO manifest themselves to have a long-lasting stable time [39]. This is due to the plenty of hydroxyl or carboxyl groups on their surface, which help their interaction with surfactants, improving their dispersion stability in non-polar mediums [170]. Besides their substantial dispersion stability, oxides have extraordinary tribological, as well as thermal, properties. CuO and ZnO nanolubricants had been investigated extensively, based on their rheological and tribological properties. They offered a remarkable intensification to both characteristics compared to other oxides, whether as a single [52,72,126,130] or hybrid additive [73,77]. Likewise, from the family of oxides, the hybrid Al_2O_3/TiO_2 nanolubricant showed a valuable performance at the level of tribological, thermal, and dispersion stability properties [50].

Regarding the thermal properties, MWCNT had been used in most of the rheological studies concerning engine-based nanolubricants, even with tiny added mounts [135,139,140,146]. This returns to the fact that MWCNT can provide considerable reinforcement to the rheological properties, owing to its high thermal conductivity value, with 3000–5000 W/mK compared to the engine lubricants, which have a value in the range of 0.0139–0.146 W/mK [171].

Furthermore, graphene and its oxide derivatives, such as graphene oxide GO and reduced graphene oxide rGO, showed a superb tribological and heat transfer performance, as mentioned in many studies [62,63,65,111,172]. This returns to the multi-layer nature of this family of nano additives that are easily sheared, due to its high chemical stability and

weak van der Waals forces between its sheets [64,172]. These characteristics of graphene and its constituents make them a worthy preference as a lubricant additive.

On top of that, GO and rGO possess better mechanical and thermal conductivity properties and dispersion stability than pure Gr [172].

Likewise, molybdenum sulphide (MoS$_2$) nano additives attract considerable attention, due to their distinctive wear properties, as mentioned in some studies [61,173]. It is believed that the friction-reduction capability of MoS$_2$ returns to its weak van der Waals primary atomic bonding that eases the slipping of MoS$_2$ layers and hence, forming the protective tribofilm [61].

As a general rule, it is necessary to consider all the nanolubricants' working system parameters. Besides their tribological and rheological features, some other attributes should be taken into account. This includes their size, surface morphology, and the internal structure of the nanoparticles, which is determined by the quality and processing of these nano constituents [172,174]. The size of the nanoparticles defines their internal physicochemical and mechanical properties, altering their tribological properties. For instance, their plasticity increases at a size range less than 10 nm [175–177], and their hardness increases with a reduction in the grain less than 100 nm, according to the Hall–Petch law [178]. Consequently, if the nanoparticles are harder than the rubbing system, this can degrade the wear effect.

For surface morphology, lamellar and platelet nanoparticles are preferred, at some points, to spherical ones. This is because nano-spheres will encounter higher pressure and more probability of rubbing surface deformation [174]. With reference to the nanoparticles' internal structure, the Schottky defect in nanostructure develops their mechanical strength by restraining the dislocation progress, then having a beneficial tribological impact [179,180].

Furthermore, new 2D nanomaterials need to be considered as engine-based lubricant additives. These 2D nanomaterials have been included in numerous recent studies as a promising lubricant additives. This includes MXenes, MOF, and CNNS [181–186]. For instance, a study by Wang reported a significant reduction in the coefficient of friction, by 63.33%, when MOF was added to 150SN base oil, with 1 wt.% as an optimum concentration [183]. In another study by Yong [187], the MXenes of $Ti_3C_2T_x$ highly exfoliated nano sheets had been used as a lubricant's nano additive. The tribological study that was conducted on ball-on-disk tribometer showed a fair consolidation in the tribological properties of the PAO base lubricant. The friction coefficient and wear volume were reduced by 10.5% and 7.7%, respectively, in contrast with the pure oil. It is believed that the enhancement in the tribological performance of MXenes returns to their ability of forming rich self-lubricating tribo-films. This is due to their low shear resistance, offered by their weak secondary interlayer bonding [184]. A common drawback of MXenes, which is mutual with other nanolubricants, is their low dispersion stability that can downgrade their tribological properties [188].

7. Future Directions and Challenges

In the context of nanolubrication, many challenges need to be considered in future studies. This includes some factors such as the dispersion stability of the colloidal system, and tribological and rheological beneficent mechanisms. Although there have been many articles on nanofluid behaviour, researchers still do not have an adequate grasping and complete vision of the complex mechanisms behind these factors. For dispersion stability, it is of high importance to form a system of homogeneous suspension. The nanofluid stability is influenced by the type of surface modification, pH value, and the sort of nanoparticles [37]. On the other hand, there are many disagreements between the experimental data and theoretical predictions, regarding the tribological and rheological characteristics [37,47,48,189]. Further, there is a need for more real engine bench and road tests that have to cover the actual working conditions of these nanolubricants [56,70].

7.1. Molecular Dynamics Simulations

To better understand the experimental results and theoretical hypotheses confined to the various properties of nanolubricants, recent studies have been directed to the atomic level simulations, using molecular dynamics for these nanofluids. Molecular dynamics (MD) simulations can recompense the shortage of experiments, and provide a clear way to understand the different characteristics of nanolubricants at the atomic level. The research studies revealed that molecular dynamics could afford a whole screening method for studying nanolubricant properties [190–192], as shown in Figure 25.
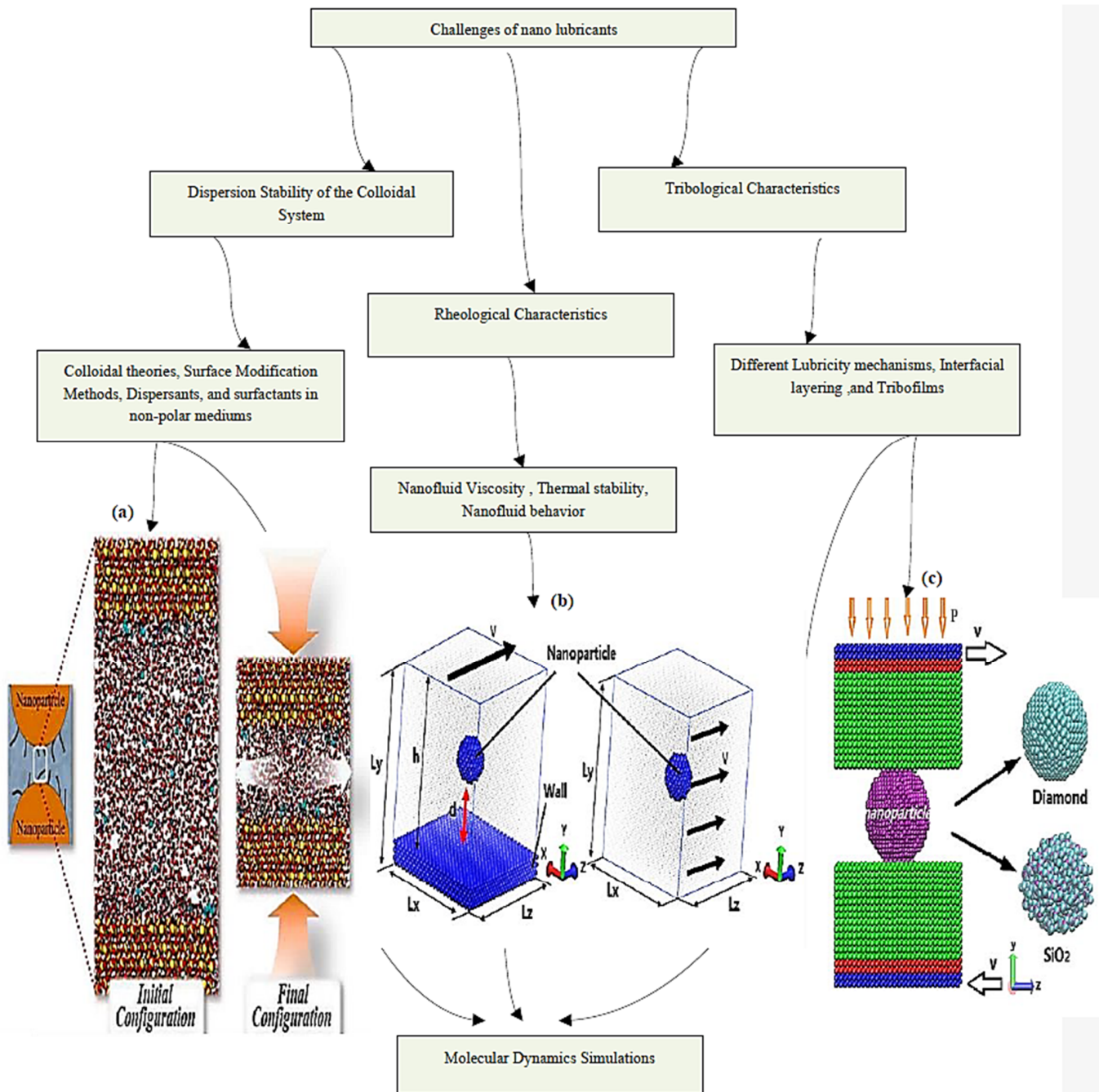
Figure 25. Molecular dynamics simulations for nanolubricants. (**a**) Dispersion stability properties [194], (**b**) rheological properties [191], (**c**) tribological properties [193]. Adapted with permission.

In a recent study, nanofluid behaviour was investigated using the near-wall and main flow model of molecular dynamics [191], as shown in Figure 25b. For the near-wall model, the nanoparticles that were too close to the wall would have a rotational motion and would not move with the mainstream of the fluid. This is due to the overlap between the adsorbed fluid layer around the nanoparticles and the solid-like layer of the particle–wall interface near the wall. For the main flow model, the nanoparticles would have both translation and rotational motions.

For the tribological characteristics, the hypotheses of the ball-bearing lubrication mechanism had been confirmed through the simulation of molecular dynamics [193]. The nanoparticles acted as ball-bearing, and the sliding motion was converted to a mix between sliding and rolling, leading to a reduction in the coefficient of friction, as shown in Figure 25c. In another recent study by Fang [194], a theoretical method was generated to quantify the aggregation and dispersion of nanofluids. The potential of mean force (free energy), based on the umbrella sampling method for nanoparticles, was considered in calculating the physical forces that govern the motion of nanoparticles. Based on PMF curves (Figure 26a), when nanoparticles approach closer, they are acquired to overcome high energy barriers.
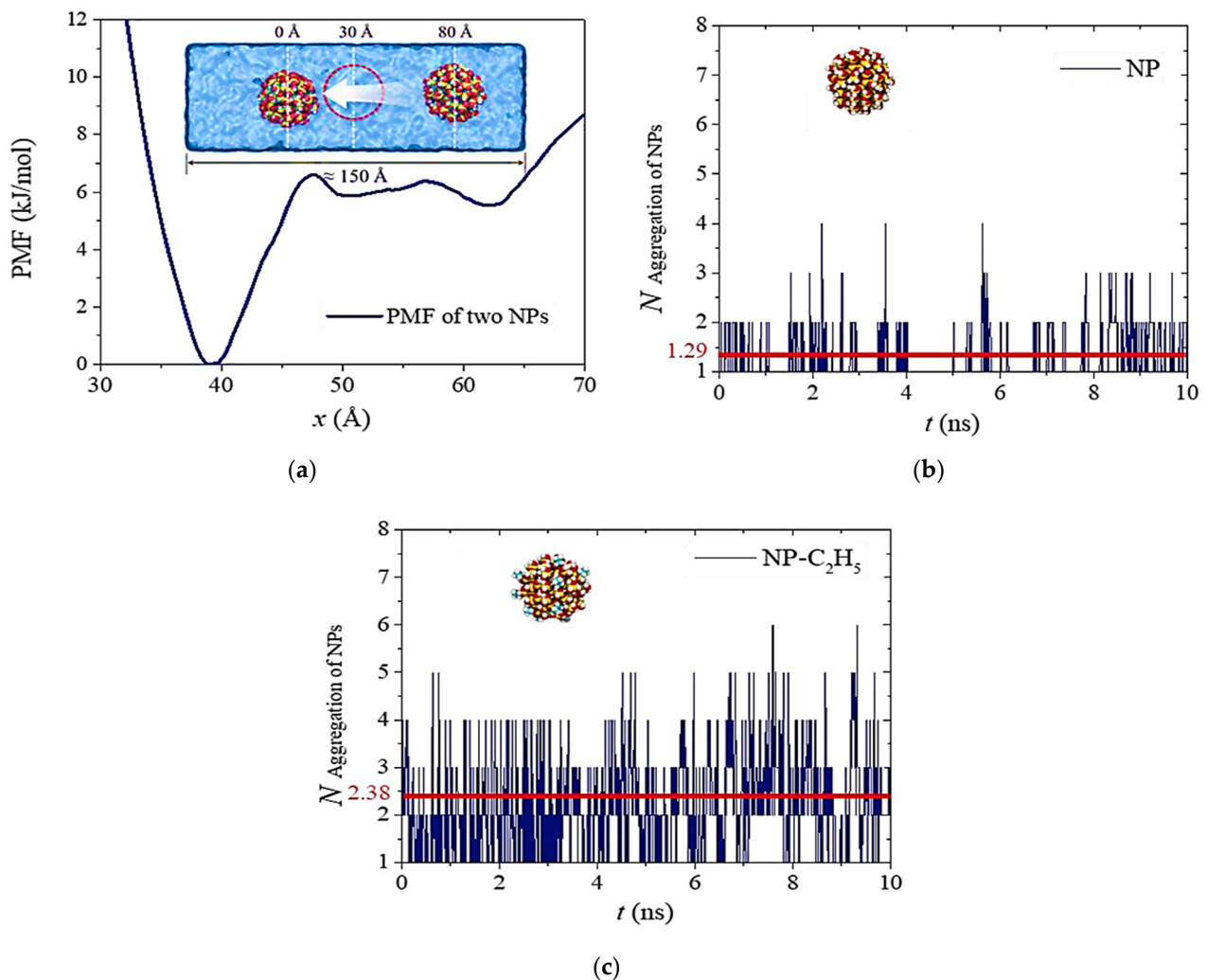

(a)

(b)

(c)

Figure 26. Molecular insight into the aggregation and dispersion behaviour of nanoparticles. (**a**) PMF curve of nanoparticle when another particle approached, (**b**,**c**) aggregation number of nanoparticles with simulation time under different grafting conditions [194]. Adapted with permission.

The difference between the particle diameter and the equilibrium distance is defined as the critical distance. When the hydroxyl chain on the surfaces of two approaching particles is less than the critical distance, the particles will be aggregated, forming a low quality of dispersion. The aggregation number, calculated by the molecular dynamics simulations, indicates the degree of aggregation. A highly dispersive nanofluid is obtained when this number increases, and vice versa (Figure 26b,c). Many studies regarding the theoretical analyses of nanofluids using molecular dynamics are shown in Table 8.

Table 8. Molecular dynamics studies of nanofluids.

Reference	Year	Substantial Findings	Studied Property
[194]	2020	Addressing of effective method to quantify aggregation/dispersion range through molecular simulation	Dispersion Stability
[195]	2021	MD simulations stated that the transformation from dispersion state to the reversible state is related to the Lennard–Jones(LJ) particle number	
[190]	2020	Providing a facile method to produce high dispersion stability of GO suspensions. MD simulations indicated that the used surface agents could form a high reaggregation barrier on the surface of nanoparticles	
[196]	2021	By increasing the receiving heat flux of nanofluid, the thermal conductivity is improved.	Rheological and Thermophysical Characteristics
[191]	2014	Discussing the hypotheses behind the flow of nanofluids using near and main flow models	
[192]	2021	The common hypotheses of the ball-bearing lubrication mechanism have been confirmed through the MD simulations, which verified the rolling motion of nanoparticles.	Tribological Characteristics
[197]	2014	A clear investigation was concluded about the effect of sliding velocity and load capacity on the formation of the nano tribo-films at the contacted surfaces	
[198]	2020	Frictional heating and anti-wear properties of the friction pair is controlled through the existence of nanoparticles	
[199]	2020	Simulations of MD clarified that Gr nano additives could form a thick layer of tribo-film that can help in reducing the coefficient of friction and friction force	
[200]	2014	Nanofluids have a higher transition pressure than the base fluid, with an excellent load-carrying capacity	
[201]	2020	Theoretical guidance was implemented for the lubrication mechanism of MOS2 nanoparticles	
[193]	2015	Confirmation of the ball-bearing lubrication mechanism of nanoparticles under mild velocities and loads	
[189]	2015	The load-carrying capacity of nanofluid is improved regarding the base oil before the rupture of the lubricant film	
[120]	2018	Atomistic simulations confirmed the mending mechanism of nanolubricants through which nanoparticles fill in valleys of the sliding asperities	

Over and above that, artificial intelligence models can also predict the different behaviours of lubricant performance, regarding their tribological and other behaviours [202–204]. One of these tools is the artificial neural network (ANN), which is considered a widely accepted novel modelling approach [203]. Basically, the ANN is composed of a network of mathematical functions, based upon the working methodology of neurons in the human brain. They can learn in a fashion similar to the way our brains do [202]. The mathematical functions use a complex dataset of experimental results as inputs, and then build a model that can predict and optimize the future results under different variations (Figure 27) [204]. In this way, the cost and time of the unaffected experimental work would be minimized.
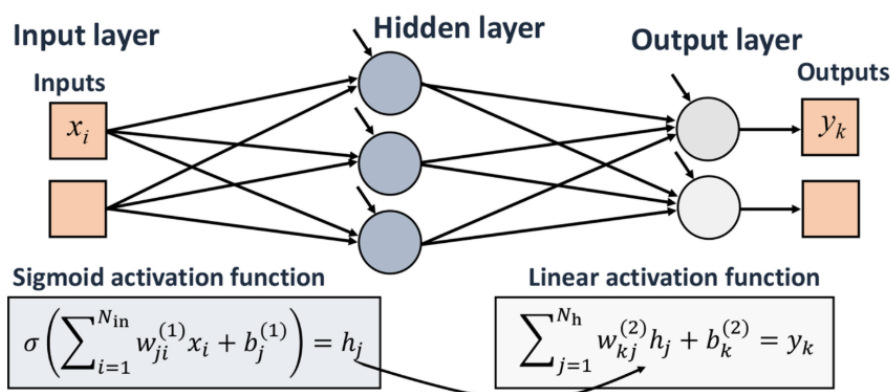
Figure 27. Working methodology of ANN as a predictive artificial intelligence tool [204]. Adapted with open access permission.

The ANN has been used in many studies to predict the performance of a tribo-system [203]. It has been used in numerous studies regarding the rheological and thermo-physical properties of these systems [73,129,133,147].

7.2. Ionic Based Nano Lubricants

As a nano concentrate for engine lubricants, ionic liquids have been developed in the last few years [18,105]. These concentrates are needed to be highlighted strongly in future studies, as they can offer valuable results regarding the friction and wear characteristics. These particular types of liquids can be used as a lubricant [205,206], lubricant additive [207–212], a carrier medium for nanoparticles in the form of a concentrated lubricant additive [105,106], and even as a surfactant to enhance the dispersion stability of nanolubricants [213]. For instance, a concentrate of hairy nano-silica (HSPs) and the ionic liquid of ([BMIM][NTF$_2$]) as a carrier medium was prepared. It was used as a lubricant additive for 10W-30 fully formulated engine lubricant [105]. The results showed an outstanding performance regarding friction reduction, prevention of noise, and scuffing as well.

Unfortunately, there is a major gap in the research field, regarding ionic engine nanol-ubricants. In addition to their significant tribological properties, many factors should be considered in future studies, regarding the use of ionic-based nano additives. This includes their thermophysical and dispersion stability properties, as well as their engine performance.

7.3. Cost and Economics of Nanolubricants

It has been indicated that the cost of nanofluids is one of the most outstanding issues in many applications [45,214]. The production cost of these fluids relies on the manufacturing method, which combines the dispersion technique into the base fluid and nanoparticles fabrication. As discussed previously, two- and single-step methods are the only approaches used for the production of nanofluids. The equipment used in these techniques, as well as dispersion testing, are expensive and very sophisticated. This includes probe and bath sonication, zeta potential, FTIR, sedimentation analysis, and UV.

The work on diminishing nanofluids production cost had been mentioned in many recent studies [215–217]. Sylwia [214] had generated a considerable model that can represent the cost estimation of any sort of nanofluids, as shown in Equation (6), as follows:

$$P_{nf} = \frac{P_{np}\rho V}{0.001} + P_{others} \tag{6}$$

where P_{nf}, is the unit price of the prepared nanofluid in EUR/dm3, P_{np} is the price of the nanoparticles in EUR/g, P_{others} the price of other operations, such as dispersion testing, sonication, and stirring. V and ρ are the base fluid volume and density.

In a recent study by Bharath [56], the cost estimation of a hybrid ZnO/TiO_2 engine-based nanolubricant had been conducted. The total fabrication cost, including preparation, nanoparticle, and surface modification expenditures, was found to be around 25% more than the retail market price of the 5W-30 base oil.

In light of the current research direction of nanolubricants, it is clear that more economic studies are needed regarding the production cost.

8. Conclusions

From the conclusions of the various mentioned studies, it can be reported that nano-materials are considered an ideal preference for improving vehicular engine performance. This would be conducted by dispersing specific concentrations of nanoparticles into the lubricating oil. A considerable and effective result of such additives is realized by fostering thermal and mechanical efficiencies of the engine. Fuel efficiency and power train durability are considered the most vigorous outcome of this interface nanotechnology. In the present study, the goal was to present an overview and critical analysis for the potentiality of engine-based nanolubricants. An entire screening of all the considerations that can affect the behaviour of these lubricants is extracted from almost all of the studies in this area over the last ten years. The preparation techniques and the dispersion stability of engine-based nanolubricants were addressed first. Then, the tribological and rheological properties of these nanofluids were introduced, with all of the hypothesized lubrication mechanisms and experimental modelling of the thermal and viscosity behaviours. Potential candidates of nano additives have been recommended, based on the combined effect of the previously mentioned factors.

Moreover, the future of this research direction, regarding molecular dynamics and its economic value, were covered. As a key output, the authors would like to concentrate on the importance of the engine lubricant's complete analysis, regarding the future studies of nano additives. This includes wear and friction properties, thermophysical and rheological analysis, dispersion stability, and actual engine performance.

References

1. Ali, M.K.A.; Xianjun, H.; Abdelkareem, M.A.A.; Elsheikh, A.H. Role of nanolubricants formulated in improving vehicle engines performance. In *IOP Conference Series: Materials Science and Engineering*; IOP Publishing: Bristol, UK, 2019; Volume 563. [CrossRef]
2. Shah, R.; Woydt, M.; Huq, N.; Rosenkranz, A. Tribology meets sustainability. *Ind. Lubr. Tribol.* **2020**. [CrossRef]
3. European Commission. *EU Good Practice in Energy Efficiency, for a Sustainable, Safer and more Competion Goes to Overcome Friction*; European Commission: Brussels, Belgium, 2017.
4. Holmberg, K.; Erdemir, A. Tribology International The impact of tribology on energy use and CO 2 emission globally and in combustion engine and electric cars. *Tribol. Int.* **2019**, *135*, 389–396. [CrossRef]
5. Biberger, J.; Füßer, H. Tribology International Development of a test method for a realistic, single parameter-dependent analysis of piston ring versus cylinder liner contacts with a rotational tribometer. *Tribol. Int.* **2017**, *113*, 111–124. [CrossRef]

6.   La, D.D.; Truong, T.N.; Pham, T.Q.; Vo, H.T.; Tran, N.T.; Nguyen, T.A.; Nadda, A.K.; Nguyen, T.T.; Chang, S.W.; Chung, W.J.; et al. Scalable fabrication of modified graphene nanoplatelets as an effective additive for engine lubricant oil. *Nanomaterials* **2020**, *10*, 877. [CrossRef]

7.   Abril, S.O.; Rojas, J.P.; Flórez, E.N. Numerical Methodology for Determining the Energy Losses in Auxiliary Systems and Friction Processes Applied to Low Displacement Diesel Engines. *Lubricants* **2020**, *8*, 103. [CrossRef]

8.   Knauder, C.; Allmaier, H.; Sander, D.E.; Sams, T. Investigations of the Friction Losses of Different Engine Concepts: Part 3: Friction Reduction Potentials and Risk Assessment at the Sub-Assembly Level. *Lubricants* **2020**, *8*, 39. [CrossRef]

9.   Knauder, C.; Allmaier, H.; Sander, D.E.; Sams, T. Investigations of the Friction Losses of Different Engine Concepts. Part 2: Sub-Assembly Resolved Friction Loss Comparison of Three Engines. *Lubricants* **2019**, *7*, 105. [CrossRef]

10.   Knauder, C.; Allmaier, H.; Sander, D.E.; Sams, T. Investigations of the Friction Losses of Different Engine Concepts. Part 1: A Combined Approach for Applying Subassembly-Resolved Friction Loss Analysis on a Modern Passenger-Car Diesel Engine. *Lubricants* **2019**, *7*, 39. [CrossRef]

11.   Aldana, P.U.; Vacher, B.; le Mogne, T.; Belin, M.; Thiebaut, B.; Dassenoy, F. Action Mechanism of WS2 Nanoparticles with ZDDP Additive in Boundary Lubrication Regime. *Tribol. Lett.* **2014**, *56*, 249–258. [CrossRef]

12.   Sharma, V.; Timmons, R.B.; Erdemir, A.; Aswath, P.B. Interaction of plasma functionalized TiO$_2$ nanoparticles and ZDDP on friction and wear under boundary lubrication. *Appl. Surf. Sci.* **2019**, *489*, 372–383. [CrossRef]

13.   Hsu, C.-J.; Stratmann, A.; Rosenkranz, A.; Gachot, C. Enhanced Growth of ZDDP-Based Tribofilms on Laser-Interference Patterned Cylinder Roller Bearings. *Lubricants* **2017**, *5*, 39. [CrossRef]

14.   Gachot, C.; Hsu, C.; Suárez, S.; Grützmacher, P.; Rosenkranz, A.; Stratmann, A.; Jacobs, G. Microstructural and Chemical Characterization of the Tribolayer Formation in Highly Loaded Cylindrical Roller Thrust Bearings. *Lubricants* **2016**, *4*, 19. [CrossRef]

15.   Vyavhare, K.; Timmons, R.B.; Erdemir, A.; Edwards, B.L.; Aswath, P.B. Tribochemistry of fluorinated ZnO nanoparticles and ZDDP lubricated interface and implications for enhanced anti-wear performance at boundary lubricated contacts. *Wear* **2021**, *474–475*, 203717. [CrossRef]

16.   Ratoi, M.; Niste, V.B.; Walker, J.; Zekonyte, J. Mechanism of Action of WS2 Lubricant Nanoadditives in High-Pressure Contacts. *Tribol. Lett.* **2013**, *52*, 81–91. [CrossRef]

17.   Bagi, S.; Aswath, P. Mechanism of Friction and Wear in MoS2 and ZDDP/F-PTFE Greases under Spectrum Loading Conditions. *Lubricants* **2015**, *3*, 687–711. [CrossRef]

18.   Sharma, V. Development of Plasma Functionalized Nano-Additives for Oils and Study of Their Tribological Properties. Ph.D. Thesis, The University of Texas at Arlington, Arlington, TX, USA, 2017.

19.   Wong, V.W.; Tung, S.C. Overview of automotive engine friction and reduction trends–Effects of surface, material, and lubricant-additive technologies. *Friction* **2016**, *4*, 1–28. [CrossRef]

20.   Srivyas, P.D.; Charoo, M.S. A Review on Tribological Characterization of Lubricants with Nano Additives for Automotive Applications. *Tribol. Ind.* **2018**, *40*, 594–623. [CrossRef]

21.   Tonk, R. The challenges and benefits of using carbon nano-tubes as friction modifier lubricant additives. *Mater. Today Proc.* **2020**, *37*, 3275–3278. [CrossRef]

22.   Kaleli, H.; Demirtaş, S.; Uysal, V.; Karnis, I.; Stylianakis, M.M.; Anastasiadis, S.H.; Kim, D.E. 920.Tribological performance investigation of a commercial engine oil incorporating reduced graphene oxide as additive. *Nanomaterials* **2021**, *11*, 386. [CrossRef]

23.   Tonk, R. The characterization analysis of multi walled carbon nanotubes coated with carboxylic group compounds to improve its dispersion properties in mineral base engine oils. *Mater. Today Proc.* **2020**, *37*, 3279–3282. [CrossRef]

24.   Shafi, W.K.; Charoo, M.S. An overall review on the tribological, thermal and rheological properties of nanolubricants, Tribology–Materials. *Surf. Interfaces* **2021**, *15*, 20–54. [CrossRef]

25.   Ali, M.K.A.; Xianjun, H. Improving the heat transfer capability and thermal stability of vehicle engine oils using Al$_2$O$_3$/TiO$_2$ nanomaterials. *Powder Technol.* **2020**, *363*, 48–58. [CrossRef]

26.   Charoo, M.S.; Hanief, M. Improving the tribological characteristics of a lubricating oil by nano sized additives. *Mater. Today Proc.* **2020**, *28*, 1205–1209. [CrossRef]

27.   Kałużny, J.; Waligórski, M.; Szymański, G.M.; Merkisz, J.; Różański, J.; Nowicki, M.; al Karawi, M.; Kempa, K. Reducing friction and engine vibrations with trace amounts of carbon nanotubes in the lubricating oil. *Tribol. Int.* **2020**, *151*. [CrossRef]

28.   Ivanov, M.; Shenderova, O. Nanodiamond-based nanolubricants for motor oils. *Curr. Opin. Solid State Mater. Sci.* **2017**, *21*, 17–24. [CrossRef]

29.   Kotia, A.; Chowdary, K.; Srivastava, I.; Ghosh, S.K.; Ali, M.K.A. Carbon nanomaterials as friction modifiers in automotive engines: Recent progress and perspectives. *J. Mol. Liq.* **2020**, *310*, 113200. [CrossRef]

30.   Vardhaman, B.S.A.; Amarnath, M.; Ramkumar, J.; Mondal, K. Enhanced tribological performances of zinc oxide/MWCNTs hybrid nanomaterials as the effective lubricant additive in engine oil. *Mater. Chem. Phys.* **2020**, *253*, 123447. [CrossRef]

31.   Mousavi, S.B.; Heris, S.Z. Experimental investigation of ZnO nanoparticles effects on thermophysical and tribological properties of diesel oil. *Int. J. Hydrog. Energy* **2020**, *45*, 23603–23614. [CrossRef]

32.   Mello, V.S.; Trajano, M.F.; Emilia, A.; Silva, D. Comparison Between the Action of Nano-Oxides and Conventional EP Additives in Boundary Lubrication. *Lubricants* **2020**, *8*, 54. [CrossRef]

33. Esfe, M.H.; Mosaferi, M. Effect of MgO nanoparticles suspension on rheological behavior and a new correlation. *J. Mol. Liq.* **2020**, *309*, 112632. [CrossRef]

34. Laad, M.; Jatti, V.K.S. Titanium oxide nanoparticles as additives in engine oil. *J. King Saud Univ. Eng. Sci.* **2016**, *30*, 116–122. [CrossRef]

35. Guo, J.; Peng, R.; Du, H.; Shen, Y.; Li, Y.; Li, J.; Dong, G. The application of nano-MOS2 quantum dots as liquid lubricant additive for tribological behavior improvement. *Nanomaterials* **2020**, *10*, 200. [CrossRef] [PubMed]

36. Karthikeyan, K.M.B.; Vijayanand, J.; Arun, K.; Rao, V.S. Thermophysical and wear properties of eco-friendly nano lubricants. *Mater. Today Proc.* **2020**, *39*, 285–291. [CrossRef]

37. Yang, L.; Ji, W.; Mao, M.; Huang, J.N. An updated review on the properties, fabrication and application of hybrid-nanofluids along with their environmental effects. *J. Clean. Prod.* **2020**, *257*, 120408. [CrossRef]

38. Mello, V.S.; Faria, E.A.; Alves, S.M.; Scandian, C. Enhancing Cuo nanolubricant performance using dispersing agents. *Tribol. Int.* **2020**, *150*, 106338. [CrossRef]

39. Chen, Y.; Renner, P.; Liang, H. Dispersion of Nanoparticles in Lubricating Oil: A Critical Review. *Lubricants* **2019**, *7*, 7. [CrossRef]

40. Rabaso, P.; Ville, F.; Dassenoy, F.; Diaby, M.; Afanasiev, P.; Cavoret, J.; Vacher, B.; le Mogne, T. Boundary lubrication: Influence of the size and structure of inorganic fullerene-like MoS2 nanoparticles on friction and wear reduction. *Wear* **2014**, *320*, 161–178. [CrossRef]

41. Shaw, D. *Introduction to Colloid and Surface Chemistry*, 4th ed.; Elsevier: Oxford, UK; Boston, MA, USA, 2013. [CrossRef]

42. Robins, M.; Fillery-Travis, A. *Colloidal Dispersions*; Russel, W.B., Saville, D.A., Schowalter, W.R., Eds.; Cambridge University Press: Cambridge, UK, 1989; Volume 17.

43. Yu, W.; Xie, H. A Review on Nanofluids: Preparation, Stability Mechanisms, and Applications. *J. Nanomater.* **2012**, *2012*, 1–17. [CrossRef]

44. Azman, N.F.; Samion, S. Dispersion Stability and Lubrication Mechanism of Nanolubricants: A Review. *Int. J. Precis. Eng. Manuf. Green Technol.* **2019**, *6*, 393–414. [CrossRef]

45. Babar, H.; Ali, H.M. Towards hybrid nanofluids: Preparation, thermophysical properties, applications, and challenges. *J. Mol. Liq.* **2019**, *281*, 598–633. [CrossRef]

46. Shafi, W.K.; Charoo, M.S. NanoLubrication Systems: An Overview. *Mater. Today Proc.* **2018**, *5*, 20621–20630. [CrossRef]

47. Asadi, A.; Aberoumand, S.; Moradikazerouni, A.; Pourfattah, F.; Żyła, G.; Estellé, P.; Mahian, O.; Wongwises, S.; Nguyen, H.M.; Arabkoohsar, A. Recent advances in preparation methods and thermophysical properties of oil-based nanofluids: A state-of-the-art review. *Powder Technol.* **2019**, *352*, 209–226. [CrossRef]

48. Jama, M.; Singh, T.; Gamaleldin, S.M.; Koc, M.; Samara, A.; Isaifan, R.J.; Atieh, M.A. Critical Review on Nanofluids: Preparation, Characterization, and Applications. *J. Nanomater.* **2016**, *2016*, 1–22. [CrossRef]

49. Ali, M.K.A.; Xianjun, H. Colloidal stability mechanism of copper nanomaterials modified by ionic liquid dispersed in polyalphaolefin oil as green nanolubricants. *J. Colloid Interface Sci.* **2020**, *578*, 24–36. [CrossRef] [PubMed]

50. Ali, M.K.A.; Xianjun, H. Role of bis2-ethylhexyl phosphate and Al_2O_3/TiO_2 hybrid nanomaterials in improving the dispersion stability of nanolubricants. *Tribol. Int.* **2021**, *155*, 106767. [CrossRef]

51. Esfe, M.H.; Saedodin, S.; Shahram, J. Experimental investigation, model development and sensitivity analysis of rheological behavior of ZnO/10W40 nano-lubricants for automotive applications. *Phys. Low-Dimens. Syst. Nanostruct.* **2017**, *90*, 194–203. [CrossRef]

52. Abdel-Rehim, A.A.; Akl, S.; Elsoudy, S. Investigation of the Tribological Behavior of Mineral Lubricant Using Copper Oxide Nano Additives. *Lubricants* **2021**, *9*, 16. [CrossRef]

53. Ali, M.K.A.; Xianjun, H.; Turkson, R.F.; Peng, Z.; Chen, X. Enhancing the thermophysical properties and tribological behaviour of engine oils using nano-lubricant additives Al_2O_3. *RSC Adv.* **2016**, *6*, 77913–77924. [CrossRef]

54. Heredia-Cancino, J.A.; Ramezani, M.; Álvarez-Ramos, M.E. Effect of degradation on tribological performance of engine lubricants at elevated temperatures. *Tribol. Int.* **2018**, *124*, 230–237. [CrossRef]

55. Kral, J.; Konecny, B.; Kral, J.; Madac, K.; Fedorko, G.; Molnar, V. Degradation and chemical change of longlife oils following intensive use in automobile engines. *Measurement J. Int. Meas. Confed.* **2014**, *50*, 34–42. [CrossRef]

56. Bharath, B.K.; Selvan, V.A.M. An Experimental Investigation on Rheological and Heat Transfer Performance of Hybrid Nanolubricant and Its Effect on the Vibration and Noise Characteristics of an Automotive Spark-Ignition Engine. *Int. J. Thermophys.* **2021**, *42*, 1–30. [CrossRef]

57. Liu, K.N.; Zhang, Y.; Dai, F.; Sun, W. Improved heat transfer of the engine oil by changing it to hybrid nanofluid: Adding hybrid nano-powders. *Powder Technol.* **2021**, *383*, 56–64. [CrossRef]

58. Gupta, H.; Rai, S.K.; Krishna, N.S.; Anand, G. Effect of silica nano-additive on flash point, pour point, rheological and tribological properties of lubricating engine oil: An experimental study. *J. Dispers. Sci. Technol.* **2021**, *42*, 622–632. [CrossRef]

59. Singh, J.P.; Singh, S.; Nandi, T.; Ghosh, S.K. Development of graphitic lubricant nanoparticles based nanolubricant for automotive applications: Thermophysical and tribological properties followed by IC engine performance. *Powder Technol.* **2021**, *387*, 31–47. [CrossRef]

60. Chouhan, A.; Sarkar, T.K.; Kumari, S.; Vemuluri, S.; Khatri, O.P. Synergistic lubrication performance by incommensurately stacked ZnO-decorated reduced graphene oxide/MoS2 heterostructure. *J. Colloid Interface Sci.* **2020**, *580*, 730–739. [CrossRef]

61. Mousavi, S.B.; Heris, S.Z.; Estellé, P. Experimental comparison between ZnO and MoS2 nanoparticles as additives on performance of diesel oil-based nano lubricant. *Sci. Rep.* **2020**, *10*, 1–17. [CrossRef]

62. Wu, B.; Song, H.; Li, C.; Song, R.; Zhang, T.; Hu, X. Enhanced tribological properties of diesel engine oil with Nano-Lanthanum hydroxide/reduced graphene oxide composites. *Tribol. Int.* **2020**, *141*. [CrossRef]

63. Ali, M.K.A.; Hou, X.; Abdelkareem, M.A.A. Anti-wear properties evaluation of frictional sliding interfaces in automobile engines lubricated by copper/graphene nanolubricants. *Friction* **2019**, *8*, 905–916. [CrossRef]

64. Wang, W.; Zhang, G.; Xie, G. Applied Surface Science Ultralow concentration of graphene oxide nanosheets as oil-based lubricant additives. *Appl. Surf. Sci.* **2019**, *498*, 143683. [CrossRef]

65. Paul, G.; Shit, S.; Hirani, H.; Kuila, T.; Murmu, N.C. Tribological behavior of dodecylamine functionalized graphene nanosheets dispersed engine oil nanolubricants. *Tribol. Int.* **2019**, *131*, 605–619. [CrossRef]

66. Ghasemi, R.; Fazlali, A.; Mohammadi, A.H. Effects of TiO 2 nanoparticles and oleic acid surfactant on the rheological behavior of engine lubricant oil. *J. Mol. Liq.* **2018**, *268*, 925–930. [CrossRef]

67. Ali, M.K.A.; Xianjun, H.; Abdelkareem, M.A.A.; Gulzar, M.; Elsheikh, A.H. Novel approach of the graphene nanolubricant for energy saving via anti-friction/wear in automobile engines. *Tribol. Int.* **2018**, *124*, 209–229. [CrossRef]

68. Kamal, M.; Ali, A.; Fuming, P.; Younus, H.A. Fuel economy in gasoline engines using Al_2O_3/TiO_2 nanomaterials as nanolubricant additives. *Appl. Energy* **2018**, *211*, 461–478. [CrossRef]

69. Demas, N.G.; Erck, R.A.; Lorenzo-martin, C.; Ajayi, O.O.; Fenske, G.R. Experimental Evaluation of Oxide Nanoparticles as Friction and Wear Improvement Additives in Motor Oil. *J. Nanomater.* **2017**, *2017*. [CrossRef]

70. Sgroi, M.F.; Asti, M.; Gili, F.; Deorsola, F.A.; Bensaid, S.; Fino, D.; Kraft, G.; Garcia, I.; Dassenoy, F. Engine bench and road testing of an engine oil containing MoS2 particles as nano-additive for friction reduction. *Tribol. Int.* **2017**, *105*, 317–325. [CrossRef]

71. Sepyani, K.; Afrand, M.; Esfe, M.H. An experimental evaluation of the effect of ZnO nanoparticles on the rheological behavior of engine oil. *J. Mol. Liq.* **2017**, *236*, 198–204. [CrossRef]

72. Ran, X.; Yu, X.; Zou, Q. Effect of Particle Concentration on Tribological Properties of ZnO Nanofluids. *Tribol. Trans.* **2017**, *60*, 154–158. [CrossRef]

73. Moghaddam, M.A.; Motahari, K. Experimental investigation, sensitivity analysis and modeling of rheological behavior of MWCNT-CuO 30–70/SAE40 hybrid nano-lubricant. *Appl. Therm. Eng.* **2017**, *123*, 1419–1433. [CrossRef]

74. Wu, H.; Qin, L.; Dong, G.; Hua, M.; Yang, S.; Zhang, J. An investigation on the lubrication mechanism of MoS2 nano sheet in point contact: The manner of particle entering the contact area. *Tribol. Int.* **2017**, *107*, 48–55. [CrossRef]

75. Esfe, M.H.; Afrand, M.; Yan, W.M.; Yarmand, H.; Toghraie, D.; Dahari, M. Effects of temperature and concentration on rheological behavior of MWCNTs/SiO220-80-SAE40 hybrid nano-lubricant. *Int. Commun. Heat Mass Transf.* **2016**, *76*, 133–138. [CrossRef]

76. Ali, M.K.A.; Xianjun, H.; Mai, L.; Bicheng, C.; Turkson, R.F.; Qingping, C. Reducing frictional power losses and improving the scuffing resistance in automotive engines using hybrid nanomaterials as nano-lubricant additives. *Wear* **2016**, *364–365*, 270–281. [CrossRef]

77. Asadi, M.; Asadi, A. Dynamic viscosity of MWCNT/ZnO-engine oil hybrid nanofluid: An experimental investigation and new correlation in different temperatures and solid concentrations. *Int. Commun. Heat Mass Transf.* **2016**, *76*, 41–45. [CrossRef]

78. Wu, L.; Zhang, Y.; Yang, G.; Zhang, S.; Yu, L.; Zhang, P. Tribological properties of oleic acid-modified zinc oxide nanoparticles as the lubricant additive in poly-alpha olefin and diisooctyl sebacate base oils. *RSC Adv.* **2016**, *6*, 69836–69844. [CrossRef]

79. Zheng, D.; Cai, Z.; Shen, M.; Li, Z.; Zhu, M. Investigation of the tribology behaviour of the graphene nanosheets as oil additives on textured alloy cast iron surface. *Appl. Surf. Sci.* **2016**, *387*, 66–75. [CrossRef]

80. Meng, Y.; Su, F.; Chen, Y. Supercritical Fluid Synthesis and Tribological Applications of Silver Nanoparticle-decorated Graphene in Engine Oil Nanofluid. *Sci. Rep.* **2016**, *6*, 1–12. [CrossRef]

81. Mungse, H.P.; Khatri, O.P. Dispersion and lubrication potential of nanosheets. *RSC Adv.* **2015**, 25565–25571. [CrossRef]

82. Koshy, C.P.; Rajendrakumar, P.K.; Thottackkad, M.V. Evaluation of the tribological and thermo-physical properties of coconut oil added with MoS2nanoparticles at elevated temperatures. *Wear* **2015**, *330–331*, 288–308. [CrossRef]

83. Jia, Z.; Chen, T.; Wang, J.; Ni, J.; Li, H.; Shao, X. Synthesis, characterization and tribological properties of Cu/reduced graphene oxide composites. *Tribol. Int.* **2015**, *88*, 17–24. [CrossRef]

84. Zin, V.; Agresti, F.; Barison, S.; Colla, L.; Mercadelli, E.; Fabrizio, M.; Pagur, C. Tribological properties of engine oil with carbon nano-horns as nano-additives. *Tribol. Lett.* **2014**, *55*, 45–53. [CrossRef]

85. Arumugam, S.; Sriram, G.; Ellappan, R. Bio-lubricant-biodiesel combination of rapeseed oil: An experimental investigation on engine oil tribology, performance, and emissions of variable compression engine. *Energy* **2014**, *72*, 618–627. [CrossRef]

86. Wan, Q.; Jin, Y.; Sun, P.; Ding, Y. Rheological and tribological behaviour of lubricating oils containing platelet MoS2 nanoparticles. *J. Nanopart. Res.* **2014**, *16*, 2386. [CrossRef]

87. Chen, T.; Xia, Y.; Jia, Z.; Liu, Z.; Zhang, H. Synthesis, Characterization, and Tribological Behavior of Oleic Acid Capped Graphene Oxide. *J. Nanomater.* **2014**, *2014*, 654145. [CrossRef]

88. Mungse, H.P.; Khatri, O.P. Chemically functionalized reduced graphene oxide as a novel material for reduction of friction and wear. *J. Phys. Chem.* **2014**, *118*, 14394–14402. [CrossRef]

89. Ettefaghi, E.o.l.; Ahmadi, H.; Rashidi, A.; Nouralishahi, A.; Mohtasebi, S.S. Preparation and thermal properties of oil-based nanofluid from multi-walled carbon nanotubes and engine oil as nano-lubricant. *Int. Commun. Heat Mass Transf.* **2013**, *46*, 142–147. [CrossRef]

90. Ettefaghi, E.O.l.; Rashidi, A.; Ahmadi, H.; Mohtasebi, S.S.; Pourkhalil, M. Thermal and rheological properties of oil-based nanofluids from different carbon nanostructures. *Int. Commun. Heat Mass Transf.* **2013**, *48*, 178–182. [CrossRef]

91. Demas, N.G.; Timofeeva, E.V.; Routbort, J.L.; Fenske, G.R. Tribological Effects of BN and MoS2 Nanoparticles Added to Polyalphaolefin Oil in Piston Skirt/Cylinder Liner Tests. *Tribol. Lett.* **2012**, *47*, 91–102. [CrossRef]

92. Materials, A.C.S.A.; Madras, T.; Madras, T. Graphene-Based Engine Oil Nanofluids for Tribological Applications Graphene-Based Engine Oil Nanofluids for Tribological Applications. *Tribol. Int.* **2011**, 4221–4227.

93. Ahmed Ali, M.K.; Xianjun, H.; Essa, F.A.; Abdelkareem, M.A.A.; Elagouz, A.; Sharshir, S.W. Friction and Wear Reduction Mechanisms of the Reciprocating Contact Interfaces Using Nanolubricant Under Different Loads and Speeds. *J. Tribol.* **2018**, *140*. [CrossRef]

94. Liu, Y.; Ge, X.; Li, J. Graphene lubrication. *Appl. Mater. Today* **2020**, *20*, 100662. [CrossRef]

95. Gulzar, M.; Masjuki, H.H.; Kalam, M.A.; Varman, M.; Zulkifli, N.W.M.; Mufti, R.A.; Zahid, R. Tribological performance of nanoparticles as lubricating oil additives. *J. Nanopart. Res.* **2016**, *18*, 223. [CrossRef]

96. Ali, M.K.A.; Xianjun, H.; Mai, L.; Qingping, C.; Turkson, R.F.; Bicheng, C. Improving the tribological characteristics of piston ring assembly in automotive engines using Al2O3 and TiO2 nanomaterials as nano-lubricant additives. *Tribol. Int.* **2016**, *103*, 540–554. [CrossRef]

97. Rajendhran, N.; Palanisamy, S.; Periyasamy, P.; Venkatachalam, R. Enhancing of the tribological characteristics of the lubricant oils using Ni-promoted MoS2 nanosheets as nano-additives. *Tribol. Int.* **2018**, *118*, 314–328. [CrossRef]

98. Kheireddin, B.A. Tribological Properties of Nanoparticle Based Lubrication Systems. Ph.D. Thesis, Texas A&M University, College Station, TX, USA, 2016.

99. Ramón-Raygoza, E.D.; Rivera-Solorio, C.I.; Giménez-Torres, E.; Maldonado-Cortés, D.; Cardenas-Alemán, E.; Cué-Sampedro, R. Development of nanolubricant based on impregnated multilayer graphene for automotive applications: Analysis of tribological properties. *Powder Technol.* **2016**, *302*, 363–371. [CrossRef]

100. Baskar, S.; Prabaharan, G.; Arumugam, S.; Nagabhooshanam, N. Modeling and Analysis of the Tribological Evaluation of Bearing Materials under the Influence of Nano Based Marine Lubricant Using D-Optimal Design. *Mater. Today Proc.* **2018**, *5*, 11548–11555. [CrossRef]

101. Zhang, Z.J.; Simionesie, D.; Schaschke, C. Graphite and hybrid nanomaterials as lubricant additives. *Lubricants* **2014**, *2*, 44–65. [CrossRef]

102. Mousavi, S.B.; Heris, S.Z.; Estellé, P. Viscosity, tribological and physicochemical features of ZnO and MoS2 diesel oil-based nanofluids: An experimental study. *Fuel* **2021**, *293*, 120481. [CrossRef]

103. Tóth, D.; Szabó, I.; Kuti, R. Tribological Properties of Nano-Sized ZrO2 Ceramic Particles in Automotive Lubricants. *FME Trans.* **2020**, *48*, 36–43. [CrossRef]

104. Thachnatharen, N.; Khalid, M.; Arulraj, A.; Sridewi, N. Materials Today: Proceedings. Tribological performance of hexagonal boron nitride hBN as nano-additives in military grade diesel engine oil. *Mater. Today Proc.* **2021**. [CrossRef]

105. Beheshti, A.; Huang, Y.; Ohno, K.; Blakey, I.; Stokes, J.R. Improving tribological properties of oil-based lubricants using hybrid colloidal additives. *Tribol. Int.* **2020**, *144*, 106130. [CrossRef]

106. Avilés, M.D.; Pamies, R.; Sanes, J.; Bermúdez, M.D. Graphene-ionic liquid thin film nanolubricant. *Nanomaterials* **2020**, *10*, 535. [CrossRef]

107. Xue, C.Y.; Wang, S.R.; Wang, Y.; Wang, G.Q.; Yan, X.Y. The Influence of Nanocomposite Carbon additive on Tribological Behavior of Cylinder Liner/Piston Ring. In *IOP Conference Series: Materials Science and Engineering*; IOP Publishing: Bristol, UK, 2019; Volume 491. [CrossRef]

108. Asnida, M.; Hisham, S.; Awang, N.W.; Amirruddin, A.K.; Noor, M.M.; Kadirgama, K.; Ramasamy, D.; Najafi, G.; Tarlochan, F. Copper II oxide nanoparticles as additve in engine oil to increase the durability of piston-liner contact. *Fuel* **2018**, *212*, 656–667. [CrossRef]

109. Borda, F.L.G.; de Oliveira, S.J.R.; Lazaro, L.M.S.M.; Leiróz, A.J.K. Experimental investigation of the tribological behavior of lubricants with additive containing copper nanoparticles. *Tribol. Int.* **2018**, *117*, 52–58. [CrossRef]

110. Cheng, Z.-L.; Li, W.; Wu, P.-R.; Liu, Z. Study on structure-activity relationship between size and tribological properties of graphene oxide nanosheets in oil. *J. Alloy. Compd.* **2017**, *722*, 778–784. [CrossRef]

111. Rasheed, A.K.; Khalid, M.; Javeed, A.; Rashmi, W.; Gupta, T.C.S.M.; Chan, A. Heat transfer and tribological performance of graphene nanolubricant in an internal combustion engine. *Tribol. Int.* **2016**, *103*, 504–515. [CrossRef]

112. Ali, M.K.A.; Xianjun, H.; Elagouz, A.; Essa, F.A.; Abdelkareem, M.A.A. Minimizing of the boundary friction coefficient in automotive engines using Al2O3 and TiO2 nanoparticles. *J. Nanopart. Res.* **2016**, *18*, 377. [CrossRef]

113. Scherge, M.; Böttcher, R.; Kürten, D.; Linsler, D. Multi-Phase Friction and Wear Reduction by Copper Nanopartices. *Lubricants* **2016**, *4*, 36. [CrossRef]

114. Jeng, Y.-R.; Huang, Y.-H.; Tsai, P.-C.; Hwang, G.-L. Tribological Performance of Oil-Based Lubricants with Carbon-Fe Nanocapsules Additive. *Tribol. Trans.* **2015**, *58*, 924–929. [CrossRef]

115. Peña-Parás, L.; Taha-Tijerina, J.; Garza, L.; Maldonado-Cortés, D.; Michalczewski, R.; Lapray, C. Effect of CuO and Al2O3 nanoparticle additives on the tribological behavior of fully formulated oils. *Wear* **2015**, *332–333*, 1256–1261. [CrossRef]

116. Padgurskas, J.; Rukuiza, R.; Prosyčevas, I.; Kreivaitis, R. Tribological properties of lubricant additives of Fe, Cu and Co nanoparticles. *Tribol. Int.* **2013**, *60*, 224–232. [CrossRef]

117. Zhang, B.S.; Xu, B.S.; Xu, Y.; Gao, F.; Shi, P.J.; Wu, Y.X. CU nanoparticles effect on the tribological properties of hydrosilicate powders as lubricant additive for steelsteel contacts. *Tribol. Int.* **2011**, *44*, 878–886. [CrossRef]

118. Abdullah, M.I.H.C.; Abdollah, M.F.B.; Amiruddin, H.; Tamaldin, N.; Nuri, N.R.M. Optimization of Tribological Performance of hBN/AL2O3Nanoparticles as Engine Oil Additives. *Procedia Eng.* **2013**, *68*, 313–319. [CrossRef]

119. Ghaednia, H. An Analytical and Experimental Investigation of Nanoparticle Lubricants. Ph.D. Thesis, Auburn University, Auburn, AL, USA, 2014.

120. Pe, L.; García-pineda, P.; Montemayor, O.E.; Nava, K.L.; Martini, A. Tribology International Effects of substrate surface roughness and nano/micro particle additive size on friction and wear in lubricated sliding. *Tribol. Int.* **2018**, *119*, 88–98. [CrossRef]

121. Vaitkunaite, G.; Espejo, C.; Wang, C.; Thi, B.; Charrin, C.; Neville, A.; Morina, A. Tribology International MoS 2 tribofilm distribution from low viscosity lubricants and its effect on friction. *Tribol. Int.* **2020**, *151*, 106531. [CrossRef]

122. Esfe, M.H.; Arani, A.A.A.; Esfandeh, S.; Afrand, M. Proposing new hybrid nano-engine oil for lubrication of internal combustion engines: Preventing cold start engine damages and saving energy. *Energy* **2019**, *170*, 228–238. [CrossRef]

123. Stachowiak, G.; Batchelor, A.W. *Engineering Tribology*, 4th ed.; Elsevier: Butterworth, Malaysia, 2014.

124. Wang, Q.J.; Chung, Y.-W. (Eds.) *Encyclopedia of Tribology*; Springer: Boston, MA, USA, 2013. [CrossRef]

125. Chhabra, R.P. Non-Newtonian Fluids: An Introduction. In *Rheology of Complex Fluids*; Springer: New York, NY, USA, 2010; pp. 3–34. [CrossRef]

126. Farbod, M.; asl, R.K.; abadi, A.R.N. Morphology dependence of thermal and rheological properties of oil-based nanofluids of CuO nanostructures. *Colloids Surf. Physicochem. Eng. Asp.* **2015**, *474*, 71–75. [CrossRef]

127. Dardan, E.; Afrand, M.; Isfahani, A.H.M. Effect of suspending hybrid nano-additives on rheological behavior of engine oil and pumping power. *Appl. Therm. Eng.* **2016**, *109*, 524–534. [CrossRef]

128. Asadi, A.; Asadi, M.; Rezaei, M.; Siahmargoi, M.; Asadi, F. The effect of temperature and solid concentration on dynamic viscosity of MWCNT/MgO 20–80–SAE50 hybrid nano-lubricant and proposing a new correlation: An experimental study. *Int. Commun. Heat Mass Transf.* **2016**, *78*, 48–53. [CrossRef]

129. Hemmat Esfe, M.; Abbasian Arani, A.A.; Esfandeh, S. Improving engine oil lubrication in light-duty vehicles by using of dispersing MWCNT and ZnO nanoparticles in 5W50 as viscosity index improvers (VII). *Appl. Therm. Eng.* **2018**, *143*, 493–506. [CrossRef]

130. Ma, J.; Shahsavar, A.; Al-Rashed, A.A.A.A.; Karimipour, A.; Yarmand, H.; Rostami, S. Viscosity, cloud point, freezing point and flash point of zinc oxide/SAE50 nanolubricant. *J. Mol. Liq.* **2020**, *298*, 112045. [CrossRef]

131. Asadi, A.; Pourfattah, F. Heat transfer performance of two oil-based nanofluids containing ZnO and MgO nanoparticles; a comparative experimental investigation. *Powder Technol.* **2019**, *343*, 296–308. [CrossRef]

132. Asadi, A.; Asadi, M.; Rezaniakolaei, A.; Rosendahl, L.A.; Wongwises, S. An experimental and theoretical investigation on heat transfer capability of Mg OH2/MWCNT-engine oil hybrid nano-lubricant adopted as a coolant and lubricant fluid. *Appl. Therm. Eng.* **2018**, *129*, 577–586. [CrossRef]

133. Motahari, K.; Moghaddam, M.A.; Moradian, M. Experimental investigation and development of new correlation for influences of temperature and concentration on dynamic viscosity of MWCNT-SiO2 20-80/20W50 hybrid nano-lubricant. *Chin. J. Chem. Eng.* **2018**, *26*, 152–158. [CrossRef]

134. Esfe, M.H.; Esfandeh, S. Investigation of rheological behavior of hybrid oil based nanolubricant-coolant applied in car engines and cooling equipments. *Appl. Therm. Eng.* **2018**, *131*, 1026–1033. [CrossRef]

135. Esfe, M.H.; Rostamian, H.; Rejvani, M.; Emami, M.R.S. Rheological behavior characteristics of ZrO 2-MWCNT/10w40 hybrid nano-lubricant affected by temperature, concentration, and shear rate: An experimental study and a neural network simulating. *Phys. Low-Dimens. Syst. Nanostruct.* **2018**, *102*, 160–170. [CrossRef]

136. Nadooshan, A.A.; Esfe, M.H.; Afrand, M. Evaluation of rheological behavior of 10W40 lubricant containing hybrid nano-material by measuring dynamic viscosity. *Physica Low Dimens. Syst. Nanostruct.* **2017**, *92*, 47–54. [CrossRef]

137. Esfe, M.H.; Rostamian, H. Non-Newtonian power-law behavior of TiO 2 /SAE 50 nano-lubricant: An experimental report and new correlation. *J. Mol. Liq.* **2017**, *232*, 219–225. [CrossRef]

138. Aberoumand, S.; Jafarimoghaddam, A. Experimental study on synthesis, stability, thermal conductivity and viscosity of Cu–engine oil nanofluid. *J. Taiwan Inst. Chem. Eng.* **2017**, *71*, 315–322. [CrossRef]

139. Alirezaie, A.; Saedodin, S.; Esfe, M.H.; Rostamian, S.H. Investigation of rheological behavior of MWCNT COOH-functionalized/MgO-Engine oil hybrid nanofluids and modelling the results with artificial neural networks. *J. Mol. Liq.* **2017**, *241*, 173–181. [CrossRef]

140. Esfe, M.H.; Afrand, M.; Rostamian, S.H.; Toghraie, D. Examination of rheological behavior of MWCNTs/ZnO-SAE40 hybrid nano-lubricants under various temperatures and solid volume fractions. *Exp. Therm. Fluid Sci.* **2017**, *80*, 384–390. [CrossRef]

141. Afrand, M.; Najafabadi, K.N.; Akbari, M. Effects of temperature and solid volume fraction on viscosity of SiO2-MWCNTs/SAE40 hybrid nanofluid as a coolant and lubricant in heat engines. *Appl. Therm. Eng.* **2016**, *102*, 45–54. [CrossRef]

142. Vakili-Nezhaad, G.R.; Dorany, A. Investigation of the effect of multiwalled carbon nanotubes on the viscosity index of lube oil cuts. *Chem. Eng. Commun.* **2009**, *196*, 997–1007. [CrossRef]

143. Desai, N.; Nagaraj, A.M.; Sabnis, N. Materials Today: Proceedings Analysis of thermo-physical properties of SAE20W40 engine oil by the addition of SiO 2 nanoparticles. *Mater. Today Proc.* **2021**, 2–7. [CrossRef]

144. Brinkman, H.C. The Viscosity of Concentrated Suspensions and Solutions. *J. Chem. Phys.* **1952**, *20*, 571. [CrossRef]

145. Esfe, M.H.; Arani, A.A.A.; Esfandeh, S. Experimental study on rheological behavior of monograde heavy-duty engine oil containing CNTs and oxide nanoparticles with focus on viscosity analysis. *J. Mol. Liq.* **2018**, *272*, 319–329. [CrossRef]

146. Esfe, M.H.; Karimpour, R.; Arani, A.A.A.; Shahram, J. Experimental investigation on non-Newtonian behavior of Al$_2$O$_3$-MWCNT/5W50 hybrid nano-lubricant affected by alterations of temperature, concentration and shear rate for engine applications. *Int. Commun. Heat Mass Transf.* **2017**, *82*, 97–102. [CrossRef]

147. Esfe, M.H.; Rostamian, H.; Sarlak, M.R.; Rejvani, M.; Alirezaie, A. Rheological behavior characteristics of TiO$_2$-MWCNT/10w40 hybrid nano-oil affected by temperature, concentration and shear rate: An experimental study and a neural network simulating. *Phys. Low-Dimens. Syst. Nanostruct.* **2017**, *94*, 231–240. [CrossRef]

148. Afrand, M.; Najafabadi, K.N.; Sina, N.; Safaei, M.R.; Kherbeet, A.S.; Wongwises, S.; Dahari, M. Prediction of dynamic viscosity of a hybrid nano-lubricant by an optimal artificial neural network. *Int. Commun. Heat Mass Transf.* **2016**, *76*, 209–214. [CrossRef]

149. Ahmed, S.A.; Ozkaymak, M.; Sözen, A.; Menlik, T.; Fahed, A. Improving car radiator performance by using TiO$_2$-water nanofluid. *Eng. Sci. Technol. Int. J.* **2018**, *21*, 996–1005. [CrossRef]

150. Wrenick, S.; Sutor, P.; Pangilinan, H.; Schwarz, E.E. Heat Transfer Properties of Engine Oils. In Proceedings of the World Tribology Congress III, ASMEDC, Washington, DC, USA, 12–16 September 2005; Volume 1, pp. 595–596. [CrossRef]

151. Yang, L.; Mao, M.; Huang, J.n.; Ji, W. Enhancing the thermal conductivity of SAE 50 engine oil by adding zinc oxide nano-powder: An experimental study. *Powder Technol.* **2019**, *356*, 335–341. [CrossRef]

152. Deepak, S.N.; Ram, C.N. Physio-chemical study of traditional lubricant SAE 20 W40 and virgin coconut oil using TiO$_2$ nano-additives. *Mater. Today Proc.* **2021**, *42*, 1024–1029. [CrossRef]

153. Aberoumand, S.; Jafarimoghaddam, A.; Moravej, M.; Aberoumand, H.; Javaherdeh, K. Experimental study on the rheological behavior of silver-heat transfer oil nanofluid and suggesting two empirical based correlations for thermal conductivity and viscosity of oil based nanofluids. *Appl. Therm. Eng.* **2016**, *101*, 362–372. [CrossRef]

154. Gupta, A.; Kumar, R. Role of Brownian motion on the thermal conductivity enhancement of nanofluids. *Appl. Phys. Lett.* **2007**, *91*, 223102. [CrossRef]

155. Shaheen, A.; Nadeem, S. Metachronal wave analysis for non-Newtonian fluid under thermophoresis and Brownian motion effects. *Res. Phys.* **2017**, *7*, 2950–2957. [CrossRef]

156. Harish, R.; Sivakumar, R. Effects of nanoparticle dispersion on turbulent mixed convection flows in cubical enclosure considering Brownian motion and thermophoresis. *Powder Technol.* **2021**, *378*, 303–316. [CrossRef]

157. Asadi, A.; Asadi, M.; Rezaniakolaei, A.; Rosendahl, L.A.; Afrand, M.; Wongwises, S. Heat transfer efficiency of Al$_2$O$_3$-MWCNT/thermal oil hybrid nanofluid as a cooling fluid in thermal and energy management applications: An experimental and theoretical investigation. *Int. J. Heat Mass Transf.* **2018**, *117*, 474–486. [CrossRef]

158. Asadi, A. A guideline towards easing the decision-making process in selecting an effective nanofluid as a heat transfer fluid. *Energy Convers. Manag.* **2018**, *175*, 1–10. [CrossRef]

159. Ettefaghi, E.; Ahmadi, H.; Rashidi, A.; Mohtasebi, S.; Alaei, M. Experimental evaluation of engine oil properties containing copper oxide nanoparticles as a nanoadditive. *Int. J. Ind. Chem.* **2013**, *4*, 28. [CrossRef]

160. Hemmati-Sarapardeh, A.; Varamesh, A.; Amar, M.N.; Husein, M.M.; Dong, M. On the evaluation of thermal conductivity of nanofluids using advanced intelligent models. *Int. Commun. Heat Mass Transf.* **2020**, *118*, 104825. [CrossRef]

161. Sulgani, M.T.; Karimipour, A. Improve the thermal conductivity of 10w40-engine oil at various temperature by addition of Al 2 O 3 /Fe 2 O 3 nanoparticles. *J. Mol. Liq.* **2019**, *283*, 660–666. [CrossRef]

162. Hamilton, R.L.; Crosser, O.K. Thermal Conductivity of Heterogeneous Two-Component Systems. *Ind. Eng. Chem. Fundam.* **1962**, *1*, 187–191. [CrossRef]

163. Tamura, K.; Kasai, M.; Nakamura, Y.; Enomoto, T. Impact of Boundary Lubrication Performance of Engine Oils on Friction at Piston Ring-Cylinder Liner Interface. *SAE Int. J. Fuels Lubr.* **2014**, *7*, 875–881. [CrossRef]

164. Holmberg, K.; Andersson, P.; Erdemir, A. Global energy consumption due to friction in passenger cars. *Tribol. Int.* **2012**, *47*, 221–234. [CrossRef]

165. Holmberg, K.; Erdemir, A. Influence of tribology on global energy consumption, costs and emissions. *Friction* **2017**, *5*, 263–284. [CrossRef]

166. Sarma, P.K.; Srinivas, V.; Rao, V.D.; Kumar, A.K. Experimental study and analysis of lubricants dispersed with nano cu and tio2 in a four-stroke two wheeler. *Nanoscale Res. Lett.* **2011**, *6*, 233. [CrossRef] [PubMed]

167. Kotia, A.; Borkakoti, S.; Ghosh, S.K. Wear and performance analysis of a 4-stroke diesel engine employing nanolubricants. *Particuology* **2018**, *37*, 54–63. [CrossRef]

168. Marcano, S.J.C.; Bensaid, S.; Deorsola, F.A.; Russo, N.; Fino, D. Nanolubricants for diesel engines: Related emissions and compatibility with the after-treatment catalysts. *Tribol. Int.* **2014**, *72*, 198–207. [CrossRef]

169. Beig, G.; Sahu, S.K.; Singh, V.; Tikle, S.; Sobhana, S.B.; Gargeva, P.; Ramakrishna, K.; Rathod, A.; Murthy, B.S. Recent developments of nanoparticles additives to the consumables liquids in internal combustion engines: Part II: Nano-lubricants. *Sci. Total Environ.* **2019**, *319*, 114156. [CrossRef]

170. Mallakpour, S.; Madani, M. A review of current coupling agents for modification of metal oxide nanoparticles. *Prog. Org. Coat.* **2015**, *86*, 194–207. [CrossRef]

171. Mamat, H. Nanofluids: Thermal Conductivity and Applications. *Ref. Modul. Mater. Sci. Mater. Eng.* **2019**. [CrossRef]

172. Sarno, M.; Scarpa, D.; Senatore, A.; Mustafa, W.A.A. rGO/GO nanosheets in tribology: From the state of the art to the future prospective. *Lubricants* **2020**, *8*, 31. [CrossRef]

173. Ripoll, M.R.; Tomala, A.M.; Totolin, V.; Remškar, M. Performance of nanolubricants containing MoS 2 nanotubes during form tapping of zinc-coated automotive components. *J. Manuf. Process.* **2019**, *39*, 167–180. [CrossRef]

174. Ali, I.; Basheer, A.A.; Kucherova, A.; Memetov, N.; Pasko, T.; Ovchinnikov, K.; Pershin, V.; Kuznetsov, D.; Galunin, E.; Grachev, V.; et al. Advances in carbon nanomaterials as lubricants modifiers. *J. Mol. Liq.* **2019**, *279*, 251–266. [CrossRef]

175. Yamakov, V.; Wolf, D.; Phillpot, S.R.; Mukherjee, A.K.; Gleiter, H. Deformation-mechanism map for nanocrystalline metals by molecular-dynamics simulation. *Nat. Mater.* **2004**, *3*, 43–47. [CrossRef] [PubMed]

176. Hahn, H.; Mondal, P.; Padmanabhan, K.A. Plastic deformation of nanocrystalline materials. *Nanostruct. Mater.* **1997**, *9*, 603–606. [CrossRef]

177. Fan, G.J.; Choo, H.; Liaw, P.K.; Lavernia, E.J. A model for the inverse Hall–Petch relation of nanocrystalline materials. *Mater. Sci. Eng.* **2005**, *409*, 243–248. [CrossRef]

178. Schiotz, J. A Maximum in the Strength of Nanocrystalline Copper. *Science* **2003**, *301*, 1357–1359. [CrossRef]

179. Bernholc, J.; Brenner, D.; Nardelli, M.B.; Meunier, V.; Roland, C. Mechanical and Electrical Properties of Nanotubes. *Annu. Rev. Mater. Res.* **2002**, *32*, 347–375. [CrossRef]

180. Gong, H.; Yu, C.; Zhang, L.; Xie, G.; Guo, D.; Luo, J. Intelligent lubricating materials: A review. *Compos. Part B Eng.* **2020**, *202*, 108450. [CrossRef]

181. Zhang, L.; Li, G.; Guo, Y.; Qi, H.; Che, Q.; Zhang, G. PEEK reinforced with low-loading 2D graphitic carbon nitride nanosheets: High wear resistance under harsh lubrication conditions. *Compos. Part A Appl. Sci. Manuf.* **2018**, *109*, 507–516. [CrossRef]

182. Rodriguez, A.; Jaman, M.S.; Acikgoz, O.; Wang, B.; Yu, J.; Grützmacher, P.G.; Rosenkranz, A.; Baykara, M.Z. The potential of Ti3C2TX nano-sheets MXenes for nanoscale solid lubrication revealed by friction force microscopy. *Appl. Surf. Sci.* **2021**, *535*, 147664. [CrossRef]

183. Wang, F.F.; Liu, Z.; Cheng, Z.L. High performance of MOF-structured lubricating material with nano- and micro-sized morphologies. *Mater. Lett.* **2019**, *248*, 222–226. [CrossRef]

184. Wyatt, B.C.; Rosenkranz, A.; Anasori, B. 2D MXenes: Tunable Mechanical and Tribological Properties. *Adv. Mater.* **2021**, *33*, 2007973. [CrossRef]

185. Malaki, M.; Varma, R.S. Mechanotribological Aspects of MXene-Reinforced Nanocomposites. *Adv. Mater.* **2020**, *32*, 202003154. [CrossRef]

186. Yin, X.; Jin, J.; Chen, X.; Rosenkranz, A.; Luo, J. Ultra-Wear-Resistant MXene-Based Composite Coating via in Situ Formed Nanostructured Tribofilm. *ACS Appl. Mater. Interfaces* **2019**, *11*, 32569–32576. [CrossRef]

187. Liu, Y.; Zhang, X.; Dong, S.; Ye, Z.; Wei, Y. Synthesis and tribological property of Ti3C2TX nanosheets. *J. Mater. Sci.* **2017**, *52*, 2200–2209. [CrossRef]

188. Yang, J.; Chen, B.; Song, H.; Tang, H.; Li, C. Synthesis, characterization, and tribological properties of two-dimensional Ti$_3$C$_2$. *Cryst. Res. Technol.* **2014**, *49*, 926–932. [CrossRef]

189. Hu, C.; Bai, M.; Lv, J.; Li, X. Molecular dynamics simulation of mechanism of nanoparticle in improving load-carrying capacity of lubricant film. *Comput. Mater. Sci.* **2015**, *109*, 97–103. [CrossRef]

190. Chen, J.; Dai, F.; Zhang, L.; Xu, J.; Liu, W.; Zeng, S.; Xu, C.; Chen, L.; Dai, C. Molecular insights into the dispersion stability of graphene oxide in mixed solvents: Theoretical simulations and experimental verification. *J. Colloid Interface Sci.* **2020**, *571*, 109–117. [CrossRef] [PubMed]

191. Hu, C.; Bai, M.; Lv, J.; Wang, P.; Zhang, L.; Li, X. Molecular dynamics simulation of nanofluid's flow behaviors in the near-wall model and main flow model. *Microfluid. Nanofluid.* **2014**, *17*, 581–589. [CrossRef]

192. Mirzaamiri, R.; Akbarzadeh, S.; Ziaei-Rad, S.; Shin, D.G.; Kim, D.E. Molecular dynamics simulation and experimental investigation of tribological behavior of nanodiamonds in aqueous suspensions. *Tribol. Int.* **2021**, *156*, 106838. [CrossRef]

193. Hu, C.; Bai, M.; Lv, J.; Kou, Z.; Li, X. Tribology International Molecular dynamics simulation on the tribology properties of two hard nanoparticles diamond and silicon dioxide confined by two iron blocks. *Tribiol. Int.* **2015**, *90*, 297–305. [CrossRef]

194. Fang, T.; Zhang, Y.; Yan, Y.; Dai, C.; Zhang, J. Molecular insight into the aggregation and dispersion behavior of modified nanoparticles. *J. Pet. Sci. Eng.* **2020**, *191*, 107193. [CrossRef]

195. Zhao, L.; Shi, Z.; Qian, Q.; Song, J.; Chen, Q.; Yang, J.; Wang, C.; Tu, Y. Association of Lennard-Jones particles in nanoconfined aqueous solution: Theory and molecular dynamics simulations. *Phys. Stat. Mech. Appl.* **2021**, *563*, 125414. [CrossRef]

196. Abu-Hamdeh, N.H.; Almatrafi, E.; Hekmatifar, M.; Toghraie, D.; Golmohammadzadeh, A. Molecular dynamics simulation of the thermal properties of the Cu-water nanofluid on a roughed Platinum surface: Simulation of phase transition in nanofluids. *J. Mol. Liq.* **2020**, *327*, 114832. [CrossRef]

197. Hu, C.; Bai, M.; Lv, J.; Liu, H.; Li, X. Applied Surface Science Molecular dynamics investigation of the effect of copper nanoparticle on the solid contact between friction surfaces. *Appl. Surf. Sci.* **2014**, *321*, 302–309. [CrossRef]

198. Hu, C.; Lv, J.; Bai, M.; Zhang, X.; Tang, D. Molecular dynamics simulation of effects of nanoparticles on frictional heating and tribological properties at various temperatures. *Friction* **2020**, *8*, 531–541. [CrossRef]

199. Zhang, L.; Lu, B.; Wu, Y.; Wang, J.; Zhang, X.; Wang, L.; Xi, D. Molecular dynamics simulation and experimental study on the lubrication of graphene additive films. *Proc. Inst. Mech. Eng. Part J J. Eng. Tribol.* **2020**, *234*, 1–16. [CrossRef]

200. Hu, C.; Bai, M.; Lv, J.; Wang, P.; Li, X. Molecular dynamics simulation on the friction properties of nanofluids confined by idealized surfaces. *Tribol. Int.* **2014**, *78*, 152–159. [CrossRef]

201. Hu, C.; Yi, C.; Bai, M.; Lv, J.; Tang, D. Molecular dynamics study of the frictional properties of multilayer MoS 2. *RSC Adv.* **2020**, *10*, 17418–17426. [CrossRef]

202. Rosenkranz, A.; Marian, M.; Profito, F.J.; Aragon, N.; Shah, R. The use of artificial intelligence in tribology—A perspective. *Lubricants* **2021**, *9*, 2. [CrossRef]

203. Friedrich, K.; Reinicke, R.; Zhang, Z. Wear of polymer composites. *Proc. Inst. Mech. Eng. Part J J. Eng. Tribol.* **2002**, *216*, 415–426. [CrossRef]

204. Argatov, I. Artificial Neural Networks ANNs as a Novel Modeling Technique in Tribology. *Front. Mech. Eng.* **2019**, *5*, 30. [CrossRef]

205. Mahrova, M.; Pagano, F.; Pejakovic, V.; Valea, A.; Kalin, M.; Igartua, A.; Tojo, E. Pyridinium based dicationic ionic liquids as base lubricants or lubricant additives. *Tribol. Int.* **2015**, *82*, 245–254. [CrossRef]

206. Zhou, Y.; Leonard, D.N.; Guo, W.; Qu, J. Understanding Tribofilm Formation Mechanisms in Ionic Liquid Lubrication. *Sci. Rep.* **2017**, *7*, 8426. [CrossRef] [PubMed]

207. Shameem, A.C.M.; Samad, B.A.; Koshy, G.; Suresh, T.G.A.; Mana, A.P. Assessment of the tribological performance of ionic liquid additive in engine oil for automotive application. *J. Tribol.* **2019**, *21*, 21–34.

208. Barnhill, W.C. Tribological Testing and Analysis of Ionic Liquids as Candidate Anti-Wear Additives for Next-Generation Engine Lubricants. Master's Thesis, University of Tennessee, Knoxville, TN, USA, 2016.

209. Bapat, A.P.; Erck, R.; Seymour, B.T.; Zhao, B.; Cosimbescu, L. Lipophilic polymethacrylate ionic liquids as lubricant additives. *Eur. Polym. J.* **2018**, *108*, 38–47. [CrossRef]

210. González, R.; Viesca, J.L.; Battez, A.H.; Had, M.; Fernández-gonzález, A.; Bartolomé, M. Two phosphonium cation-based ionic liquids as lubricant additive to a polyalphaolefin base oil. *J. Mol. Liq.* **2019**, *293*, 111536. [CrossRef]

211. Zhou, Y.; Qu, J. Ionic liquids as lubricant additives: A review. *ACS Appl. Mater. Interfaces* **2017**, *9*, 3209–3222. [CrossRef]

212. Oulego, P.; Blanco, D.; Ramos, D.; Viesca, J.L.; Díaz, M.; Battez, A.H. Environmental properties of phosphonium, imidazolium and ammonium cation-based ionic liquids as potential lubricant additives. *J. Mol. Liq.* **2018**, *272*, 937–947. [CrossRef]

213. Guo, J.; Barber, G.C.; Schall, D.J.; Zou, Q.; Jacob, S.B. Tribological properties of ZnO and WS2 nanofluids using different surfactants. *Wear* **2017**, *382–383*, 8–14. [CrossRef]

214. Wciślik, S. A simple economic and heat transfer analysis of the nanoparticles use. *Chem. Pap.* **2017**, *71*, 2395–2401. [CrossRef] [PubMed]

215. Alirezaie, A.; Hajmohammad, M.H.; Ahangar, M.R.H.; Esfe, M.H. Price-performance evaluation of thermal conductivity enhancement of nanofluids with different particle sizes. *Appl. Therm. Eng.* **2018**, *128*, 373–380. [CrossRef]

216. Maji, N.C.; Krishna, H.P.; Chakraborty, J. Low-cost and high-throughput synthesis of copper nanopowder for nanofluid applications. *Chem. Eng. J.* **2018**, *353*, 34–45. [CrossRef]

217. Esfe, M.H.; Arani, A.A.A.; Badi, R.S.; Rejvani, M. ANN modeling, cost performance and sensitivity analyzing of thermal conductivity of DWCNT–SiO2/EG hybrid nanofluid for higher heat transfer. *J. Therm. Anal. Calorim.* **2018**, *131*, 2381–2393. [CrossRef]